“Post-transcriptional regulation of phytohormone signal transduction in *Arabidopsis* immunity”

Dissertation

zur Erlangung des Doktorgrades der Naturwissenschaften (Dr. rer. nat.)

der

Naturwissenschaftlichen Fakultät I

– Biowissenschaften –

der Martin-Luther-Universität

Halle-Wittenberg

vorgelegt

von Herr Mohammad Abukhalaf

geb. am 15.04.1989 in Damaskus

Gutachter:

Prof. Dr. Markus Pietzsch

Prof. Dr. Bettina Hause

Prof. Dr. Sacha Baginsky

Verteidigt am 20.05.2022

Acknowledgement

Alhamdulillah, finally I am finishing my PhD which was not possible without the support of many people. First of all, this project would not have been possible without Dr. Wolfgang Hoehenwarter and all his support and guidance throughout the years, he was always there for helping me even in the simplest things, and he was and will always be as a big brother to me. I should also appreciate my colleague and friend Mohamed Ayash for the discussions and collaborative work on multiple projects. Moreover, I would like to thank Domenika Thieme and Carsten Proksch for their endless support in the lab work and the LC-MS measurements of all the protein samples.

I would like to express my deepest thanks to Prof. Markus Pietzsch for giving me the opportunity to come to Germany and be part of the international masters of Pharmaceutical and Industrial Biotechnology which was a turning point that allowed me to pursue my dream to become a scientist. Also, I would like to thank him for the continuous support and supervision throughout the PhD project.

I would also like to express my gratitude to Prof. Bettina Hause for the endless support and guidance during this project. Moreover, I must thank Prof. Tina Romeis for allowing me to continue my research project in her department. And I would also like to thank Prof. Sacha Baginsky for accepting to review this dissertation.

I should also appreciate Dr. Jörg Ziegler for his help in the preparation and measurements of plant hormones. Also, I would like to acknowledge the help of Dr. Lennart Eschen-Lippold in the qPCR experiments. And I would like to thank all the BPI members especially Sylvia Krüger for all the help in the lab stuff and experiments.

I would like to pay my special regards to my love Kriti who motivated and empowered me throughout the times till now and to come in my life. Furthermore, I want to thank all my friends, who were always next to me in the best and worst times and who encouraged me in multiple ways especially Rafa'a, Amr, Laith, Ali Khamis, Bandar, Firas, Ghanem, Mohamad Saoud, Ali Kanish, Ibrahim, Khaled Al Sakran and Khaled Jibreel.

However, all of this was not possible without my family. Words cannot express the support and help of my mom and dad throughout my life till this point. They were always with me even in the hardest times, and I am proud to be their son. Also, my brothers Majd and Nidal, and my sister Joud who have been encouraging me to pursue my higher studies and were always supportive. Finally, I would like to thank my cousin and brother Anas Abukhalaf for teaching me Deutsch and encouraging me to pursue studies in Germany.

Contents

List of Abbreviations ..... **v**

1. Introduction **1**

1.1. Proteomics 1

1.1.1. Evolution of proteomics 1

1.1.2. Quantitative proteomics 2

1.1.3. Parallel Reaction Monitoring (PRM) 5

1.2. Plant Immunity 7

1.2.1. Pattern Triggered Immunity (PTI) 7

1.2.2. Jasmonic Acid (JA) biosynthesis and signaling 9

1.2.3. PTI effect on Auxin transport 10

1.3. Protein Turnover rates 11

1.4. Aim of the Study 13

2. Materials and Methods **14**

2.1. Materials 14

2.2. Methods 21

2.2.1. Preparation of seedling cultures to study flg22 effects 21

2.2.2. Preparation of seedling cultures to the study the effect of media exchange 21

2.2.3. ^{15}N metabolic labeling of seedling cultures 21

2.2.4. Extraction of proteins 22

2.2.5. Determination of protein concentration (2D-Quant kit) 22

2.2.6. Filter Assisted Sample Preparation (FASP) 22

2.2.7. STAGE-Tip C18 peptide desalting (Stop-and-Go Extraction) 23

2.2.8. Flg22 extraction from media 23

2.2.9. LC-MS for protein analysis 23

2.2.10. LC-MS for flg22 Analysis 25

2.2.11. PRM data Analysis 25

2.2.12. Protein turnover rates Analysis (K_s and K_d) 26

2.2.13. RNA extraction 28

2.2.14. cDNA synthesis 29

2.2.15. qPCR preparation and analysis 29

2.2.16. Sample preparation for hormone analysis 30

3. Results 32

3.1. Proteome Remodeling Under Pattern Triggered Immunity (PTI) 32

3.2. Validation of the Experimental Design 33

3.2.1. Flg22 analysis in the media 33

3.2.2. Effects of media exchange on target proteins 34

3.3. Studying the PTI Response 36

3.3.1. Response in *Arabidopsis thaliana* Col-0 36

3.3.2. Response in *Arabidopsis thaliana myc234* 45

3.4. Protein Turnover Rates Measurements 51

3.4.1. Target proteins turnover rates measurement under normal conditions (control) 52

3.4.2. Target proteins turnover measurements under flg22 56

4. Discussion 60

4.1. PRM coupled retention time (Rt) scheduling achieves sensitive and accurate quantification of hundreds of peptides 60

4.2. Secondary metabolites pathways play a role in defense priming 61

4.3. Auxin efflux transporters PIN3 and PIN7 are important for growth-defense transition 63

4.4. MYC controlled Jasmonic Acid Oxidase 2 (JOX2) and IAA-Alanine Resistant 3 (IAR3) inactivates JA and JA-Ile in PTI 64

4.5. Downregulation of photosynthesis in PTI and the involved MYC control 67

4.6. Transcriptional regulation is not a direct determinant of gene expression especially in PTI 67

4.7. ^{15}N metabolic labeling LC-MS protein turnover rates measurements and its application in steady state situations 68

4.8. Protein turnover rates measurements in non-steady state PTI 69

5. Summary 71

6. **References 73**

7. **Appendix 89**

List of Abbreviations

°C	Degree Celsius
µg	Microgram
µL	Microliter
µM	Micromolar
12-OH-JA	12-Hydroxy Jasmonic Acid
2-D	Two Dimensional
2DE	Two-Dimensional Gel Electrophoresis
4CL1	4-Coumarate: CoA Ligase 1
4CL2	4-Coumarate: CoA Ligase 2
4MOI3M	4-Methoxy-Indol-3-Ylmethyl Glucosinolate
AAO1	Aldehyde Oxidase 1
AAs	Amino Acids
ABA	Abscisic Acid
ACN	Acetonitrile
ACO2	ACC Oxidase 2
ACX1	Acyl-CoA Oxidase 1
AGC	Automatic Gain Control
AOC1	Allene Oxide Cyclase 1
AOC2	Allene Oxide Cyclase 2
AOC4	Allene Oxide Cyclase 4
AOS	Allene Oxide Synthase
ASA2	Anthranilate Synthase 2
AUC	Area Under the Curve
AUX1	Auxin1
AXR4	Auxin Resistant 4
BABA	B-Aminobutyric Acid
BAK1	BRI1-Associated Receptor Kinase 1
bHLH	basic-Helix-Loop-Helix
BIK1	Botrytis-Induced Kinase 1
BSA	Bovine Serum Albumin
BTH	Benzothiadiazole
C4H	Cinnamate 4-Hydroxylase
CDPKs	Calcium Dependent Protein Kinases
CID	Collision-Induced Dissociation
COI1	Coronatine Insensitive 1
CUL1	Cullin 1
CYP81F2	Cytochrome P450, Family 81, Subfamily F, Polypeptide 2

CYP83A1	Cytochrome P450, Family 83, Subfamily A, Polypeptide 1
CYP83B1	Cytochrome P450, Family 83, Subfamily B, Polypeptide 1
CYP94B1	Cytochrome P450, Family 94, Subfamily B, Polypeptide 1
CYP94B3	Cytochrome P450, Family 94, Subfamily B, Polypeptide 3
CYP94C1	Cytochrome P450, Family 94, Subfamily C, Polypeptide 1
Da	Dalton
DDA	Data Dependent Acquisition
ddH_2O	Double-Distilled Water
DIA	Data Independent Acquisition
EB	Extraction Buffer
EDS5	Enhanced Disease Susceptibility 5
EFR	EF-Tu Receptor
EIN3	Ethylene Insensitive 3
elf18	18 Amino Acid Epitope of *Escherichia Coli* Elongation Factor (EF) Tu
ELISA	Enzyme Linked Immunosorbent Assay
ER	Endoplasmic Reticulum
ESI	Electrospray Ionization
ET	Ethylene
ETI	Effector Triggered Immunity
FA	Formic Acid
FASP	Filter Assisted Sample Preparation
FCP	Fold Change Protein
FDR	False Discovery Rate
flg ns	Non-Steady State Flg22 Elicited PTI
flg ss	Steady State Flg22 Elicited PTI
flg22	Flagellin 22
FLNC	Filamin C
FLS2	Flagellin-Sensitive 2
FNR1	Ferredoxin-NADP (+)-Oxidoreductase 1
FTICR	Fourier Transform Ion-Cyclotron Resonance
g	Relative Centrifugal Force
GS	Glucosinolates
H_2O	Water

HL	Hydrophilic Loops
HPLC	High-Performance Liquid Chromatography
hrs	Hours
I4-FFL	Incoherent Type-4 Feed-Forward Loop
IAA	Indole-3-Acetic Acid
IAR3	IAA-Alanine Resistant 3
ICATs	Isotope Coded Affinity Tags
ICS1	Isochorismate Synthase 1
IF	Intensity Factor
IGPS	Indole-3-Glycerol Phosphate Synthase
INA	2,6-Dichloro-Isonicotinic Acid
IT	Injection Time
iTRAQ	Isobaric Tags for Relative and Absolute Quantification
JA	Jasmonic Acid
JA-Ile	Jasmonic Acid Isoleucine
JAR1	Jasmonate Resistant 1
JAZ	Jasmonate ZIM Domain
JOX2	Jasmonic Acid Oxidase 2
K_d	Degradation Rate
K_{dil}	Growth Rate (Dilution Factor)
K_{loss}	Apparent Degradation Rate
K_s	Synthesis Rate
kV	Kilovolts
L	Liter
LAX	Like AUXIN1
LC	Liquid Chromatography
LC-MS	Liquid Chromatography – Mass Spectrometry
LHCB3	Light-Harvesting Chlorophyll B-Binding Protein 3
LOX2	Lipoxygenase 2
M	Molar
m/z	Mass / Charge
MALDI	Matrix Assisted Laser Desorption Ionization
MAPKs or MPKs	Mitogen Activated Protein Kinases
MeJA	Methyl Jasmonate
MEKKs	MKK Kinases
MeOH	Methanol
mg	Milligram
min	Minutes
MKKs	MAPK Kinases
MKS1	MPK Substrate 1
mL	Milliliter
mM	Millimolar

mm	Millimeter
MS	Mass Spectrometry
ms	Millisecond
NGS	Next Generation Sequencing
NINJA	Novel Interactor Of JAZ
NIT4	Nitrilase 4
nL	Nanoliter
NTL9	Nac Transcription Factor-Like 9
OGs	Oligogalacturonides
OPDA	12-Oxophytodienoic Acid
OPR3	Oxophytodienoate-Reductase 3
PAD4	Phytoalexin Deficient 4
PAL1	Phenylalanine Ammonia-Lyase 1
PAMPs	Pathogen Associated Molecular Patterns
PASEF	Parallel Accumulation–Serial Fragmentation
PAT	Polar Auxin Transport
PAT1	Phosphoribosyl Anthranilate Transferase 1
PDH-E1 ALPHA	Pyruvate Dehydrogenase E1 Alpha
PEN2	Penetration 2
PIN3	PIN-Formed 3
PIN7	PIN-Formed 7
PM	Plasma Membrane
Pmol	Picomole
PP2A	Protein Phosphatase 2A Subunit A3
ppm	Part Per Million
PQI	Protein Quantification Index
PRM	Parallel Reaction Monitoring
PRRs	Pattern Recognition Receptors
PSMs	Peptide Spectral Matches
PTI	Pattern Triggered Immunity
PTMs	Post Translational Modifications
QIT	Quadruple Ion Trap
QqQ	Triple Quadruple
QTOF	Quadruple Time of Flight
RIA	Relative Isotopic Abundance
ROS	Reactive Oxygen Species
rpm	Revolutions Per Minute
RSTDE	Relative Standard Error
Rt	Retention Time

RT	Room Temperature
SA	Salicylic Acid
SAR	Systemic Acquired Resistance
SC	Spectral Counting
SCF^{COI1}	Coronatine Insensitive1 Skp1/Cullin/F-Box Complex
secs	Seconds
SILAC	Stable Isotope Labeling by Amino Acids in Cell Culture
SKP1	S Phase Kinase-Associated Protein 1
SOT16	Sulfotransferase 16
SRM	Selected Reaction Monitoring
SUR1	Superroot 1
TCP22	TCP Domain Protein 22
TDA	Targeted Data Dependent Acquisition
TFA	Trifluoroacetic Acid
TFs	Transcription Factors
TIM	Triosephosphate Isomerase
TMTs	Tandem Mass Tags
TPL	Topless
TPR	Topless-Related
TQ	Triple Quadruple
TSA1	Tryptophan Synthase Alpha Chain
TSB1	Tryptophan Synthase Beta-Subunit 1
U	Units
UBC21	Ubiquitin-Conjugating Enzyme 21
UGT74B1	UDP-Glucosyl Transferase 74B1
UGT74F2	UDP-Glucosyltransferase 74F2
V	Volts

1. Introduction

1.1. Proteomics

1.1.1. Evolution of proteomics

The analysis of the full set of proteins encoded by the genome in an organism, tissue or cell in multiple conditions, is termed proteomics (Ferguson and Smith, 2003, Wilkins et al., 1996). The developments in the field of genomics were important as open reading frames are the blueprints for the expressed proteins (Tyers and Mann, 2003). Proteomics approaches were faced by multiple challenges, such as protein abundance, degradation, post translational modifications (PTMs), alternative splicing, instability of the proteome and others that shaped the development of proteomics techniques in the last 20 years (Altelaar et al., 2013).

Before the introduction of mass spectrometry (MS), proteins were sequenced by Edman degradation (Edman and Begg, 1967) a laborious method that is suited for characterization of N-terminal sequence tags of particular proteins. In the mid-1990s, (Henzel et al., 1993) and (Shevchenko et al., 1996) used two-dimensional gel electrophoresis (2DE) to separate intact

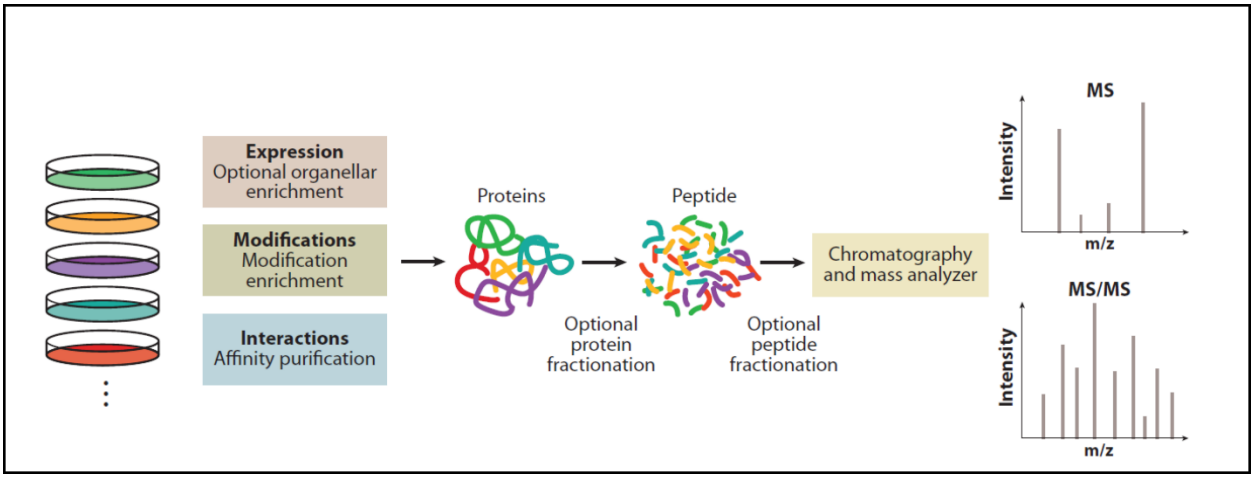

Figure 1-1. Outline of a generic shotgun proteomics workflow. The typical proteomics workflow starts with the protein extract which can be then used a whole, enriched or purified depending on the type of study. Proteins are then digested with enzymes, such as trypsin or Lys-C, to multiple smaller peptides. These peptides are then separated by liquid chromatography and analyzed by mass spectrometry (LC-MS) which collects MS and tandem MS (MS/MS) spectra linked to each peptide. These spectra disclose information of the peptide sequence and quantity in the sample which can be interpreted for protein identification and quantitation. m/z, mass-to-charge ratio. (Cox and Mann, 2011)

proteins followed by matrix-assisted laser desorption ionization MS (MALDI-MS) of the tryptic digested proteins obtained from the 2DE spots and further data analysis, to cover 10 and 150 proteins in *Escherichia coli* and yeast, respectively. Limitation of the 2DE separation in complex protein mixtures prompted the use of other separation techniques such as liquid chromatography (LC). Samples are first separated by the LC which is coupled online to the MS by the use of the electrospray ionization (ESI) (Fenn et al., 1989) (LC-MS). This technique was used later in the development of the shotgun proteomics workflow (Cox and Mann, 2011) (Figure 1-1). This "bottom up" approach starts with the extraction of the proteins from organisms or cells, then these proteins are digested by trypsin, which cleaves at lysine and arginine carboxy termini, to peptides which can be separated by nanoscale high-performance liquid chromatography (HPLC) and analyzed by tandem MS (MS/MS). Tandem MS technique uses two mass analyzers with a collision cell in the middle (McLafferty, 1981). After separation by HPLC, peptides are further separated in the first mass analyzer and then the separated peptide enters the collision cell where collision-induced dissociation (CID) or other fragmentation regimes of peptides result in fragments that are analyzed afterwards by the second mass analyzer (Steen and Mann, 2004). Different combinations of analyzers were used such as triple quadrupole (TQ), quadrupole ion trap (QIT), Fourier transform ion-cyclotron resonance (FTICR), or quadrupole time-of-flight (QTOF) mass spectrometers. However, the introduction of the orbitrap (Makarov, 2000) ,the cheaper alternative to FTICR with high resolution and accuracy, in a hybrid linear ion trap/orbitrap MS revolutionized shotgun proteomics. Finally, generated MS/MS spectra are analyzed by different programs which use variable algorithms to match them to the theoretically generated peak lists of corresponding peptides and later to proteins.

Another approach, is "top down" where proteins are separated and then analyzed as a whole by MS/MS (McLafferty et al., 2007). Despite its advantage in the coverage of protein sequence and PTMs, limitations in instrumentation, separation and data analysis hindered the use of this approach (Kellie et al., 2010). Developments on all the levels of the proteomics workflow in the last decade including sample preparation, LC techniques, MS analyzers and data analysis advanced proteomics and made it an important tool for systems biology (Bensimon et al., 2012, Cox and Mann, 2011).

1.1.2. Quantitative proteomics

After earlier developments established peptide and protein identification, quantitation of proteins became the main part of proteomic studies (Bantscheff et al., 2012). Quantitative proteomics are divided into two main approaches (Figure 1-2): Isotopic labeling and Label-free.

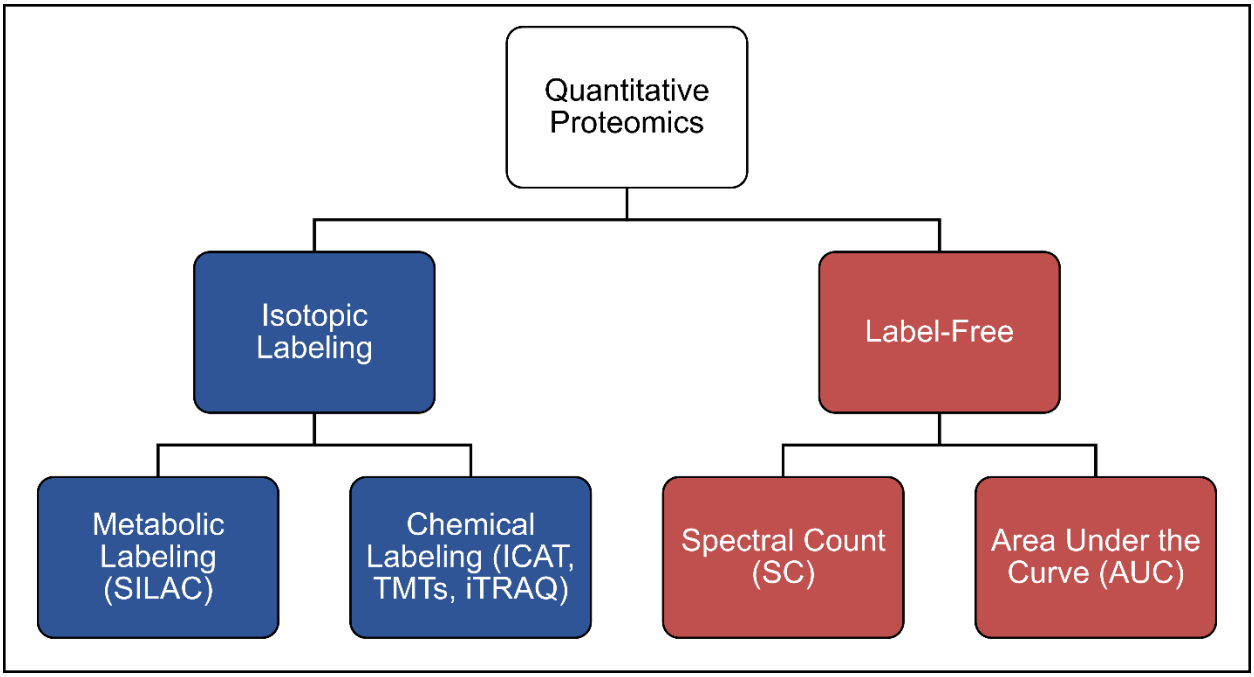

Figure 1-2. Summary of the quantitative proteomics approaches. Two main approaches are used depending on labeling with isotopes or not. Explanation of each approach is discussed in the text.

Isotopic labeling techniques have been developing over the years. In 1999, isotopic-coded affinity tags (ICATs) were introduced (Gygi et al., 1999) to quantify differences in protein abundance in the yeast *Saccharomyces cerevisiae* under ethanol vs. galactose as a carbon source. In this workflow, cysteine side chain residues of the proteins are derivatized with an ICAT reagent (which consists of Biotin, a linker (light or heavy isotope) and a Thiol-specific reactive group) with a light linker in one sample and a heavy linker in the other. The two samples are mixed and digested resulting in a mixture of peptides where some are tagged (heavy or light). Then using avidin affinity chromatography, tagged peptides are separated and then analyzed by MS. Data analysis software then can relatively quantify the ratios of heavy to light linked peptide pairs, thus allowing relative protein quantification between samples (Li et al., 2003). In 2002, stable isotope labeling by amino acids in cell culture (SILAC) was introduced by (Ong et al., 2002),where it was used to relatively quantify protein abundance during muscle cell differentiation processes. In this workflow, cell cultures are grown in a media either containing naturally occurring amino acids (AAs) or isotopic labeled (heavy) AAs. Subsequently proteins are extracted and mixed (heavy and light), digested, then separated and analyzed by LC-MS. This technique nullifies the effects of sample preparation as samples are combined at the earliest stage in the experiments (Chahrour et al., 2015). Later in 2004, a multiplexing quantitation strategy of proteins was

introduced by (Ross et al., 2004) where isobaric tags are added at the N-termini and lysine side chains of peptides. The resulting peptides are isobaric and elute at the same retention times, however, after collision in the MS analyzer they produce different reporter ions which can be quantified. The advantage of this approach is that it does not expand proteome complexity and enables the comparison of multiple states in one measurement. Two main reagents are widely used: isobaric tags for relative and absolute quantification (iTRAQ) and Tandem Mass Tags (TMTs) which were used in up to 8-plex (Choe et al., 2007) and 10 plex (Keshishian et al., 2015) experiments, respectively.

The other popular approach is label-free quantitation. It can overcome the expensive costs of isotopic labeling (Neilson et al., 2011). However it was not robust, until the introduction of MS instruments which can achieve high resolution high mass accuracy measurements, such as the Hybrid Linear Ion Trap/Orbitrap Mass Spectrometer (Makarov et al., 2006). The quantitation in this approach uses two main methods: Area Under the Curve (AUC) and Spectral Counting. (SC) (Figure 1-2). In the first method, the MS1 signal peak area in the ion chromatogram is integrated representing the quantity of the peptide of choice (Mueller et al., 2008). It has been established that the abundance of the peptide is proportional to the AUC (Chelius and Bondarenko, 2002), where concentrations of tryptic digests of myoglobin in amounts of 10 fmol to 100 pmol were linearly correlated with the AUC (R^2 = 0.991). The second method is more dependent on the shotgun workflow, where the first MS analyzer selects the highest abundant peptides (usually top 10 or 20) to be fragmented by CID and analyzed by the second MS resulting in the MS/MS spectra. The idea behind this method, is that the more times a peptide is selected by the MS1 the more abundant it is in the sample. This was validated by (Liu et al., 2004), where the concentration of marker proteins spiked in yeast cell lysates were linearly correlated with their respective spectral counts ($R^2 \approx 0.99$). A comparison between the two label-free methods reported the superiority of SC in sensitivity to detect changing proteins, yet its inferiority to AUC in the accuracy of protein ratios estimation (Old et al., 2005). Moreover, label-free approaches are considered comparable to isotopic labeling (Turck et al., 2007), however, the main problems arise as different samples should be analyzed individually. For example, the variable efficiency of the MS and the retention time shifts between different runs are challenges in the AUC method that multiple software tackle by peak detection and peak alignments (America and Cordewener, 2008). On the other hand, the MS/MS spectra quality can affect the SC method as errors in its assignments to peptides introduce errors in protein quantification (Mueller et al., 2008). However, solutions based on statistical procedures demonstrated the ability to distinguish incorrect MS/MS spectral assignments to peptides (Keller et al., 2002).

Developments in bioinformatics introduced multiple powerful free and commercial tools for the quantitative analysis of large proteomics data sets. For example, MaxQuant with the MaxLFQ algorithm (Cox et al., 2014) ,that is based on the AUC method, is now widely accepted as a quantification index in label-free proteomics experiments. Moreover, Peptide Spectrum Matches (PSMs) ,a scoring incorporated into Mascot (Perkins et al., 1999) and SEQUEST (Eng et al., 1994) search engines, is another accepted quantification index based on SC method. All of these developments facilitated the quantification of thousands of proteins in biological systems under different conditions.

1.1.3. Parallel Reaction Monitoring (PRM)

Despite the credibility of label-free quantification methods, some limitations in accuracy of quantification are accepted (Al Shweiki et al., 2017). Therefore, verification of the label-free results by orthogonal techniques such as western blotting (Xie et al., 2010) and Enzyme Linked Immunosorbent Assay (ELISA) (Piersma et al., 2010) is important, nonetheless, these approaches are limited in the number of proteins to be analyzed. Accordingly, targeted MS approaches have been developed which are more accurate and sensitive and could be used for the verification of the label-free results (Neilson et al., 2011).

Targeted proteomic approaches are based on the utilization of the MS instruments acquisition methods to select target mass to charge (m/z) ratios. In a discovery proteomics, a data dependent acquisition (DDA) scan strategy is used, where intact peptide ions with the highest intensity (Top10 or 20) are selected to be fragmented in the collision cell, and then spectra of the resulting fragments are acquired. An important method in targeted proteomics is selected reaction monitoring (SRM) (Lange et al., 2008) where the precursor ion is specifically selected at the first quadrupole mass analyzer Q1 and then fragmented in q2 followed by further isolation of a selected fragment ion in Q3 which is then recorded (Figure 1-3 A). This method was used before in small molecules analysis (Baty and Robinson, 1977), however, developments in the proteomics instrumentation transferred this method to targeted proteomics experiments (Anderson and Hunter, 2006). To overcome the pitfalls in the SRM method such as the difficulties in selection of the best fragment ions and the restricting need of triple quadruple (QqQ) instruments, parallel reaction monitoring (PRM) was developed (Figure 1-3 B) (Peterson et al., 2012). In comparison to SRM, all peptide fragment ions are recorded by the MS2 analyzer (Orbitrap or TOF), expanding the use of QqOrbi or QqTOF from discovery to targeted experiments. PRM has been established to be comparable to SRM with the advantage of higher specificity and less effort in the method development (Schiffmann et al., 2014, Ronsein et al., 2015). Moreover, it has been used for the

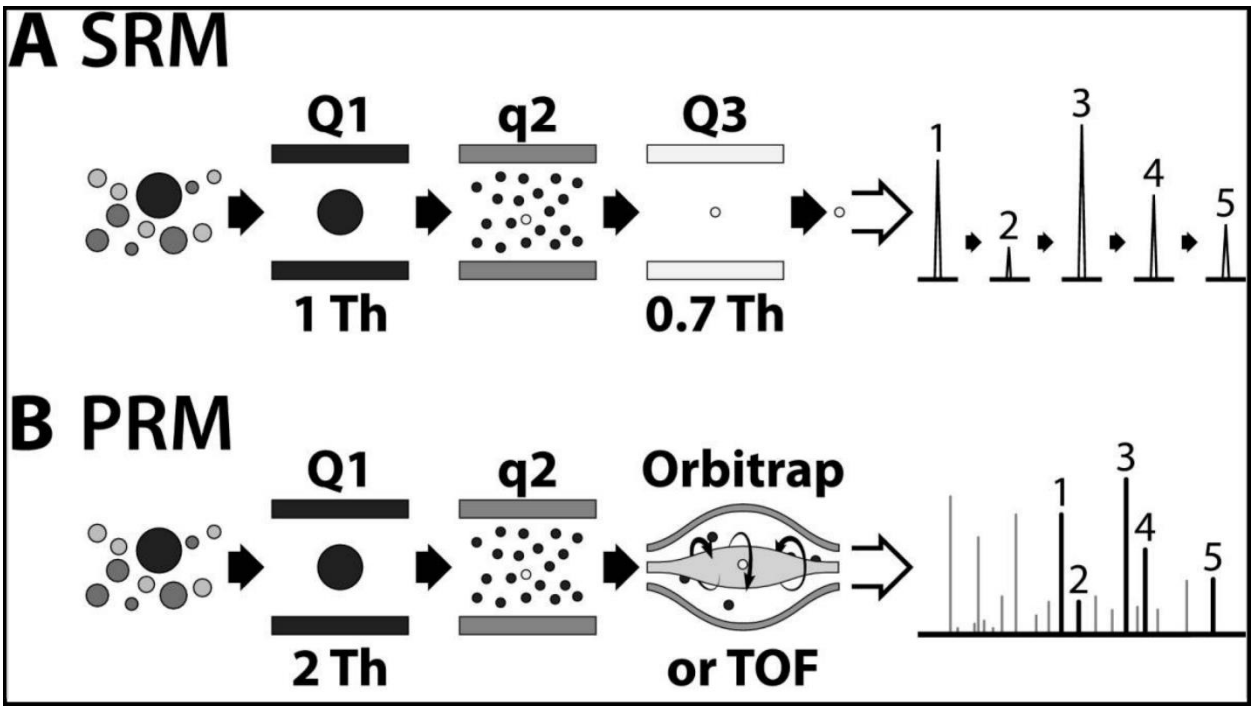

Figure 1-3. Comparison between Selected Reaction Monitoring (SRM) and Parallel Reaction Monitoring (PRM) acquisition strategies. In SRM method, the first quadruple (Q1) selects the precursor ion which is fragmented in the second quadruple (q2) and then a fragment ion is selected in the third quadruple (Q3) (A). However, in PRM method, Q3 is replaced by an orbitrap or time of flight (TOF) analyzer which records all the fragments spectra (B). Th: Thomson (mass to charge ratio). (Peterson et al., 2012)

validation of relative protein quantitation from discovery label and label-free experiments such as verifying relative abundance of ten proteins of the equine monocyte-derived macrophages infected with equine infectious anemia virus (Du et al., 2015) and relative abundance of desmin and filamin C (FLNC) in desminopathy (Maerkens et al., 2013), respectively. Targeted experiments had a limitation in the number of scans (8-10) across a chromatographic peak (Gallien and Domon, 2015). Therefore, coupling of scheduled retention time (Rt) windows of target peptides m/z throughout chromatographic elution was developed to cover hundreds of m/z in a single run (Gallien et al., 2012b, Majovsky et al., 2014).

In general, quantitation in these targeted techniques is based on the integration of the peak areas of peptide fragment ions which infers the quantities of their cognate proteins (Picotti and Aebersold, 2012). Therefore, it is important to choose peptides which are unique to the proteins to be analyzed, termed proteotypic peptides (Mallick et al., 2007). Other criteria should be considered when choosing peptides such as peptide length, modifications, precursor charge,

chromatographic peak shape and signal intensity (Rauniyar, 2015). Advances in bioinformatics and artificial intelligence contributed to the development of tools that can predict those proteotypic peptides such as deep peptide observability predictor (Zimmer et al., 2018). Moreover, analysis of the targeted LC-MS data became uncomplicated with the introduction of free powerful programs such as Skyline (MacLean et al., 2010, Pino et al., 2020).

1.2. Plant Immunity

1.2.1. Pattern Triggered Immunity (PTI)

Plants normally protect themselves from multiple biotic and abiotic stresses through physical barriers such as the cell wall (Hamann, 2012) and cuticles (Yeats and Rose, 2013). Furthermore, healthy plants constantly produce active antimicrobials such as saponins and inactive precursors such as cyanogenic glycosides and glucosinolates which are directly activated upon pathogen attack (Osbourn, 1996). Nonetheless, pathogens usually overcome these barriers thus activating the immune response. The interaction of the pattern recognition receptors (PRRs) on the plant plasma membrane with the pathogen associated molecular patterns (PAMPs) from the pathogen induces multiple responses such as stomatal closure (Melotto et al., 2008), secondary metabolites (with antimicrobial activity) production and secretion (Ahuja et al., 2012, Bednarek, 2012a) and reactive oxygen species (ROS) production (O'Brien et al., 2012), all of which are termed pattern triggered immunity (PTI). Mostly, PTI response is adequate for the plant to survive a pathogen attack, however, some pathogens have evolved to suppress the PTI by secreting effectors which interrupt the plant immune response (Chisholm et al., 2006). Accordingly, plants also developed R proteins which recognize these effectors leading to the activation of the effector triggered immunity (ETI) (Dangl and Jones, 2001). Studies of the main two parts of the inducible plant immunity (PTI and ETI) introduced the 'zig-zag' model that describes a dichotomy of PTI and ETI (Jones and Dangl, 2006). On the other hand, another model termed "Invasion model" was proposed by (Cook et al., 2015) to broaden the understanding of the plants microbes interactions.

Multiple PAMPs with their corresponding PRRs have been identified such as the 22 amino acid N terminal epitope of *Pseudomonas syringae* flagellin (flg22) and the 18 amino acid epitope of *Escherichia coli* elongation factor (EF) Tu (elf18) that interacts with flagellin-sensitive 2 (FLS2) and EF-Tu receptor (EFR), respectively (Gómez-Gómez and Boller, 2000, Zipfel et al., 2006). Once flg22 binds to FLS2, it induces the formation of a stable heteromer of FLS2 and BRI1-associated receptor kinase 1 (BAK1) and the phosphorylation of these receptors in seconds

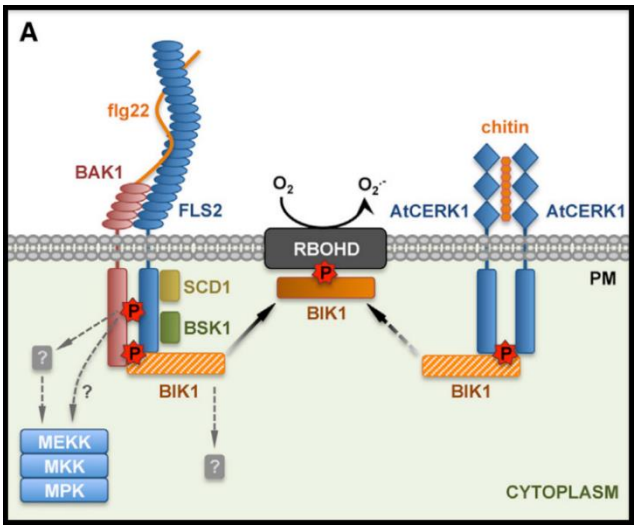

Figure 1-4. Flg22 signaling cascade by binding to FLS2. Flg22 binds to flagellin sensitive 2 (FLS2) stabilizing its heterodimerization with BRI1-associated receptor kinase 1 (BAK1) which leads to a cascade of phosphorylation leading to ROS generation and Mitogen Activated Protein Kinases (MPKs) activation. (Macho and Zipfel, 2014) (more information provided in the text).

(Chinchilla et al., 2007, Schulze et al., 2010). Furthermore, FLS2 and BAK1 phosphorylation prompts phosphorylation of receptor-like cytoplasmic kinases such as Botrytis-Induced Kinase 1 (BIK1) (Lu et al., 2010) that also phosphorylates NADPH oxidase (RBOHD) which is responsible for ROS generation in PTI (Kadota et al., 2014) (Figure 1-4). Another early response to flg22 is the Ca^{+2} burst which activates other membrane transporters and depolarization of the plasma membrane (Jeworutzki et al., 2010). It was also demonstrated that the Ca^{+2} burst is dependent on BIK1 (Li et al., 2014). Signal transduction cascades activated by flg22 affect and involve different important protein kinases. Calcium Dependent Protein Kinases (CDPKs), precisely CPK4/5/6/11, are activated as early as 5 minutes after PAMP perception and were shown to be involved in ROS generation and transcriptional reprogramming (Boudsocq et al., 2010). Moreover, two main cascades involving Mitogen Activated Protein Kinases (MPKs), MAPK kinases (MKKs) and MKK kinases (MEKKs) have been identified to be induced by flg22. The first involves MEKK1, MKK4/5 and MPK3/6 which activates WRKY22/29 transcription factors (Asai et al., 2002) and the second involves MEKK1, MKK1/2 and MPK4 which phosphorylates MPK Substrate 1 (MKS1) releasing WRKY33 transcription factor (Gao et al., 2008, Qiu et al., 2008). The effect of MPKs on these transcription factors and others important in immunity such as MYC2 (Sethi et al., 2014) and EIN3 (Yoo et al., 2008) was demonstrated in the effect of flg22 on the expression of genes of important pathways such as tryptophan, secondary metabolites and the biosynthesis and signaling of the hormones integral to immunity Jasmonic Acid (JA), Salicylic Acid (SA) and Ethylene (ET) (Denoux et al., 2008).

PTI also affects photosynthesis and carbohydrate metabolism processes in plants (Rodríguez-Moreno et al., 2008). Using chlorophyll fluorescence as an indicator of the photosynthesis activity, bacterial infection with *Pseudomonas syringae* led to a decrease of photosynthesis (Bonfig et al.,

2006, Ishiga et al., 2009). Moreover, gene expression analysis showed downregulation of photosynthesis after flg22 treatment or *Pseudomonas syringae* infection (Denoux et al., 2008, Zou et al., 2005). Previous proteomics studies also reported downregulation of the abundance of proteins involved in photosynthesis due to infection or PAMP treatment (Göhre et al., 2012, Pineda et al., 2010, Zhou et al., 2006). This was also confirmed recently, as 43 proteins were downregulated in *Arabidopsis thaliana* seedlings 16 hrs after flg22 treatment (Abukhalaf et al., 2020).

1.2.2. Jasmonic Acid (JA) biosynthesis and signaling

Hormones, mainly JA, SA and ET, are involved in the plant immune response (PTI and ETI), however, the crosstalk and interconnection of these hormone signaling pathways complicates the understanding of their individual effects. In general, it has been believed that SA and JA/ET responses are related to biotrophic or hemi-biotrophic pathogens and necrotrophic pathogens, respectively (Glazebrook, 2005). Yet, JA was found to be involved in the resistance to biotrophic pathogens too (Abukhalaf et al., 2020, Hillmer et al., 2017, Nickstadt et al., 2004).

JA Biosynthesis starts in the plastid with the conversion of α-linolenic acid (18:3) (α-LeA) to (13S)-hydroperoxyoctadecatrienoic acid (13-HPOT) by lipooxygenases (LOXs) (Feussner and Wasternack, 2002) such as LOX2 (Glauser et al., 2009). Then, the enzymes allene oxide synthase (AOS) and allene oxide cyclase (AOC) converts 13-HPOT to cis-(+)-12-oxophytodienoic acid (cis-OPDA) which is then transported to the peroxisome forming JA under the effect of OPDA reductase 3 (OPR3) and acyl-coenzyme A oxidases (ACX) such as ACX1 (Schilmiller et al., 2007, Wasternack and Hause, 2013). JA is further metabolized to the more active JA-Isoleucine (JA-Ile) by the enzyme JA conjugate synthase (JAR1) (Staswick and Tiryaki, 2004).

A breakthrough in the understanding of the JA signaling pathway was the discovery of the Jasmonate ZIM domain (JAZ) proteins which are a group of direct repressors of different immune responsive transcription factors (TFs) such as MYC2 (Chini et al., 2007). These JAZs interact with the F-Box protein Coronatine Insensitive1 Skp1/Cullin/F-box complex (SCF^{COI1}), an E3 Ubiquitin ligase, in the presence of JA or JA-Ile leading to the ubiquitinylation and further degradation of JAZs (Pauwels and Goossens, 2011). Other interaction partners in this signaling pathway have been also discovered such as the Novel Interactor of JAZ (NINJA), TOPLESS (TPL) and TPL related (TPRs) (Pauwels et al., 2010). The main result is the release of the repressed TFs and the transcriptional activation of the immune responsive genes. The TF MYC2 has been recognized as the master regulator of the JA signaling by regulating a wide range of responses in the JA pathway (Kazan and Manners, 2013).

Other JA metabolites in which JA or JA-Ile is hydroxylated or carboxylated have been identified. These include 12-hydroxy JA and JA-Ile (12-OH-JA and 12-OH-JA-Ile) and 12-carboxy JA-Ile (12-COOH-JA-Ile) which are known to be biologically inactive (Wasternack and Hause, 2013). Cytochrome P450 (CYP) B1, B3 and C1 have been recognized to be responsible for the conversion of JA-Ile to 12-OH-JA-Ile and 12-COOH-JA-Ile (Heitz et al., 2012, Koo et al., 2014). Moreover, Jasmonic Acid Oxidases (JOXs) were identified as enzymes that hydroxylate JA itself leading to the formation of the inactive 12-OH-JA (Caarls et al., 2017, Smirnova et al., 2017). This inactivation has been recognized as a direct route for turning off JA signaling thus regulating the plant immune response (Miersch et al., 2008).

1.2.3. PTI effect on Auxin transport

Auxin plays a central role in plant's growth and development (Benková et al., 2003). In order to achieve this, auxin has to be transported throughout the plant. After synthesis in the shoot apex or developing leaves, auxin is transported through vascular tissues or from cell to cell by polar auxin transport (PAT) through different transporters (Swarup and Bennett, 2003, Swarup and Péret, 2012). Different transporters have been identified such as AUXIN1/LIKE-AUX1 (AUX/LAX), PIN-FORMED (PIN), ATP-binding cassette (ABC) transporters and others (Geisler et al., 2017, Krecek et al., 2009, Péret et al., 2012). PINs are important auxin efflux carriers that regulate a range of developmental events in plants. They are a family of eight proteins which are localized in the plasma membrane (PM) or the endoplasmic reticulum (ER) depending on the size of their hydrophilic loops (HL) (Ganguly et al., 2014). PIN1, 2, 3, 4 and 7 are localized to PM while PIN5, 6 and 8 are localized to the ER (Adamowski and Friml, 2015). The direction of auxin flow is dependent on the asymmetric localization of PINs. For instance, PIN1 and 7 have been shown to play an important role in the apical -basal axis formation of *Arabidopsis* embryos (Friml et al., 2003). Moreover, PIN3 was shown to be accumulated at the lateral cell surface upon gravity stimulation, thus regulating lateral auxin transport and tropic growth (Friml et al., 2002).

In PTI, the signaling pathway of JA and SA have been shown to affect and be affected by auxin. SA causes downregulation of auxin related genes and interferes with auxin signaling (Wang et al., 2007). Moreover, auxin repressed genes of the JA biosynthesis pathway in *Arabidopsis* seedlings (Jun and Xiu-Jie, 2006). In contrast, multiple studies demonstrated a positive interaction between JA and auxin in necrotrophic pathogen resistance (Kazan and Manners, 2009). PIN transporters ,on the other hand, were downregulated 16 hrs after JA treatment (Qi et al., 2012). Also, flg22 led to mislocalization of PIN1 in *Arabidopsis* seedlings to become intracellular by the effect of MPK6 activation (Dory et al., 2018). Moreover, SA has been shown to be involved in the

activation of phosphorylation of PIN2 (Tan et al., 2020). Recently, PIN3 and 7 protein abundance was decreased 16 hrs after flg22 treatment, emphasizing their possible importance in the growth-defense trade-off (Abukhalaf et al., 2020).

1.3. Protein Turnover rates

The dynamic nature of proteins and their amino acids (AAs) have been demonstrated by Schoenheimer in rats as early as 1939 (Schoenheimer et al., 1939). One year later, the same observations were made in Tobacco (Vickery et al., 1940). Studies of protein synthesis and degradation, termed protein turnover, have been done in plants, using radiolabeling for measurement of total protein turnover (Hellebust and Bidwell, 1964, Kemp and Sutton, 1971, Trewavas, 1972). Recently, introduction of the systems biology approach and -omics techniques encouraged studies on the gene, transcript and protein level and their regulation. Systematic approaches to measure genes, transcripts and proteins were made possible with the developments in next generation sequencing (NGS) and LC-MS proteomics (Cox and Mann, 2011, Mutz et al., 2013). Moreover, regulation of transcripts such as their synthesis, degradation rates and the amount translated is becoming an important aspect (Rabani et al., 2011). Likewise, the importance of proteins synthesis and degradation rates have been demonstrated in recent studies (Cambridge et al., 2011).

Wide scale protein turnover rates measurement using LC-MS proteomics with SILAC labelling exposed the ability of this approach to measure thousands of protein synthesis and degradation rates in mammalian cells (Schwanhausser et al., 2011). Furthermore, protein turnover rates in bacteria, yeast and plant cell cultures were measured with the same approach (Gruhler et al., 2005, Jayapal et al., 2010, Pratt et al., 2002). However, it is tricky to apply the SILAC approach in intact plants due to the dynamics of amino acid metabolism, synthesis and transfer between plant tissues (Nelson et al., 2014b). To overcome this, metabolic labeling with the basic elements of AAs; Carbon (C), Nitrogen (N), Oxygen (O) and Hydrogen (H), was introduced (Chen et al., 2011, Li et al., 2012). For instance, partial ^{15}N labelling was used to measure turnover rates of up to 500 and 1228 proteins in barely and *Arabidopsis* leaves, respectively (Li et al., 2012, Li et al., 2017).

In a partial labeling experiment, plants are grown on unlabeled media and then transferred to labeled media. Plants then need some time until the labeling is incorporated in the AAs pool, this term is referred to as “Lag time” (Nelson et al., 2014a). In general, the decrease in the amount of unlabeled proteins is caused by degradation only as they existed before labeling. On the other

hand, newly synthesized proteins, which should all be labeled, are affected by synthesis and degradation. Calculations of protein turnover rates depend on the measurement of the ratio of naturally abundant proteins to the total protein population including isotopically labeled ones. This could be measured using MS and expressed as relative isotopic abundance (RIA) (Zhang et al., 2011). Due to the complexity of these mass spectrometry data, a limited number of programs are available for their analysis. Many are provided as source coded programs that might not always work as expected and further analysis and filtration of the resulting data might be needed (Lyon et al., 2014, Martin et al., 2012). Another main aspect to consider in the calculation, is the biological system status. Most mathematical models are built on the assumption that the system is in steady state; synthesis and degradation rates (K_d and K_s) are equal (Hinkson and Elias, 2011). In this status, changes in protein abundance are assumed to be caused by growth only which could be verified by an exponential growth curve of the plant in the study. Then, the growth rate should be factored into the calculations as a dilution factor (K_{dil}) as the increase in the newly synthesized proteins by growth causes a decrease in the RIA (Nelson et al., 2014b).

On the other hand, any effect on the system such as the immune response perturbs the status into a non-steady state. In this case, changes in protein abundance should be considered in the calculations of synthesis and degradation rates (Li et al., 2012). The immune response effect on transcriptional and translational regulation in plants has been demonstrated in previous studies using NGS techniques (Meteignier et al., 2017, Tabassum et al., 2020, Xu et al., 2017). However, proteomic studies measuring turnover rates in an immune response are still lacking.

1.4. Aim of the Study

Pattern Triggered Immunity (PTI) is a main part of the plant immune response that leads to the activation of multiple signaling pathways including those of major phytohormones (JA, SA, ET). Transcriptional regulation in PTI has been demonstrated previously by studies on plants treated with flg22 or other PAMPs. Our recent study characterized proteome remodeling in PTI where 1774 and 915 proteins were upregulated and downregulated, respectively, after 16 hrs 1 µM flg22 treatment (Abukhalaf et al., 2020). Furthermore, a model was presented including target proteins of several of the main enzymatic and signaling pathways in PTI.

This study aims to validate that model and use it to understand regulation on transcript, protein and hormone levels in a multi-omics approach. The main objective is to follow these processes in the early and late time transition from growth to PTI and vice versa. Using a targeted (label-free) proteomics PRM approach, qPCR and LC-MS hormone measurements in *Arabidopsis thaliana* wild type (Col-0) seedlings treated with flg22 should generate valuable data regarding the activity and interaction of relevant pathways. Moreover, comparison to *myc234* knockouts lacking an important part of the JA signaling pathway, expands our understanding of JA role in PTI.

Two main challenges are considered in this study. The first resides in the limitation in the number of quantifiable peptides in the PRM workflow. The second is in the development of a workflow that combines partial ^{15}N metabolic labeling with LC-MS measurements, to calculate protein turnover rates even in steady state shifts between growth and PTI.

2. Materials and Methods

2.1. Materials

Table 2.1 lists all chemicals, which have been used as received or further processed. Table 2.2 shows the composition of frequently used buffers and solutions. All instruments used are summarized in Table 2.3.

Table 2.1 : An overview of the chemicals used

Chemical	Supplier
2-(N-morpholino) ethane sulfonic acid (MES)	Carl Roth GmbH (Karlsruhe, Germany)
2D Quant Kit	GE Healthcare (Buckinghamshire, UK)
5x QPCR Mix EvaGreen®(Rox)	Bio&SELL GmbH (Nürnberg, Germany)
Acetic Acid	Carl Roth GmbH (Karlsruhe, Germany)
Acetone	Sigma-Aldrich Laborchemikalien GmbH (Seelze, Germany)
Acetonitrile	Honeywell (Seelze, Germany)
Ammonium Acetate	Carl Roth GmbH (Karlsruhe, Germany)
Ammonium Bicarbonate	Carl Roth GmbH (Karlsruhe, Germany)
Ammonium Nitrate	Carl Roth GmbH (Karlsruhe, Germany)
Ammonium Nitrate-$^{15}N_2$	Sigma-Aldrich Chemie GmbH (Steinheim, Germany)
Calcium Chloride Dihydrate	Merck (Darmstadt, Germany)
Chromabond® HR-XC sorbent	Macherey-Nagel (Duren, Germany)
DEAE-Sephadex A-25	Cytiva (Massachusetts, USA)

Dithiothreitol (DTT)	SERVA Electrophoresis GmbH (Heidelberg, Germany)
DNase I, RNase-free	Thermo Fisher Scientific Baltics UAB (Vilnius, Lithuania)
Ethanol	J.T.Baker (Arnhem, Netherlands)
Ethylenediaminetetraacetic Acid (EDTA) Dihydrate	Sigma-Aldrich Chemie GmbH (Steinheim, Germany)
Flg22 peptide-1 mg	GenScript (Leiden, Netherlands)
Formic Acid	Merck (Darmstadt, Germany)
Hydrochloric Acid	Carl Roth GmbH (Karlsruhe, Germany)
Iodoacetamide (IAA)	SERVA Electrophoresis GmbH (Heidelberg, Germany)
Magnesium Sulfate-Heptahydrate	Merck (Darmstadt, Germany)
Methanol	Carl Roth GmbH (Karlsruhe, Germany)
Murashige & Skoog Medium (MS Medium) Including Vitamins and MES buffer	Duchefa Biochemie (Haarlem, Netherlands)
Murashige and Skoog Basal Salt Micronutrient Solution	Sigma-Aldrich Chemie GmbH (Steinheim, Germany)
Murashige and Skoog Vitamin Solution 1000x	Sigma-Aldrich Chemie GmbH (Steinheim, Germany)
Potassium Dihydrogen Phosphate	Merck (Darmstadt, Germany)
Potassium Hydroxide	Carl Roth GmbH (Karlsruhe, Germany)
Potassium Nitrate	Merck (Darmstadt, Germany)

Potassium Nitrate-^{15}N	Sigma-Aldrich Chemie GmbH (Steinheim, Germany)
Protease Inhibitor cocktail for plants	Sigma-Aldrich Laborchemikalien GmbH (Seelze, Germany)
RevertAid First Strand cDNA Synthesis Kit	Thermo Fisher Scientific Baltics UAB (Vilnius, Lithuania)
rLys-C	Promega
Sodium Hydroxide	Merck (Darmstadt, Germany)
Sucrose	Sigma-Aldrich Laborchemikalien GmbH (Seelze, Germany)
SV Total RNA Isolation System	Promega Corporation (Madison, USA)
Trifluoroacetic Acid (TFA)	Merck (Darmstadt, Germany)
Tris Base	Carl Roth GmbH (Karlsruhe, Germany)
Trypsin	Promega
Urea	SERVA Electrophoresis GmbH (Heidelberg, Germany)
Water (LC-MS Ultra CHROMASOLV^{TM})	Honeywell (Seelze, Germany)

Table 2.2 : Buffers and solutions composition

Buffer and solution	Chemical composition
25% MS medium (1 L)	1.226 g MS Medium Including Vitamins and MES buffer, 0.375 g MES buffer, 2.5 g Sucrose (pH 5.7)
25% MS medium (1 L) (Only in Protein turnover experiments)	0.748 mM $CaCl_2$, 0.313 mM KH_2PO_4, 0.375 mM $MgSO_4$, 4.7 mM KNO_3 (475 mg), 5.15 mM NH_4NO_3 (413 mg), 2.35 mM MES buffer, 0.25x Basal Salt Micronutrients solution, 0.25x Vitamin solution (pH 5.7)
25% MS medium ^{15}N (1 L) (Only in Protein turnover experiments)	0.748 mM $CaCl_2$, 0.313 mM KH_2PO_4, 0.375 mM $MgSO_4$, 4.7 mM $K^{15}NO_3$ (480 mg), 5.15 mM $^{15}NH4^{15}NO_3$ (423 mg), 2.35 mM MES buffer, 0.25x Basal Salt Micronutrients solution, 0.25x Vitamin solution (pH 5.7)
2-D Quant kit	Color reagent A, Color reagent B, Co-Precipitant, Precipitant, Copper solution, Bovine Serum Albumin (BSA) standard solution (2 mg/mL)
Alkylating solution (UAI)	50 mM Tris Base, 8 M Urea, 50 mM IAA (pH 8.0)

Digestion solution (ABC)	50 mM NH_4HCO_3 (pH 8.0)
Extraction Buffer (EB)	50 mM Tris base, 10 mM EDTA, 10 mM DTT, 4% SDS, 1.5% Protease inhibitor cocktail for plants (pH 8.0)
Reducing solution (UAD)	50 mM Tris Base, 8 M Urea, 100 mM DTT (pH 8.0)
RevertAid First Strand cDNA Synthesis Kit	5x buffer, 100µM Oligo(dT)18 Primer, 10 mM dNTPs, RiboLock 20 U/µL, RevertAid Reverse Transcriptase 200 U/µL
SV Total RNA Isolation System	RNA Lysis buffer, RNA dilution buffer, RNA Wash solution, DNase I enzyme, $MnCl_2$ 0.09M, Beta-Mercaptoethanol 97.4%, Yellow core buffer, DNase stop solution, Nuclease-free water
Urea Solution (UA)	50 mM Tris Base, 8 M Urea (pH 8.0)

Table 2.3 : An overview of the equipment used

Instrument Name	Model	Supplier
Amicon® Ultra – 0.5mL 30K	UFC503096	Merck Millipore Ltd. (Carrigtwohill, Ireland)
Analytical balance	CPA64	Sartorius AG (Göttingen, Germany)
Avanti J-26XP in JS-5.3	J-26XP	Beckman coulter, USA
Centrifuge	5415D	Eppendorf GmbH (Hamburg, Germany)
	5810R	
Chromabond® Multi 96-Monoblock ,96x0.5 mL, leer	738651	Macherey-Nagel (Duren, Germany)
EASY-nLC 1000 Liquid Chromatograph	LC120	Thermo Fisher Scientific Inc. (Massachusetts, USA)
Erlenmeyer flasks 250 mL, wide neck	82.2.1055.3	Duran GmbH (Mainz, Germany)
Flatbed shaker	HS 250	IKA-Werke GmbH & Co. KG (Staufen, Germany)
Laboklav	25	SHP Steriltechnik AG (Germany)
Magnetic stirrer	Reo	IKA-Werke GmbH & Co. KG (Staufen, Germany)
MX3005P qPCR System	MX3005P	Agilent Technologies, Inc. (California, USA)
NanoDrop™ 8000 Spectrophotometer	8000	Thermo Fisher Scientific Inc. (Massachusetts, USA)

pH meter	Seveneasy	Mettler-Toledo AG (Switzerland)
Q Exactive™ Plus Hybrid Quadrupole-Orbitrap™ Mass Spectrometer	Q Exactive™ Plus	Thermo Fisher Scientific Inc. (Massachusetts, USA)
Rotational Vacuum Concentrators	AVC2-25CD plus	Martin Christ Gefriertrocknungsanlagen GmbH (Harz, Germany)
Savant Speed Vac Concentrator	SC210 A	Thermo Fisher Scientific Inc. (Massachusetts, USA)
Spectrophotometer	DU 800	Beckman coulter, USA
Spin tip adaptors	#sp-990-8	Protea Biosciences (West Virginia, USA)
Stainless Steel Beads, 5 mm	69989	QIAGEN (Hilden, Germany)
Thermomixer C	5328	Eppendorf AG (Hamburg, Germany)
Ultrasonicator bath	Sponorex super (RK 106)	Bandelin electronic (Berlin, Germany)
Vortex	Genie 2	Bender & Hobein (Zurich, Switzerland)

2.2. Methods

2.2.1. Preparation of seedling cultures to study flg22 effects

Each flask was filled with 50 mL 25% MS medium and then 250 seeds of *Arabidopsis thaliana* Col-0 or *myc234* were added to each flask. The flasks were covered and then were left on a shaker at 45 rpm in a chamber under long day conditions (16 hrs light and 8 hrs dark) and at 22°C. After 10 days, seedlings representing 0 hrs were taken and flg22 was added to a final concentration of 1 µM in medium to the rest of the flasks and replaced on the shaker. Samples were taken at 1 hrs, 3 hrs and 16 hrs after flg22 addition and then the rest of the seedlings were transferred to new flasks with fresh 50 mL 25% MS media. Afterwards, samples were taken at 1 hrs, 3 hrs and 16 hrs after the transfer (17, 19 and 32 hrs). Four and three independent seedling cultures were collected at each time point in Col-0 and *myc234*, respectively. The seedlings were kept frozen at -80°C after harvest.

2.2.2. Preparation of seedling cultures to the study the effect of media exchange

Same procedure was used as above but instead of adding flg22, autoclaved water was added and seedlings were taken at time points 0, 16, 17 and 19 hrs.

2.2.3. ^{15}N metabolic labeling of seedling cultures

Each flask was filled with 50 mL 25% MS media and then 250 seeds of *Arabidopsis thaliana* Col-0 were added to each flask. The flasks were covered and then were left on a shaker at 45 rpm in a chamber under long day conditions (16 hrs light and 8 hrs dark) and at 22°C. After 10 days, seedlings representing 0 hrs were taken and the rest were treated differently depending on the experiment.

Under normal conditions, the rest of the seedlings were transferred to 25% MS media ^{15}N and samples were taken at 8, 9, 10, 12, 24, 36, 48, 72 and 96 hrs after media exchange. Three independent seedling cultures were collected at each time point, weighed and kept frozen at -80°C.

Under flg22 effect, the rest of the seedlings were transferred to 25% MS media ^{15}N and after 8 hrs of media exchange seedlings representing 0 hrs flg22 were taken. flg22 was added to a final concentration of 1 µM in medium to the rest of the flasks and samples were taken at 2, 4, 6, 8, 16, 24, 32, 48, 72 and 96 hrs after flg22 addition. Three independent seedling cultures were collected at each time point weighed and kept frozen at -80°C.

2.2.4. Extraction of proteins

Seedling were ground in liquid nitrogen. 1 mL EB was added to 500 mg of ground tissue and vortexed for 30 secs and then kept in a thermomixer at 600 rpm at 95°C for 10 min. Samples were vortexed again for 30 secs and then returned to a thermomixer at 600 rpm at 22°C for 20 min. The extracts were centrifuged 16,000 g for 10 min at 10°C. The supernatants were transferred to new tubes and again centrifuged at 20,000 g for 30 min at 10°C. The supernatants were retained and protein concentration was determined by 2D-Quant.

2.2.5. Determination of protein concentration (2D-Quant kit)

Bovine serum albumin (BSA) standards of 0, 10, 20, 30, 40, 50 µg of BSA were prepared, 5 µL of protein extracts were pipetted into 2 mL Eppendorf tubes. Then, 500 µL of precipitant were added and then mixed. 500 µL of co-precipitant were added and then mixed. The samples were centrifuged at 10,000 g for 5 min at Room Temperature (RT). Then, the supernatants were discarded and proteins left to dry for 5 min. 100 µL of the copper solution and 400 µL of ddH_2O were added to each sample and then mixed. 1 mL of Working color solution (300 µL Color Reagent B with 30 mL Color Reagent A) were added to each sample and then mixed. The reaction was allowed to proceed for 15 min. Then, the absorbance was measured at 480 nm with ddH_2O as a blank.

2.2.6. Filter Assisted Sample Preparation (FASP)

Our procedure was developed based on previously published protocols (Song et al., 2018, Su et al., 2018, Wisniewski et al., 2009). Amicon® Ultra 30K filters were kept in 5% Tween-20 shaking overnight at 60 rpm. Filters were washed with ddH_2O by shaking at 60 rpm for 30 minutes, this was repeated twice. Filter units were assembled and 100 µg of proteins in solution were volume adjusted to 200 µL with UA and then added to each filter. Then the filter units were centrifuged at 16,100 g for 10 min at RT, the flow throughs were discarded. The filter units were washed with 200 µL UA three times by centrifugation at 16,100 g for 10 min at RT, the flow throughs were discarded. 100 µL of UAD were added to each sample and incubated in a thermomixer at 600 rpm for 1 hrs at 22°C, then samples were centrifuged at 16,100 g for 10 min at RT, the flow throughs were discarded. 100 µL of UAI were added, samples were mixed in a thermomixer at 600 rpm for 1 hrs at 22°C in the dark and centrifuged at 16,100 g for 10 min at RT, the flow throughs were discarded. After that, filter units were washed three times with 200 µL UA by centrifugation at 16,100 g for 10 min at RT, the flow throughs were discarded. 100 µL of ABC were added to each sample and then centrifuged at 16,100 g for 10 min at RT, this was repeated

twice. Then 50 µL of ABC with 10 µL Lys-C (0.05 µg/µL) were added to filter units and samples were incubated in a thermomixer at 600 rpm for 4 hrs at 37°C. Afterwards, 10 µL (0.2 µg/µL) Trypsin were added to each sample and then kept in thermomixer overnight at 600 rpm at 37°C. Filters were transferred to new collection tubes and then centrifuged at 16,100 g for 10 min at RT, the flow throughs were kept. 40 µL ABC were added to each filter and then centrifuged again at 16,100 g for 10 min at RT, the flow throughs were kept, this step was repeated once. Then samples were dried in a vacuum concentrator. Digested peptides were desalted afterwards.

2.2.7. STAGE-Tip C18 peptide desalting (Stop-and-Go Extraction)

Dried digested protein samples were dissolved in 200 µL 0.1% formic acid (FA). STAGE-Tips were produced in-house by packing six layers of compacted C18 matrix into 100 µl pipette tips. STAGE-Tips were inserted into 2 mL Eppendorf tubes and conditioned with 100 µL 80% acetonitrile (ACN), 0.1% FA and centrifuged at 1,500 g for 2 min at RT. The flow-throughs were discarded. Tips were equilibrated two times with 100 µL 0.1% FA with subsequent centrifugation at 1,500 g for 2 min at RT. The flow throughs were discarded. 100 µL of proteins in solution were applied to STAGE-Tips and centrifuged at 1,500 g for 2 min at RT then flow-throughs were discarded. This step was repeated once. The STAGE-Tips were washed twice with 100 µL 0.1 % FA and centrifuged as before. The flow-throughs were discarded. STAGE-Tips were inserted into new 1.5 mL Eppendorf tubes and elution was done by adding 50 µL of 80% ACN, 0.1% FA followed by centrifugation at 1500 g for 1 min at RT. The eluates were retained. Another 50 µL 80% ACN, 0.1% FA were added and centrifuged as before to elute all remaining peptides. The peptides were dried in a vacuum concentrator.

2.2.8. Flg22 extraction from media

1 mL media samples were taken at time points 0, 1, 16, 17 and 19 hrs. Amicon® Ultra 30K filters were kept in 5% Tween-20 shaking overnight at 60 rpm. Filters were washed with ddH_2O by shaking at 60 rpm for 30 minutes, this was repeated twice. 300 µL of the media sample were added to the filter and then centrifuged at 16,100 g for 10 min at RT. The filtrates were kept and dried in a vacuum concentrator and the resulting dried samples were desalted on STAGE-Tips C18. The final dried peptide samples were dissolved in 136 µL 5% ACN, 0.1% TFA to reach a final concentration of 2.2 µM flg22 for LC-MS analysis.

2.2.9. LC-MS for protein analysis

Proteotyipc peptides for target proteins were selected by first measuring the sample using a conventional data dependent acquisition (DDA) scan strategy. The up to three identified peptides

with the highest number of peptide spectral matches (PSMs) unique to target proteins (mapping exclusively to target protein master protein groups in Proteome Discoverer™ v 2.1 (Thermo Fisher Scientific) with unique (m/z) were used to populate a peptide target list for parallel reaction monitoring (PRM) analysis of all 99 target proteins. Target proteins lacking three proteotypic peptides at this stage were subjected to d::pPop (Zimmer et al., 2018) analysis for in silico determination of proteotypic peptides with favorable ESI response and corresponding m/z. Samples were then analyzed with a targeted data dependent acquisition (TDA) scan strategy targeting *in silico* determined m/z followed by non-retention time (Rt) scheduled parallel reaction monitoring (PRM) of any remaining m/z not leading to proteotypic peptide identification in the earlier two MS measurements (DDA and TDA). The results from the three iterative MS scan strategies allowed construction of a PRM target list that contained at least one measured proteotypic peptide m/z for every target protein plus corresponding Rts for Rt scheduling. A Rt window of +/- 7 min was placed around measured Rts for retention time scheduling of the XX peptides in quantitative PRM analysis.

Dried peptides were dissolved in 5% acetonitrile, 0.1% trifluoroacetic acid, and injected into an EASY-nLC 1000 liquid chromatography system. Peptides were separated using liquid chromatography C18 reverse phase chemistry employing a 180 min gradient increasing from 5% to 40% acetonitrile in 0.1% FA, and a flow rate of 250 nL/min. Eluted peptides were electrosprayed on-line into a Q Exactive™ Plus mass spectrometer. The spray voltage was 1.9 kV, the capillary temperature 275°C and the Z-Lens voltage 240 V. A full MS survey scan was carried out with chromatographic peak width set to 15 s, resolution 35,000, automatic gain control (AGC) 1E+06 and a max injection time (IT) of 100 ms. The full scan was followed by Rt scheduled PRM scanning without multiplexing with HCD fragmentation. MS/MS scans were acquired with resolution 17,500, AGC 2E+05, IT 100 ms, loop count 10, isolation width 1.6 m/z, isolation offset 0.5 and a normalized collision energy 27.

Peptides and proteins were identified using the Mascot software v 2.5.0 (Matrix Science) (Perkins et al., 1999) linked to Proteome Discoverer™ v 2.1. The enzyme was set to trypsin. A precursor ion mass error of 5 ppm and a fragment ion mass error of 0.02 Da were tolerated in searches of the TAIR10 database amended with common contaminants (35934 sequences, 14486974 residues). Carbamidomethylation of cysteine was set as a fixed modification and oxidation of methionine (M) tolerated as a variable modification. A PSM, peptide and protein level false discovery rate (FDR) was calculated for all identified spectra and peptides and proteins based on

the target-decoy database model. The significance threshold α was set at 0.01 to accept PSM, peptide and protein identifications.

2.2.10. LC-MS for flg22 Analysis

Dried peptides were dissolved in 5% acetonitrile, 0.1% trifluoroacetic acid, and injected into an EASY-nLC 1000 liquid chromatography system. Peptides were separated using liquid chromatography C18 reverse phase chemistry employing a 60 min gradient increasing from 5% to 40% acetonitrile in 0.1% FA, and a flow rate of 250 nL/min. Eluted peptides were electrosprayed on-line into a Q Exactive™ Plus mass spectrometer. The spray voltage was 1.9 kV, the capillary temperature 275°C and the Z-Lens voltage 240 V. A full MS survey scan (DDA top10) was carried out with chromatographic peak width set to 15 s, resolution 70,000, automatic gain control (AGC) 3E+06 and a max injection time (IT) of 100 ms. MS/MS scans were acquired with resolution 17,500, AGC 5E+04, IT 50 ms, loop count 10, isolation width 1.6 m/z, isolation offset 0.0 and a normalized collision energy 28.

Flg22 peptides were identified using the Mascot software v 2.5.0 (Matrix Science) linked to Proteome Discoverer™ v2.1. The enzyme was set to none. A precursor ion mass error of 5 ppm and a fragment ion mass error of 0.02 Da were tolerated in searches of the flg22 sequence as a database. Oxidation of methionine (M) tolerated as a variable modification. A PSM, peptide and protein level false discovery rate (FDR) was calculated for all identified spectra and peptides and proteins based on the target-decoy database model. The significance threshold α was set at 0.01 to accept PSM, peptide and protein identifications.

2.2.11. PRM data Analysis

Quantitative analysis of PRM data was done with the Skyline software v 19.1.0 (MacLean et al., 2010). A spectral library was created using the DDA, TDA and PRM measurements described above. All target protein primary structures were concatenated in a FASTA file and imported. Raw PRM data was imported with the following “Transition Settings”: Filter tab: “Precursor charges” were set to 2,3, “Ion charges” were set to 1,2 and “Ion types” were set to y, b, p, “Product ion selection” was set from m/z > precursor to 6 ions. Library tab: “Pick” was set to 6 product ions. Instrument tab: “Method match tolerance m/z” kept at a default of 0.055. Full-Scan tab: “Isotope peaks included” set to Count, “precursor mass analyzer” set to Orbitrap, “Peaks” set to 3, “Resolving power” set to 30,000 at 400 m/z. Under MS/MS filtering, the “Acquisition method” was set to Targeted, “product mass analyzer” set to Orbitrap, “resolving power” set to 17,500 at 400

m/z. In retention time filtering, “Include all matching scans” was selected. The sum of six picked product ion signal peak areas was extracted as (Protein Quantification Index) PQI.

The matrix of target peptide PQI values in all measured samples was analyzed in excel (2019). PQI values were normalized (later termed PQI also) by multiplication with an intensity factor for each sample (equation 1):

$$\text{Intesity Factor (IF)} = \frac{MMax\ I_{all}}{Max\ I_s} \text{----------}(1)$$

Where MMax I_{all} is the highest maximum MS1 intensity in all samples and Max I_s is the maximum MS1 intensity of the sample.

PQI values of technical replicates were averaged for each biological replicate then $\log_2(x)$ transformed, and grouped by conditions (0, 1, 3, 16, 17, 19, 32 hrs). A probability-based student t-test was used to assess the significance of changes in peptide abundance between each condition and 0 hrs using a significance value of 5% (p-value < 0.05). For each peptide, its mean untransformed PQI in the two replicate sample measurements was used as an estimate of its abundance and used to calculate fold changes of abundance for each of the four or three samples per condition (i.e., flg22 1 hrs/Control (0 hrs), flg22 3 hrs/Control,…). Peptide fold changes were $\log_2(x)$ transformed and median peptide fold changes for each protein were used to infer fold changes in protein abundance in the four or three samples per condition, respectively. Median protein $\log_2(x)$ and standard deviation for each condition were used to show the results. Protein fold changes were considered significant if at least one of the peptides used for inference showed a statistically significant change in PQI between the conditions as determined above.

2.2.12. Protein turnover rates Analysis (K_s and K_d)

To analyze the raw MS data, “protover” a python-based code program was used which measure the relative isotopic abundance (RIA) of ^{15}N in peptides (Lyon et al., 2014) (eq.2). Raw data were converted to (.MzML) format using msconvert (Chambers et al., 2012). A list of proteotypic peptides with their average retention times from PRM experiments were used as an input file for the program. A retention time windows of 5 min was used in the filters and “RIA increasing” filter was disabled. Results were then analyzed using excel (2019) which contained peptides and their RIA at different time points. Peptides were filtered to contain at least five-time points RIA values in at least one biological replicate. Then the median RIA of peptides for each protein were used to infer RIA of that protein in the three samples per time point.

$$RIA = \frac{15N}{15N + 14N} \text{----------(2)}$$

Where 15N represent heavy isotope population and 14N are the naturally abundant population.

Control experiment

In the control experiment, the apparent degradation rate (K_{loss}) was calculated for each protein from the slope of plotted -ln(1-RIA) over time as in equation 3:

$$K_{loss} * t = -\ln(1 - RIA) \text{----------(3)}$$

Where t is time in days.

Then proteins were filtered by K_{loss} of a relative standard error (RSTDE) of less than or equal to 40% and R^2 median of 0.5. between replicates, and proteins with negative K_{loss} values were discarded. Moreover, to calculate the degradation rate constant (K_d) equation 4 was used:

$$K_d = K_{loss} - K_{dil} \text{----------(4)}$$

Where K_{dil} is the doubling constant.

K_{dil} was calculated by fitting an exponential model to the increase of the weights of the seedling through time as proxy for the increase of total protein amount over time as in equation 5:

$$A_t = A_0 * e^{K_{dil}*t} \text{----------(5)}$$

Where A_t is the total amount of proteins at time (t) and A_0 is the proteins amount at time (0).

To calculate the synthesis rate constant (K_s/A), equation 6 (Li et al., 2017) was used:

$$\frac{K_s}{A} = \frac{FCP - e^{-K_d*t}}{1 - e^{-K_d*t}} * K_d \text{----------(6)}$$

Where FCP is Fold Change Protein.

By reorganizing eq.5 FCP can be calculated as follows:

$$FCP = \frac{A_t}{A_0} = e^{K_{db}*t}$$

And by substituting this in eq.6, then (K_s/A) can be calculated as in equation 7:

$$\frac{K_s}{A} = \frac{e^{K_{dil}*t} - e^{-K_d*t}}{1 - e^{-K_d*t}} * K_d \text{----------(7)}$$

A mean time of 2 days was used to calculate K_s/A for all filtered proteins (later as K_s).

Flg22 experiment

This experiment was divided into two phases: non-steady state and steady state. The non-steady state was considered in the earlier time points 0, 2, 4, 6, 8 and 16 hrs after flg22 treatment. To calculate the Kd, the slope of plotting -ln (FCP*(1-RIA)) equation 8 was used:

$$K_d * t = -\ln(FCP * (1 - RIA))\text{----------}(8)$$

However, FCP here was calculated by fitting a polynomial second order model to the PRM data using median FCP at time points 0, 1, 3 and 16 hrs. Only proteins with FCPs of 1.5 or more **or** 0.75 or less at any of the time points 1, 3 or 16 hrs were considered in the non-steady state calculations. A calculated FCP derived from the model fits for the time points 2, 4, 6, 8 and 16 hrs was used to calculate K_d (Supplementary Table 10/ p.105). Calculated FCPs were considered the same at all biological replicates. Proteins with an RIA value in a minimum of 4 time points in at least one biological replicate were considered for K_d calculations. Afterwards, proteins were filtered by RSTDE of K_d of less than or equal to 40% and a median R^2 of 0.5. In the steady state situation, the same method as the one in the control experiment was used and time points 0, 8, 16, 24, 32, 48, 72 and 96 hrs after flg22 were used in the K_{loss} and K_{dil} calculations. Moreover, K_s in the two phases steady state and non-steady state was calculated using eq.7 and eq.6, respectively.

2.2.13. RNA extraction

All materials used were from SV Total RNA Isolation System (Promega) and protocol provided based on (Kobs, 1998). 30 mg of ground plant tissue was dissolved in 175 µL of the RNA Lysis buffer, then 350 µL RNA dilution buffer was added and the solution mixed by inversion 10 times and then centrifuged at 16,100 g for 10 min at RT. 200 µL of 95% Ethanol were added to the supernatant and mixed for 3-4 times by pipetting, then the mixture was transferred to the spin column assembly. The assembly was centrifuged at 13,000 g for 1 min at RT, then the filtrate was discarded and 600 µL of RNA Wash Solution were added to the spin column and centrifuged again at 13,000 g for 1 min at RT. Meanwhile, DNase incubation mix was prepared freshly by mixing 40 µL yellow buffer, 5 µL $MnCl_2$ and 5 µL DNase I enzyme for each sample. Then, the filtrate was discarded and 50 µL of DNase incubation mix was added to the spin column with incubation at 22° C for 15 minutes. 200 µL of DNase stop solution were added to the column and then centrifuged at 13,000 g for 1 min at RT. 600 µL RNA wash solution were added to the column and centrifuged again at 13,000 g for 1 min at RT. The filtrate was discarded and 250 µL RNA wash solution were added to the column and the assembly centrifuged at 16,100 g for 2 min at

RT. Afterwards, the spin column was transferred to the elution tubes provided and 100 µL of Nuclease-free water added then the assembly centrifuged at 13,000 g for 1 min at RT. The filters were discarded and the filtrate containing RNA was kept on ice to measure its concentration. NanoDrop™ 8000 Spectrophotometer (Thermo Fischer) was used to check the absorbance at 260 nm, 280 nm and 230 nm (A260, A280 and A230, respectively). 1 unit of A260 equals 40 µg of RNA. The A260/ A280 and A260 / A230 ratios were used to assess the purity of the RNA. Then extracted RNA was stored at -80° C.

2.2.14. cDNA synthesis

To make sure again that there is no DNA contamination a DNase step was done first. 1 µL of DNase I, RNase-free (1 U/µL) (Thermo Fisher) with 1 µL 10 x buffer was added to 500 ng RNA and autoclaved ddH_2O to a final volume of 10 µL. This solution was incubated for 30 min at 37° C, then 1 µL 25 mM EDTA pH 8 was added and incubated for 10 min at 65° C to stop the enzyme.

All materials further used were from Revert Aid First Strand cDNA Synthesis Kit (Thermo Fisher). A sufficient amount of the mastermix containing per sample (4 µL 5x buffer, 1 µL 100 µM Oligo(dT)18 Primer, 2 µl 10 mM dNTPs, 1 µL RiboLock 20 U/µL, 1 µL RevertAid Reverse Transcriptase 200 U/µL) was prepared. Then, 9 µL of mastermix were added to each 11 µL from the previous step and incubated in a PCR machine: 5 min 37° C, 60 min 42° C, 10 min 70° C. The resulting cDNA 20 µL was then diluted with 200 µL Nuclease-free water and stored at -20° C.

2.2.15. qPCR preparation and analysis

5x QPCR Mix EvaGreen®(Rox) (Bio & Sell) was diluted to 2x with an autoclaved ddH_2O. Then an amount needed of the mastermix containing per reaction (0.18 µL Forward primer (100 pmol/µL), 0.18 µL Reverse primer (100 pmol/µL), 10 µL 2x QPCR Mix EvaGreen®(Rox) and 6.64 µL autoclaved ddH_2O) was prepared. In each well 3 µL diluted cDNA from the synthesis step was mixed with 17 µL mastermix. Two technical replicates were prepared for each biological replicate. qPCR analysis was done using MX3005P qPCR System. Each run was done with a thermal profile of 15 min initial incubation at 95° C then 40 cycles each composed of: 15 secs denaturation at 95°C then 40 secs annealing and elongation at 65°C then collecting fluorescence. Disassociation curves for the primers were performed to control the primer efficacy. Data analysis was done using MxPro v 4.1 and the results were exported and further analyzed by excel (2019). UBC21 (AT5G25760) and PP2A (AT1G13320) were used as internal standards and relative

quantification using ΔCq method (Schmittgen and Livak, 2008) relative to the mean of (UBC21 and PP2A) was done (later termed as relative expression).

2.2.16. Sample preparation for hormone analysis

To measure the absolute amounts of the hormones an internal standard mixture containing per sample 2 ng of ABA-D6, 5 ng IAA-D5, 5 ng JA-D2, 0,75 ng JA-Ile-D2, 30 ng OPDA-D5, 45 ng ACC-D4, and 0.75 ng SA-D4 as internal standards was prepared.

One 5 mm steel bead was added to each sample of 95-100 mg of ground plant tissue in 2 mL Eppendorf tubes. Tissue homogenization in 2x bead beater at 25 /s for 50 secs at -80° C was done (temperatures were maintained by using porcelain tube holders pre-cooled in liquid N_2). 200 µL MeOH containing the standard mixture described above was added to the plant tissue then vortexed on a vortex platform for 20 min. Samples were centrifuged at 10,000 g for 5 min at RT, then supernatants were transferred to new tubes and centrifuged again at 10,000 g for 5 min at RT. Supernatants were kept at -80°C for the next day.

Chromabond® Multi 96 plate with 50 mg/well Chromabond® HR-XC sorbent was conditioned with 1 mL MeOH in each well and then centrifuged at 500 g in Avanti J-26XP in JS-5.3 Swing out rotor centrifuge for 5 min at 4°C. The eluate was discarded and plate was equilibrated with 1 mL ddH_2O in each well then centrifuged as before. Meanwhile, 1 mL 2% Acetic Acid (in water) were added to each extracted sample and mixed. Afterwards, eluate was discarded and samples were loaded on the plate 2 times each with a max loading of 1 mL sample and centrifuging as before. Eluate was discarded and the plate was washed with 1 mL ddH_2O and centrifuged as before. The plate was transferred to a new 96 deep well block and contents eluted with 1 mL MeOH and centrifugation as before. The eluate was kept at 4°C for the next step.

DEAE Sephadex plates were prepared by adding 400 µL DEAE-Sephadex (Acetate form in MeOH, 50 mg) in each well of an SPE 96 plate and filter on top. The plate was centrifuged at 500 g for 5 min at 4°C. Eluate was discarded and the eluate from the previous step was added to each well and then centrifuged as before. Eluate was discarded and the plate was washed with 1 mL MeOH and centrifuged as before. The plate was transferred into a new 96 deep well block and the metabolites eluted using 1 mL 3 M Acetic Acid in MeOH.

Eluates were transferred to 2 mL Eppendorf tubes and the solvent was evaporated in Savant SC210 A Speed Vac Concentrator at 45°C for 1 hour. 40 µL 20% MeOH in water were added to each tube and after 3 min 40 µL ddH_2O were added. After 3 min samples were centrifuged at

10,000 g for 10 min at RT. Supernatants were transferred to CHROMABOND Multi 96-Monoblock, 96x0,5 mL, then analyzed by LC-MS as in (Ziegler et al., 2014).

3. Results

3.1. Proteome Remodeling Under Pattern Triggered Immunity (PTI)

As it was reported before (Abukhalaf et al., 2020), a deep proteomics approach showed that proteins related to important immune response pathways including: Tryptophan, Auxin, Jasmonic Acid (JA), Salicylic Acid (SA), Ethylene (ET) and plant defense compounds biosynthesis, JA signaling, JA metabolism, photosynthesis and primary metabolism responded to treatment with the PTI elicitor flg22. Furthermore, targeted proteomics experiments 16 hrs post flg22 treatment, using retention time scheduled Parallel Reaction Monitoring (PRM) of 224 proteotypic peptides representing 99 of the proteins in these various pathways (Supplementary Table 1/ p.89) complemented the deep proteomics data by accurately quantifying proteins. Retention time scheduling coupled to PRM in the liquid chromatography-mass spectrometry (LC-MS) experiment was used to overcome the restrictions to the number of targets imposed by the limited number of scans (8-10) an MS analyzer can perform at a chromatographic peak with a reasonable duty cycle duration of around 1 second. This allowed coverage of a large number of peptides targeted in a

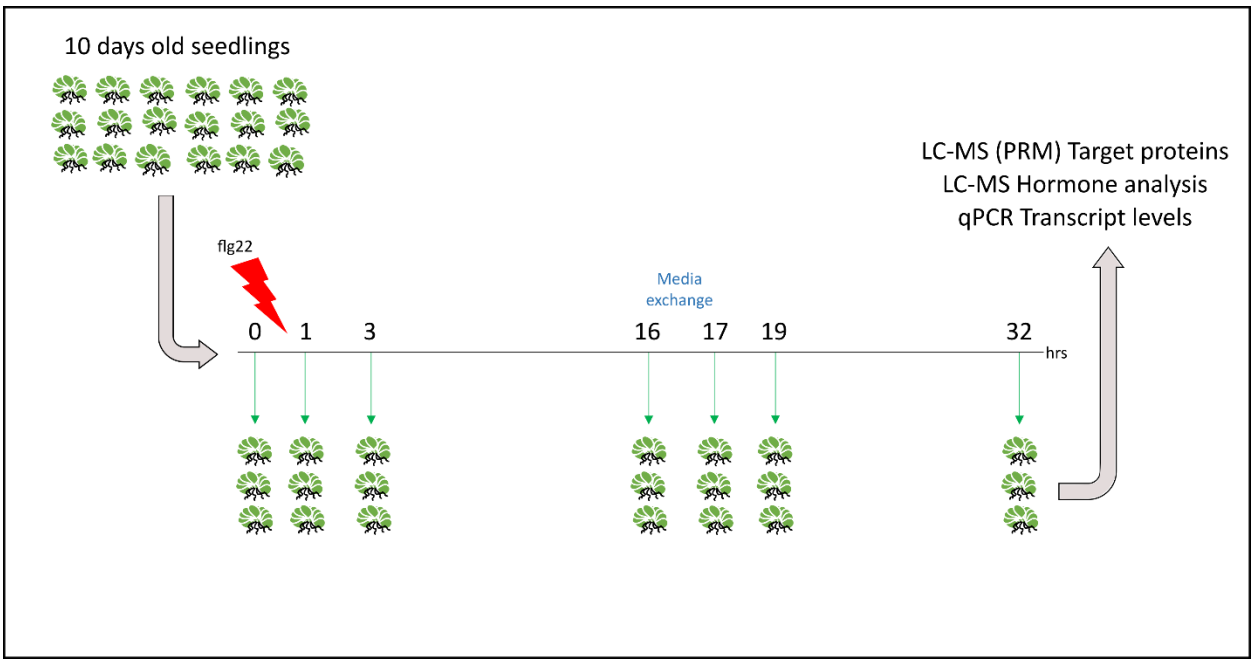

Figure 3-1. Experimental Design. 10 days old *Arabidopsis thaliana* (Col-0 or *myc234*) seedlings were grown in a liquid culture and samples were taken at 0 hrs and 1, 3 and 16 hrs after flg22 was added to a concentration of 1 µM in medium. Subsequently, seedlings were transferred to fresh media and samples were taken 1, 3 and 16 hrs (17,19 and 32 hrs) after media change. Multi-omics approach was used to analyze target proteins, target transcripts and hormone levels.

single LC-MS run. As in the deep proteomics experiment, all of the 99 targeted proteins showed a change in their abundance to some extent under the effect of flg22 (PTI). However, this only models the steady state effect of fully induced PTI 16 hrs after exposure to flg22. Thus, an experiment was designed to determine the effect of flg22 on the target proteins in earlier non-steady state situations and to study the transitions from growth to PTI and vice versa (Figure 3-1).

Arabidopsis thaliana Col-0 were grown in liquid medium for 10 days and then tissue samples were taken. This represents a control time point of 0 hrs. Subsequently flg22 was added to all the remaining seedling cultures and samples were taken at 1 and 3 hrs post exposure, representing the early response to flg22 (PTI). Another sample was taken after 16 hrs of flg22 treatment taken to represent fully induced steady state PTI. Afterwards, the rest of the seedlings were moved to fresh media and samples were taken 1 and 3 hrs (17 and 19 hrs from the start) representing the early response to a return to growth after PTI. The last samples were taken at 16 hrs after media exchange (32 hrs from the start) which should represent steady state growth and would be expected to be comparable to the control. Proteins and phytohormones as well as cognate transcripts of a selected sub-set of the targets were extracted from sampled tissue and analyzed using a multi-omics approach.

3.2. Validation of the Experimental Design

Several aspects of the experiment required control at different points. Firstly, flg22 was added to the media at the start of the experiment at time point 0 hrs and its effect was studied at 1,3 and 16 hrs after culture inoculation in which time the peptide may have been degraded and so not be seen at the later time points. Moreover, residual amounts of flg22 should not be found in the fresh media after the media exchange. Secondly, transfer of the seedlings to new media may lead to physical stress responses that might affect our interpretation of the data. These two main points were studied further.

3.2.1. Flg22 analysis in the media

Samples were taken from media in which seedlings were grown at time points 0, 1, 16, 17 and 19 hrs and were analyzed by LC-MS to check for the presence of flg22. Mean peptide spectral matches (PSMs) were used as a proxy for the amount of the flg22 and its degradation products (Figure 3-2). As expected, there was no flg22 in the media at 0, 17 and 19 hrs (Figure 3-2). On the other hand, flg22 was found at 1 and 16 hrs along with a variety of truncated species. After 1 hrs these ranged in size from the full length peptide of 22 AAs (comprising 9.4% of flg22 species in the sample) to a minimum size of 10 AAs (comprising 8.1%). Different sizes with a loss of a C

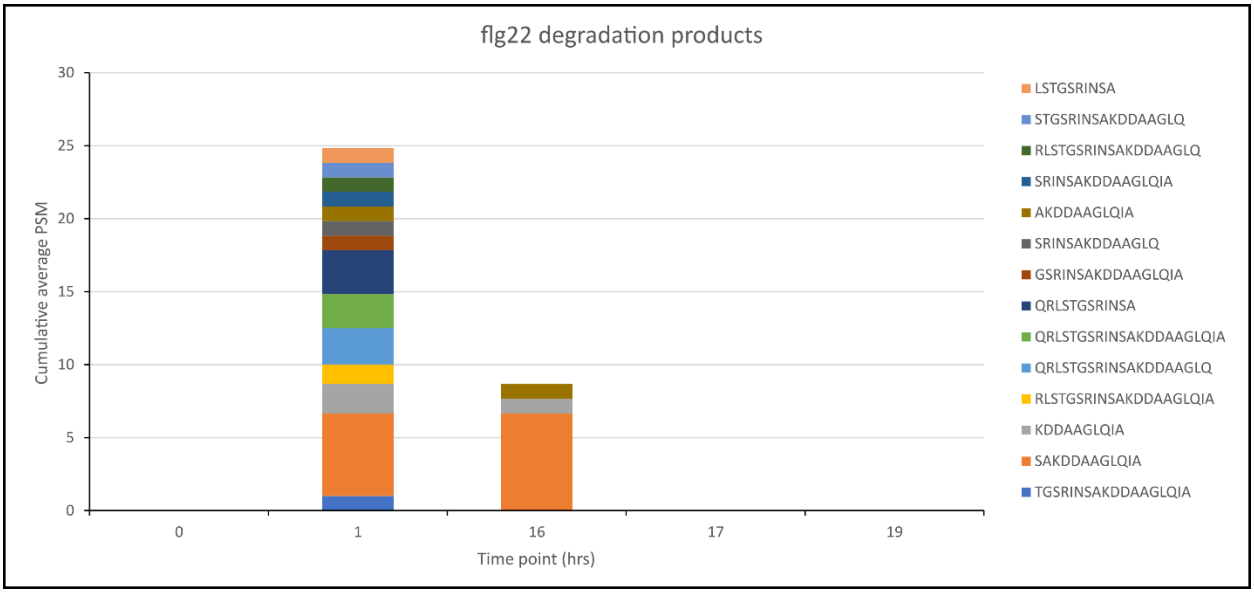

Figure 3-2. Flg22 degradation products. Full length flg22 was degraded as early as 1 hrs. After 16 hrs the C-terminal 12 amino acids (SAKDDAAGLQIA) of flg22 represented 77.9% of peptide species. After the media exchange (17 and 19 hrs) no residual parts of the peptides were measured. The y-axis represents the cumulative average peptide spectral matches (PSMs) (n=3).

terminus or an N terminus or both were found. The most abundant was (SAKDDAAGLQIA) which is a 12 AAs C terminal flg22 degradation product comprising 22.8% and 77.9% at 1 and 16 hrs, respectively. This suggests that flg22 is degraded rapidly in regard to the duration of the experiment, however, smaller sizes of the peptides are known to be active (Meindl et al., 2000) .

3.2.2. Effects of media exchange on target proteins

To discover any effects of physically moving the seedlings to fresh media, a mock experiment based on the original design (Figure 3-1) was conducted. However, instead of flg22 water was added and samples were taken at 0, 16, 17 and 19 hrs. Only targeted protein analysis (PRM) was performed. Data analysis was done on perseus v 1.6.6.0 (Tyanova et al., 2016) where protein quantification indexes (PQIs) were $\log_2$ and then Z-score transformed. The Z-scored data was then heirarchaly clustered on rows and columns based on pearson and spearman correlations, respectively (Figure 3-3). Both row and column cluster patterns were random without any discernible relationship to sampling time indicating protein abundance did not change significantly across the time points (Figure 3-3 A). One of the two main clusters contained 92 proteins in which protein levels were not changing in relation to time points (Figure 3-3 B). Also, time points after change of media (17 and 19 hrs) were not separated from 16 hrs or even 0 hrs. In addition to this,

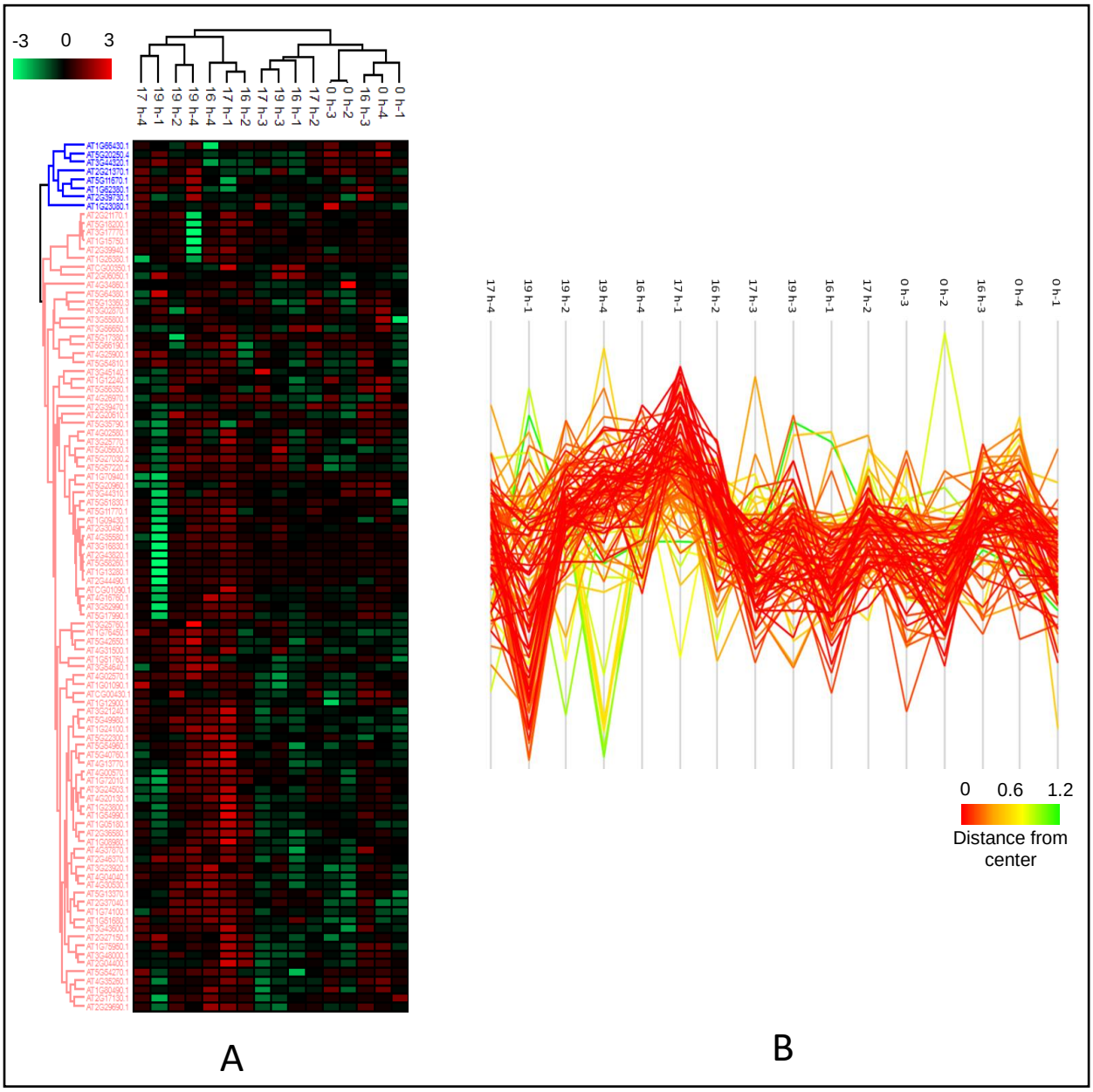

Figure 3-3. Hierarchal clustering of the target proteins under the effect of media exchange. Log_2 and Z-score transformed protein quantification index (PQI) values were hierarchaly clustered using pearson and spearman correlation for row and column dendrograms, respectively (A). A major cluster consisting of 92 proteins, presented a random pattern in relation to time points (B).

log_2 protein fold changes in respect to 0 hrs (FCP) were calculated and then were statistically tested by one sample T-test (FDR multiples testing corrected α=0.01) where the null hypotheis (H_0) is no change between all time points (log_2 FCP of zero) (Supplementary Table 2/ p.96). All of the proteins did not show significant differences except for PAL1 which increased to around

2.5 fold after 16 hrs and then remained stable even after the change of media. All of this proves that the media switch did not affect protein expression of our targets thus validating the experimental design. Furthermore, as the samples were taken at different time points during the day, stability of protein abundances insures that circadian rhythm had no effect on our targets.

3.3. Studying the PTI Response

3.3.1. Response in *Arabidopsis thaliana* Col-0

Target proteins (99) were quantified at all the time points (Supplementary Table 3/ p.97), in addition to transcript levels of 34 of them and an extra 4 that could not be measured using the PRM approach. These were Cytochrome P450 family 94 subfamily B polypeptides 1 and 3 (CYP94B1 and CYP94B3), Cytochrome P450 family 94 subfamily C polypeptide 1 (CYP94C1) and Isochorismate Synthase 1 (ICS1) (Supplementary Table 5/ p.101). Moreover, phytohormones which have important functions in defense and growth were quantified including Abscisic Acid (ABA), Indole-3-Acetic Acid (IAA), JA, JA-Isoleucine (JA-Ile), 12-hydroxy-JA (12-OH-JA), (+)-12-Oxo-Phytodienoic Acid (OPDA) and Salicylic Acid (SA) (Supplementary Table 7/ p.103).

Early response in the production of the defense compounds was detected in our experiment. The effect of the flg22 was remarkably observed on pathways like tryptophan, glucosinolate and phenylpropanoid biosynthesis on both protein and transcript levels as early as 1 hrs after flg22 treatment (Figure 3-4). Proteins in the tryptophan biosynthesis pathway such as PAT1, IGPS, TSA1 and TSB1 increased gradually reaching a significant FCP as early as 3 hrs (except PAT1) and a maximum significant FCP at 16 hrs of 3.2, 2.7, 3.4 and 5.4, respectively. A different trend was detected on the transcript level where the effect was greater and more notable at earlier time points of 1 and 3 hrs. The mean relative expression for PAT1, TSA1 and TSB1 increased to 21, 64 and 20 fold at 3 hrs, respectively. On the other hand, it decreased to 3, 5 and 1 fold at 16 hrs, respectively. Proteins in the glucosinolate biosynthesis pathway followed the same trend as in tryptophan biosynthesis, with FCPs ranging from 1.5 to 16 at 16 hrs and maximum relative transcript expression of 68 fold for SOT16 as early as 1 hrs (Figure 3-4). The same held true for the phenylpropanoids biosynthesis pathway. In general, it was quite evident, that the accumulation of transcripts precedes the accumulation of proteins in the response to the PTI elicitor. So, it appeared that the transcript levels increased at early time points leading to the subsequent increase in the abundance of proteins, that needed time to be synthesized, reaching their highest levels at the 16 hrs sampling point.

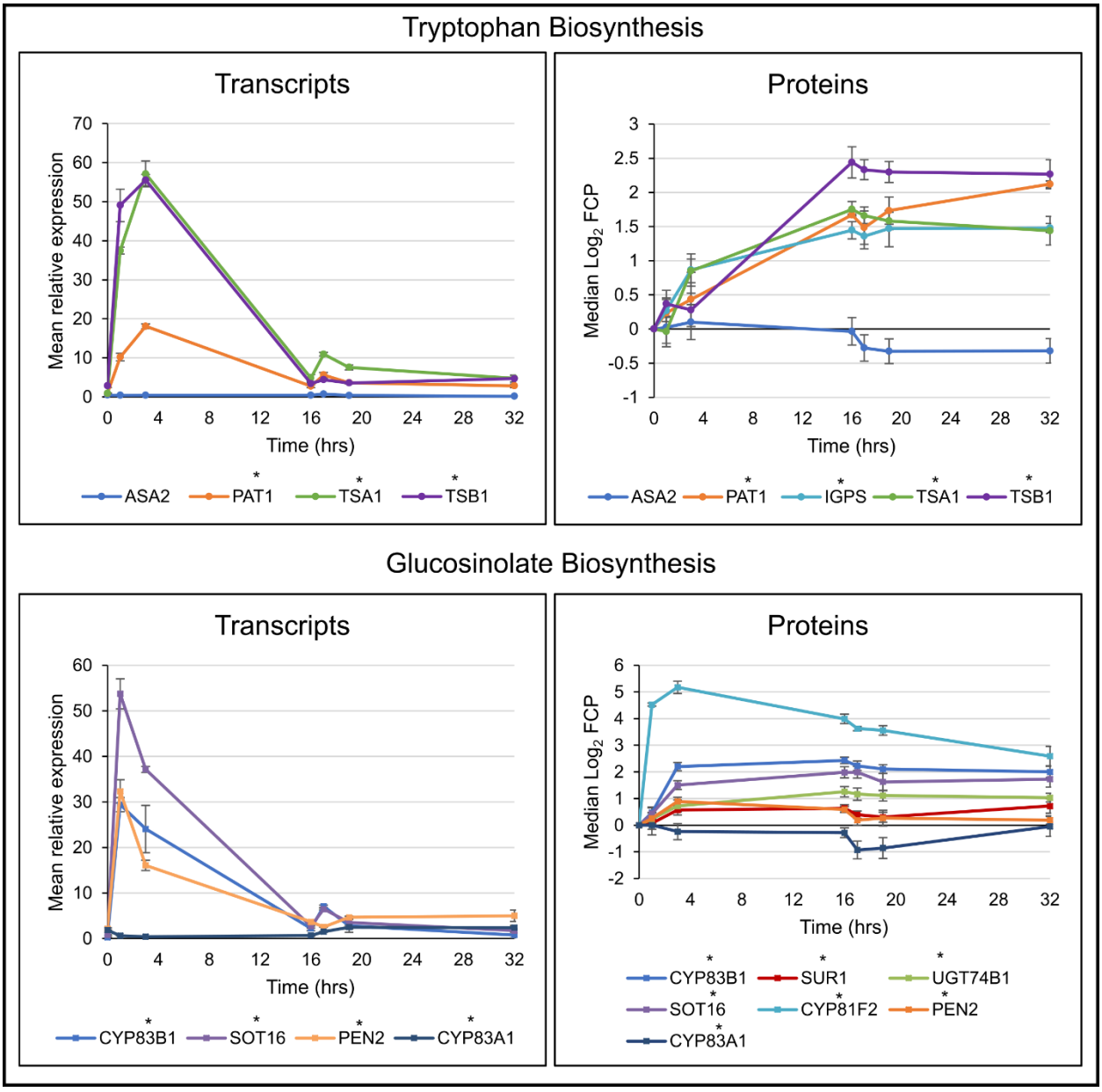

Figure 3-4: Flg22 effect on the transcript and protein levels of glucosinolate and tryptophan biosynthesis in *Arabidopsis thaliana* Col-0. The transcripts in the tryptophan and glucosinolate biosynthesis pathways were at their highest after 3 and 1 hrs, respectively. On the protein level the trend was different where most proteins increased to highest levels at 16 hrs. For transcripts mean relative expression (n=3) to the mean of PP2A and UBC21 are shown. For proteins median $\log_2$ fold changes (FCP) (to 0 hrs) (n=4) are plotted. Error bars represent standard error. Asterisks (*) represent statistically significant changes at 1, 3 or 16 hrs in respect to 0 hrs (two-tailed t-test, $\alpha = 0.05$).

Contrary to expectations, protein levels did not return to basal levels (0 hrs) after 32 hrs which again resembled steady state growth. For some proteins like CYP81F2, abundance decreased by 62% from 16 hrs till 32 hrs. For the most however the decrease in abundance was less pronounced with an average of 15% which was not significant compared to the 16 hrs sampling point. On the other hand, a significant increase in abundance of around 20% at 32 hrs in regard to 16 hrs was observed for proteins like PAT1, SUR1 and C4H. On the transcript level, the trend was different as most transcripts already decreased at 16 hrs post elicitation, however, they were still significantly higher than at 0 hrs. Also, at 32 hrs transcripts returned to normal levels (0 hrs) or did not change as for PAT1 and TSA1. This implies again that transcripts alone cannot be used as a functional reference of gene expression in non-steady state situations. Moreover, proteins in these pathways did not decrease even after the removal of the elicitor, indicating constant production of defense compounds and priming of the immune response.

One of the most important hormones in PTI is JA (Figure 3-5). Transcripts of the JA biosynthesis pathway were significantly upregulated at the early time point of 1 hrs to 11, 7 and 3 fold for AOC1, OPR3 and ACX1, respectively. This was reflected later at 16 hrs in protein abundance with a significant FCP of 1.6 and 1.5 for OPR3 and ACX1 and a non-significant FCP of 1.7 for AOC1. Other proteins like LOX2, AOS, AOC2 and AOC4 did not show significant changes in their abundance. However, JA levels increased significantly to 5.5 ng/g at 3 hrs and remained the same (5 ng/g) until 16 hrs. OPDA, a JA precursor, significantly increased in abundance as early as 1 hrs to 950 ng/g and remained at this level until 16 hrs (1096 ng/g) (Supplementary Table 7/ p.103). After media exchange, OPR3, AOC1 and ACX1 transcripts decreased reaching basal levels at 32 hrs for the first two. Nonetheless, protein levels did not significantly change after 16 hrs, remaining elevated throughout the recovery phase up until 32 hrs. Interestingly, LOX2 transcripts increased significantly (in relation to 16 hrs) after the media exchange to a maximum of 7 fold at 32 hrs and this was echoed in a significant upregulation of protein abundance at 32 hrs (in relation to 16 hrs). JA and OPDA levels did not change significantly after 16 hrs and remained in the same range until 32 hrs.

To further study JA related pathways, proteins playing roles in JA conjugation and metabolism were targeted (Figure 3-5). JAR1 protein and transcript levels did not change over the whole time of the experiment. JA-Ile levels increased to a maximum of 1 ng/g at 3 hrs and then decreased to generally non-significant levels afterwards. JOX2 and IAR3 transcripts significantly increased as early as 1 hrs to 11 and 15 fold, then decreased to 9 and 2 folds at 16 hrs, respectively. On the protein level, IAR3 reached a significant FCP of 1.4 after 16 hrs and remained at the same level

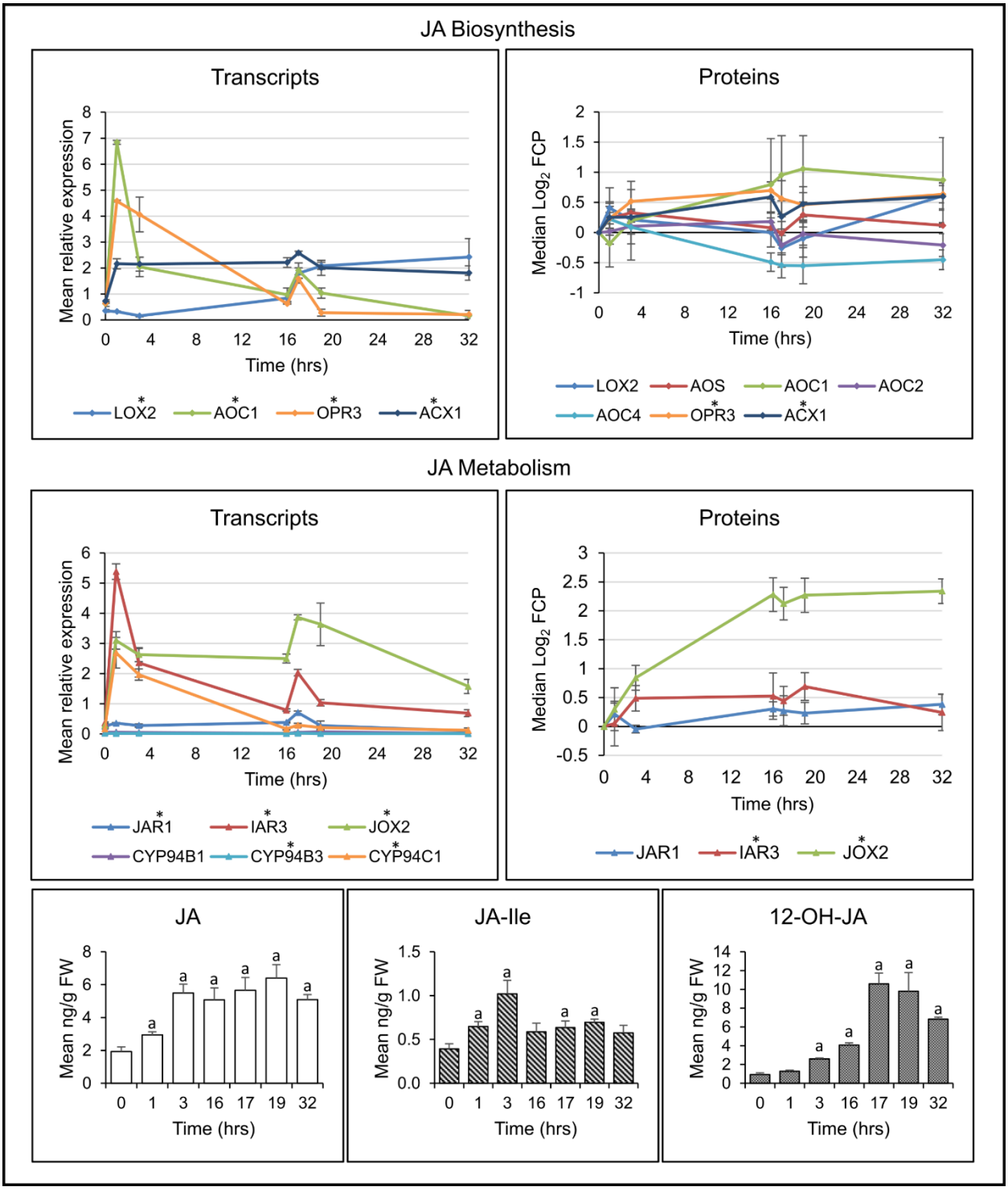

Figure 3-5: Flg22 effect on jasmonic acid (JA) biosynthesis and metabolism in *Arabidopsis thaliana* Col-0 (description on the next page)

Figure 3-5: The early increase in the abundance of transcripts and proteins of the JA biosynthesis pathway led to an increase in JA levels as early as 1 hrs. The active compound JA-Ile followed the same trend, however, the two of them did not increase after 3 hrs. On the other hand, the inactive 12-OH-JA increased continuously as JOX2 and IAR3 protein levels remained high throughout the experiment. Mean relative expression (n=3) to the mean of PP2A and UBC21 for transcripts, median log_2 fold change (FCP) (to 0 hrs) (n=4) for proteins and mean ng/g fresh weight (FW) (n=4) for hormones are plotted. Error bars represent standard error. Asterisks (*) and (a) represent statistically significant changes at 1, 3 or 16 hrs to 0 hrs and at each time point to 0 hrs, respectively (two-tailed t-test, $\alpha = 0.05$).

with a significant 1.2 FCP (to 0 hrs) at 32 hrs. JOX2 was significantly upregulated at 3 hrs with an FCP of 1.8 and reached 4.9 FCP at 16 hrs, however, after the media exchange it did not change up until 32 hrs (5 FCP). Other enzymes in JA metabolism pathways such as CYP94B1, B3 and C1 were not quantified on the protein level but their transcripts were quantified. CYP94B1 and B3 did not show any significant change, however, CYP94C1 increased significantly to 16 and 11 fold at 1 and 3 hrs, respectively. One of the main products of these metabolic pathways is the inactive 12-OH-JA which gradually increased reaching statistically significant levels of 2.6 ng/g at 3 hrs and 4.1 ng/g at 16 hrs. After the media exchange its amount increased further to 10.6 ng/g and remained high even at 32 hrs (6.8 ng/g), which was significant when compared to both 0 and 16 hrs time points. This was expected as JOX2 and IAR3 remained high after 16 hrs leading to production of more 12-OH-JA. All of this points to the importance of these two enzymes in the regulation of JA metabolism.

The growth regulating hormone auxin (IAA) decreased significantly by 30% at 16 hrs and did not increase after the media exchange with no significant difference in IAA levels at 32 hrs (as opposed to 16 hrs). Proteins in IAA biosynthesis pathways did not change in their abundance throughout the whole experiment except for AAO1 which reached a significant 2.6 FCP at 16 hrs and decreased to 1.8 FCP at 32 hrs. AAO1 transcript levels also followed the same trend with 3 fold at 16 hrs and 2 at 32 hrs. Furthermore, proteins involved in Auxin/JA signaling pathways did not seem to be affected by flg22. However, auxin efflux transporters PIN3 and PIN7 were significantly downregulated up until 16 hrs reaching 0.5 and 0.4 FCP. Their abundance increased significantly after media exchange reaching 0.7 and 0.6 FCP at 32 hrs, respectively (Figure 3-6). Likewise, PIN7 transcripts levels decreased significantly as early as 1 hrs to 0.2 fold and decreased further to 0.1 fold at 16 hrs. Thereafter, levels increased significantly (relative to 16

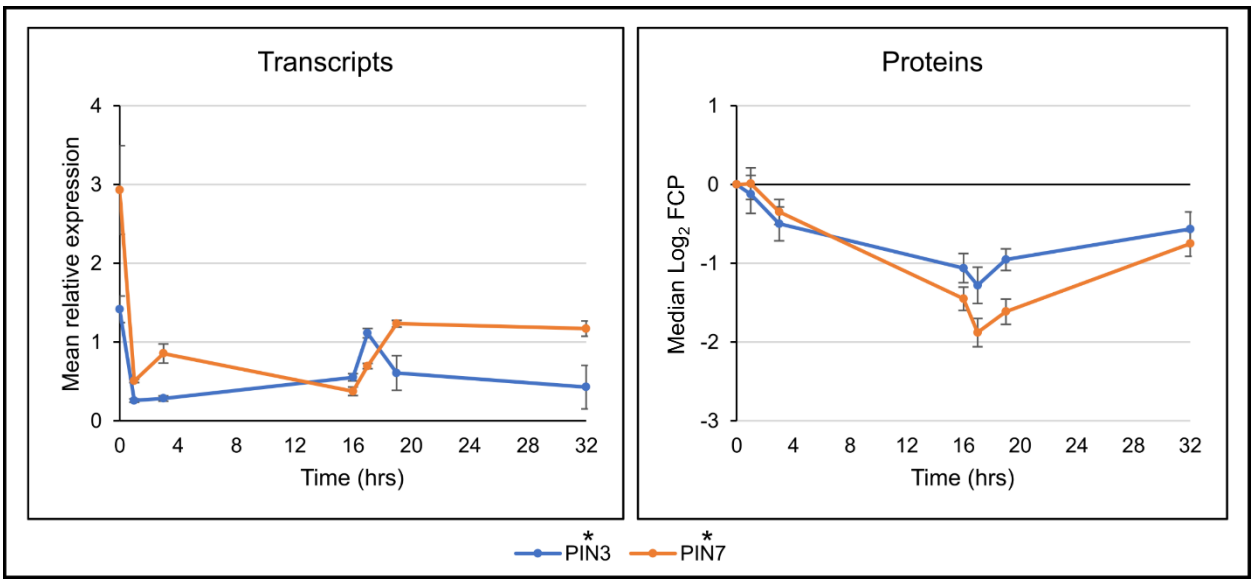

Figure 3-6: Flg22 effect on the auxin efflux transporters PIN3 and 7 in *Arabidopsis thaliana* Col-0. Transcript and protein levels of these PINs decreased as early as 1 hrs and 3 hrs, respectively. The protein levels recovered after the media exchange nearly reaching basal levels after 32 hrs. Mean relative expression (n=3) to the mean of PP2A and UBC21 is plotted for transcripts. Median log_2 fold change (FCP) (to 0 hrs) (n=4) is plotted for proteins. Error bars represent standard error. Asterisks (*) represent statistically significant change at 1, 3 or 16 hrs in respect to 0 hrs (two-tailed t-test, $\alpha = 0.05$).

hrs) to 0.4 fold at 32 hrs. Furthermore, PIN3 transcripts decreased to a significant 0.2 fold at 1 hrs and increased to 0.4 fold at 16 hrs but did not change significantly afterwards. Repeatedly, transcripts and cognate proteins levels were not directly correlated even in targets whose abundance decreased over time. Moreover, these proteins increased immediately after the removal of the elicitor, suggesting an important role in the transition to growth.

Another important hormone in PTI is SA (Figure 3-7). To produce SA, Isochorismate is produced in the plastid by ICS1 and then transported to the cytosol to become SA (Ding and Ding, 2020). In our study, ICS1 was not detected by MS, however, its transcripts were quantified. Transcripts increased to a significantly high level of 22 fold at 3 hrs and remained high at 16 hrs declining in the recovery phase to basal levels at 32 hrs. Transcriptional activators of ICS1, NTL9 and TCP22, were quantified on the protein level but their abundance did not change significantly throughout the experiment. The UDP-glucosyltransferase (UGT74F2), which glycosylates SA to inactive SAG or SGE, significantly increased 1.5 fold at 16 hrs remaining at this level up until 32 hrs. On the other hand, its transcripts initially dropped significantly at 1 and 3 hrs and then increased to a

peak level of 7 fold at 16 hrs to decrease gradually again to 3 fold at 32 hrs. SA hormone levels increased significantly at 3 hrs to 116 ng/g and continued to reach a maximum of 157 ng/g at 16 hrs, dropping abruptly to 104 ng/g at 17 hrs to rise again to 141 ng/g at 32 hrs (not significant to 16 hrs).

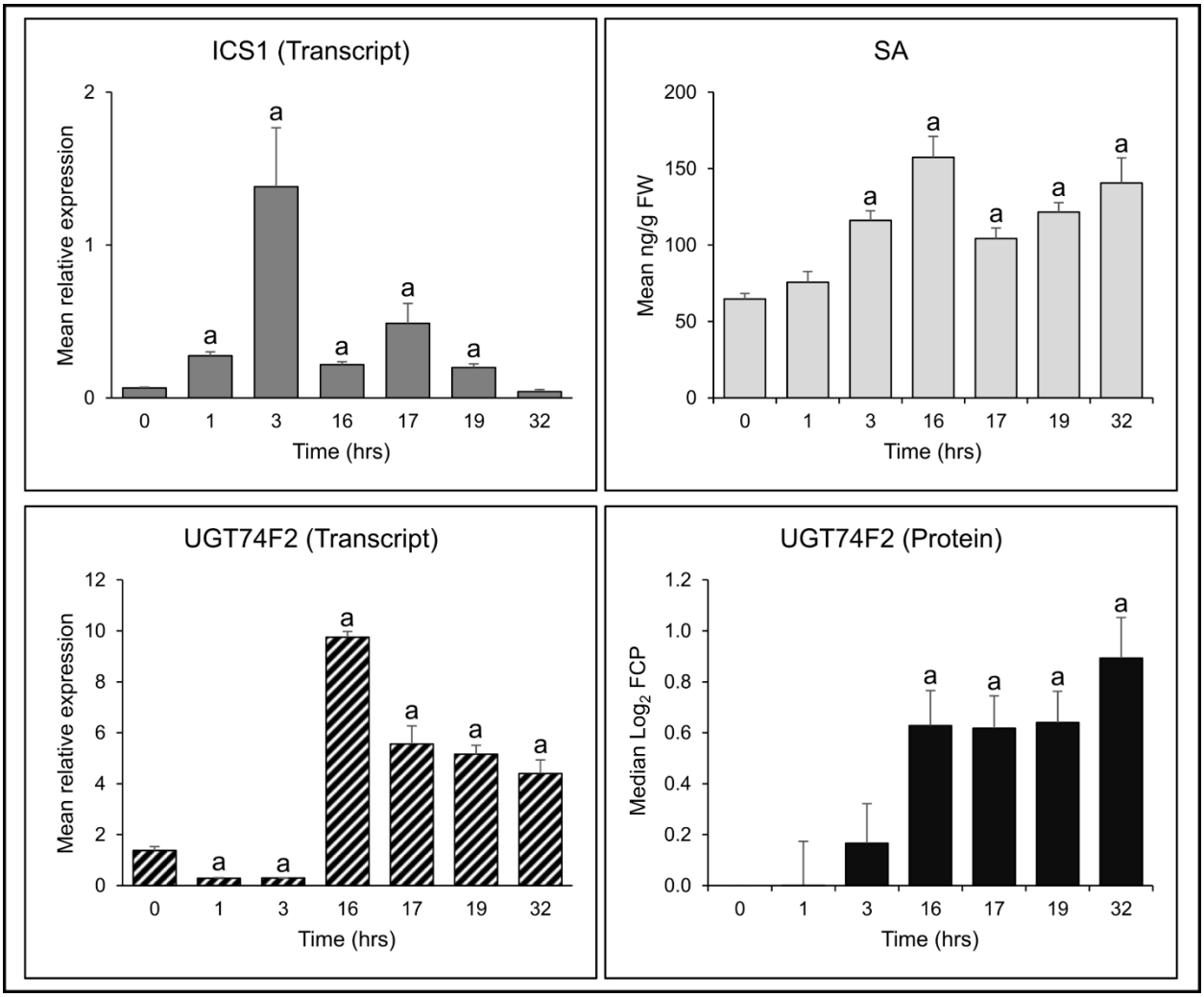

Figure 3-7: Flg22 effect on salicylic acid (SA) biosynthesis and metabolism in *Arabidopsis thaliana* Col-0. Isochorismate synthase 1 (ICS1) transcripts increased as early as 1 hrs leading to an increase of SA at 3 hrs and to a higher level at 16 hrs. UDP-glucosyltransferase (UGT74F2) increased after 16 hrs on both the transcript and protein levels to inactivate SA as SA levels remained high up until 32 hrs. Mean relative expression (n=3) to the mean of PP2A and UBC21 for transcripts, median log_2 fold change (FCP) (to 0 hrs) (n=4) for proteins and mean ng/g fresh weight (FW) (n=4) for hormones are plotted. Error bars represent standard error. (a) indicates a statistically significant change at each time point to 0 hrs (two-tailed t-test, $\alpha = 0.05$).

An important protein in the biosynthesis of ET, which also acts in the PTI response, is ACO2. ACO2 did not change significantly on the protein level, however, transcript levels increased significantly to 3.4 fold at 16 hrs and decreased (significant to 16 hrs) to 1.7 fold at 32 hrs. Another indicator of the biosynthesis of ET, NIT4, which plays a role in cyanide detoxification that is released from the oxidation step of ACC by ACO2 (Piotrowski et al., 2001), increased strongly on the protein level to a maximum FCP of 49 at 16 hrs and then declined to 28 FCP (significant to 16 hrs) at 32 hrs. Moreover, its transcript level increased significantly, reaching a high of 204 fold at 3 hrs and decreasing to 7 fold at 32 hrs.

Proteins involved in photosynthesis were also targeted and demonstrated interesting results. The abundance of a large number of proteins, 43 in all, playing integral roles in various photosynthesis reactions was shown to decrease 16 hrs after flg22 exposure (Abukhalaf et al., 2020). Twenty-three of these proteins were targeted in the experiments described here, 8 of them assigned to the photosynthesis light reaction by MapMan (PS.light reaction)). Proteins which were significantly changing after flg22 treatment (1,3 or 16 hrs) (Figure 3-8) were found to decline to a mean of 0.7 FCP at 16 hrs and remained low till the end of the experiment. Transcripts of only 4 photosynthesis proteins were quantified including: PDH-E1 alpha, TIM, FNR1 and LHCB3 (last two assigned to PS.light reaction), they decreased significantly at 3 hrs to 0.55, 0.43, 0.27 and 0.06 folds, respectively.

LHCB3 (Photosystem II) transcripts increased to normal levels at 16 hrs and to even significantly higher level 1.8 folds at 19 hrs, however, it dropped to an extremely low level at 32 hrs (0.05 folds). TIM transcripts returned to normal levels at 16 hrs and remained the same (Protein levels did not show significant change throughout the experiment). PDH-E1 alpha and FNR1 transcripts continued in the same levels till 32 hrs. As expected, immune response had a negative effect on the photosynthesis.

Out of the 24 proteins assigned to primary metabolism affected by flg22 in the deep proteomics study (Abukhalaf et al., 2020)), 15 of them were significantly upregulated at 16 hrs to a mean of 1.4 FCP with 10 of them remaining at this level and 4 of them rising further (significantly in respect to the 16 hrs time point) to a mean of 1.7 FCP at 32 hrs.

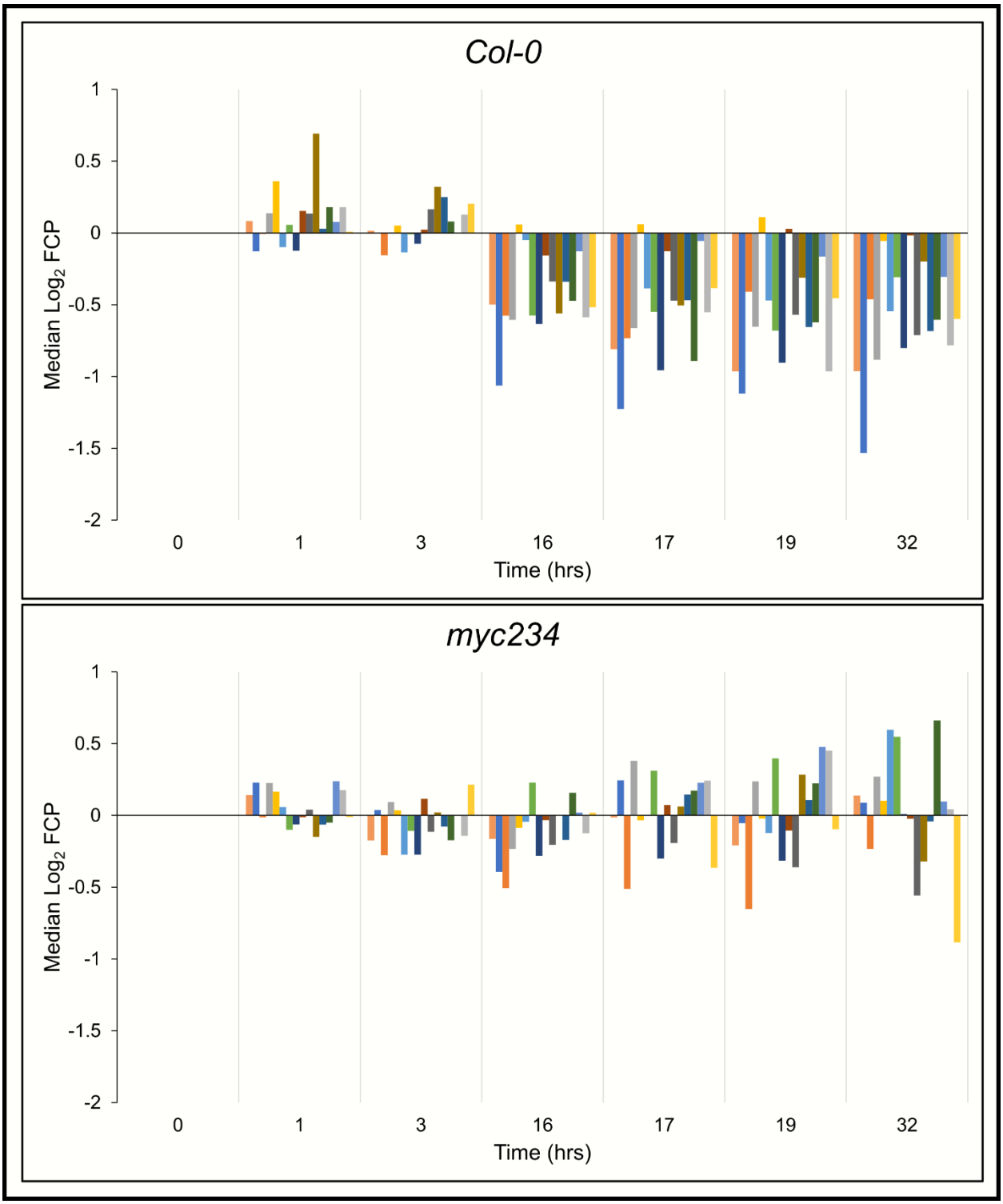

Figure 3-8. Comparison of flg22 effect on proteins playing roles in photosynthesis between *Arabidopsis thaliana* Col-0 and *myc234*. Significantly changing proteins (1, 3 or 16 hrs) annotated to photosynthesis decreased generally after 16 hrs of flg22 exposure in Col-0, however, this effect was not seen in *myc234*. Median log_2 fold change (FCP) (to 0 hrs) (n=4) in Col-0 and (n=3) in *myc234* are plotted.

3.3.2. Response in *Arabidopsis thaliana myc234*

MYC2 a transcription factor from basic-helix-loop-helix (bHLH) family is known to play a fundamental role in JA signaling and crosstalk between different phytohormones signaling pathways (Kazan and Manners, 2013). To study the effect of flg22 on plants with a defect in the JA signaling pathway, *myc234* mutants were used which does not contain MYC2 and its closely related homologs MYC3 and MYC4. The same experiments as described above for the Col-0 were then performed in the *myc234* background. (Supplementary Table 4/ p.99, Supplementary Table 6/ p.102, Supplementary Table 8/ p.103).

The abundance of proteins in the tryptophan, glucosinolate and phenylpropanoid biosynthesis pathways were upregulated much as in Col-0 (Figure 3-9), however, there were some minor differences. For instance, IGPS and TSA1 reached significant 1.3 and 1.4 FCPs at 3 hrs (lower than Col-0) and maximum of 3.1 and 4.2 FCPs at 16 hrs (higher than Col-0), respectively. Proteins in the glucosinolate and phenylpropanoid biosynthesis pathway rose to high levels at 16 hrs with mean of FCPs of 7.7 and 9.6, respectively (also higher than a mean 4.5 and 3.2 FCP in Col-0 at 16 hrs, respectively). Here also, proteins did not return to normal levels at 32 hrs. The abundance of most of the proteins increased or remained the same at 32 hrs, however, other proteins like PAT1, TSB1, CYP81F2, PAL1, and 4CL1 & 2 decreased by a mean of 45%. On the transcript level, PAT1, TSA1 and TSB1 increased significantly to their respective maxima of 19, 70 and 16 fold at 3 hrs, respectively, then decreased at 16 hrs to 5, 10 and 2 fold. After media exchange, PAT1 and TSA1 decreased significantly (in respect to 16 hrs) but TSB1 remained at the same level. CYP83B1, SOT16 and PEN2 also increased to a maximum of 216, 88 and 8 fold, respectively, at 3 hrs and decreased at 16 hrs to 33, 5 and 2 fold, respectively. After that, only SOT16 significantly decreased (respective to 16 hrs) to 3 fold at 32 hrs. In general, mean relative expression of genes in these pathways were higher and more affected at 1 hrs in Col-0, thus suggesting a delay in the PTI response in *myc234*. Here also, proteins did not return to basal levels even after 16 hrs of PAMP (flg22) removal.

Most of the JA biosynthesis pathway proteins did not change or even decrease at early time points (1 and 3 hrs), however, they increased to a mean FCP of 1.4 (except for AOC1) at 16 hrs (Figure 3-10). Moreover, all of them continued to increase reaching a mean FCP of 2 at 32 hrs (significant to 16 hrs and 0 hrs). On the transcript level the situation was different as AOC1 and ACX1 increased at 1 hrs to 5 and 2 fold, respectively, while OPR3 increased to a significant 4 fold at 3 hrs. After that, OPR3 and AOC1 decreased to basal levels, while ACX1 levels remained constant up until 32 hrs and LOX2 increased to 15 fold at 32 hrs. The mean relative expression of those

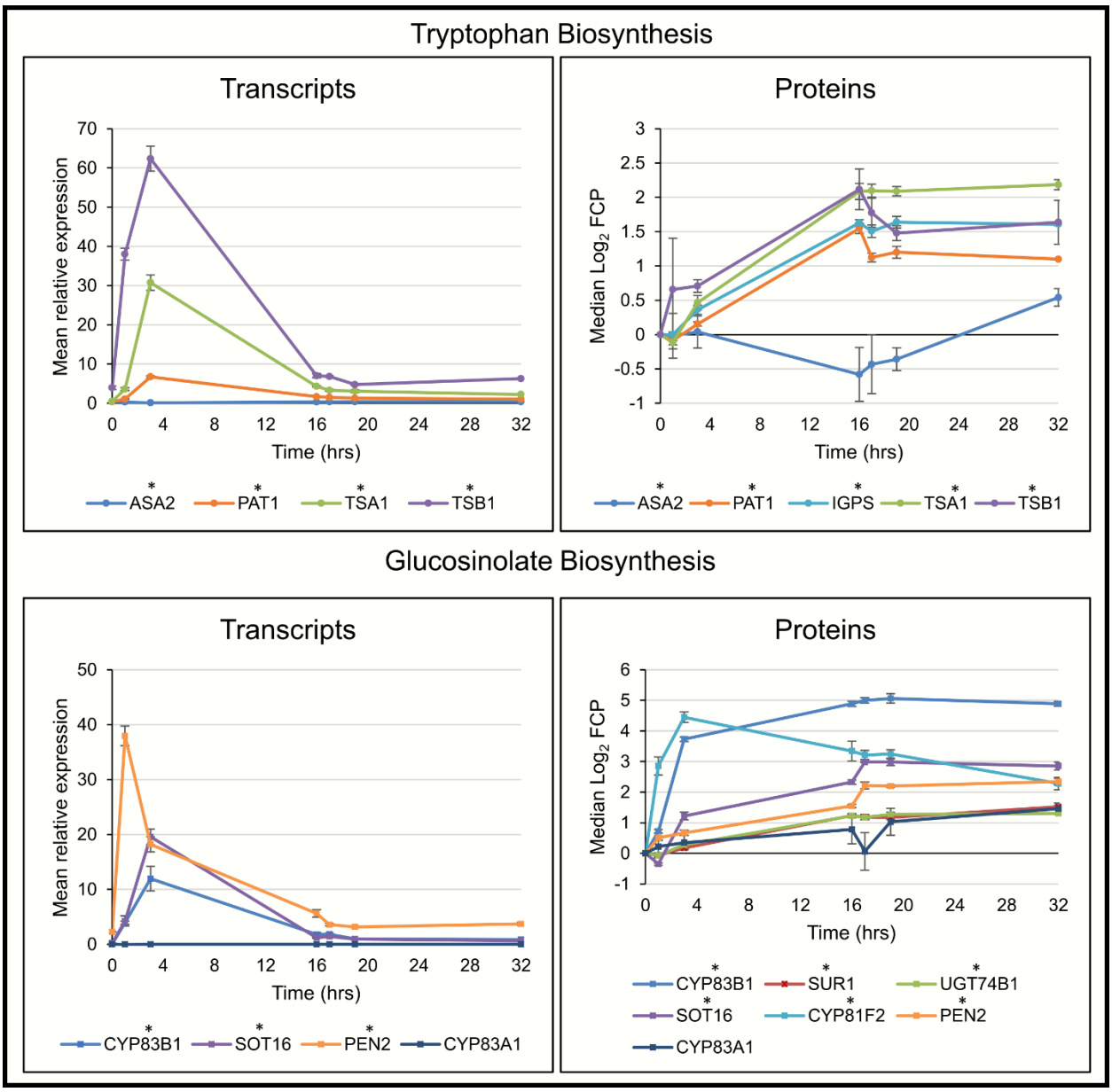

Figure 3-9: Flg22 effect on the transcript and protein levels of glucosinolate and tryptophan biosynthesis pathways in *Arabidopsis thaliana myc234*. The transcripts in the tryptophan and glucosinolate biosynthesis pathways reached their highest levels after 3 hrs and in general were much lower than in Col-0 before and after flg22 treatment. On the protein level the trend is different where most proteins increased to the highest levels at 16 hrs and remained high up until 32 hrs (fold changes were generally comparable to Col-0). Mean relative expression (n=3) to the mean of PP2A and UBC21 is plotted for transcripts. Median $\log_2$ fold change (FCP) (to 0 hrs) (n=3) is plotted for proteins. Error bars represent standard error. Asterisks (*) represent a statistically significant change at 1, 3 or 16 hrs in respect to 0 hrs (two-tailed t-test, $\alpha = 0.05$).

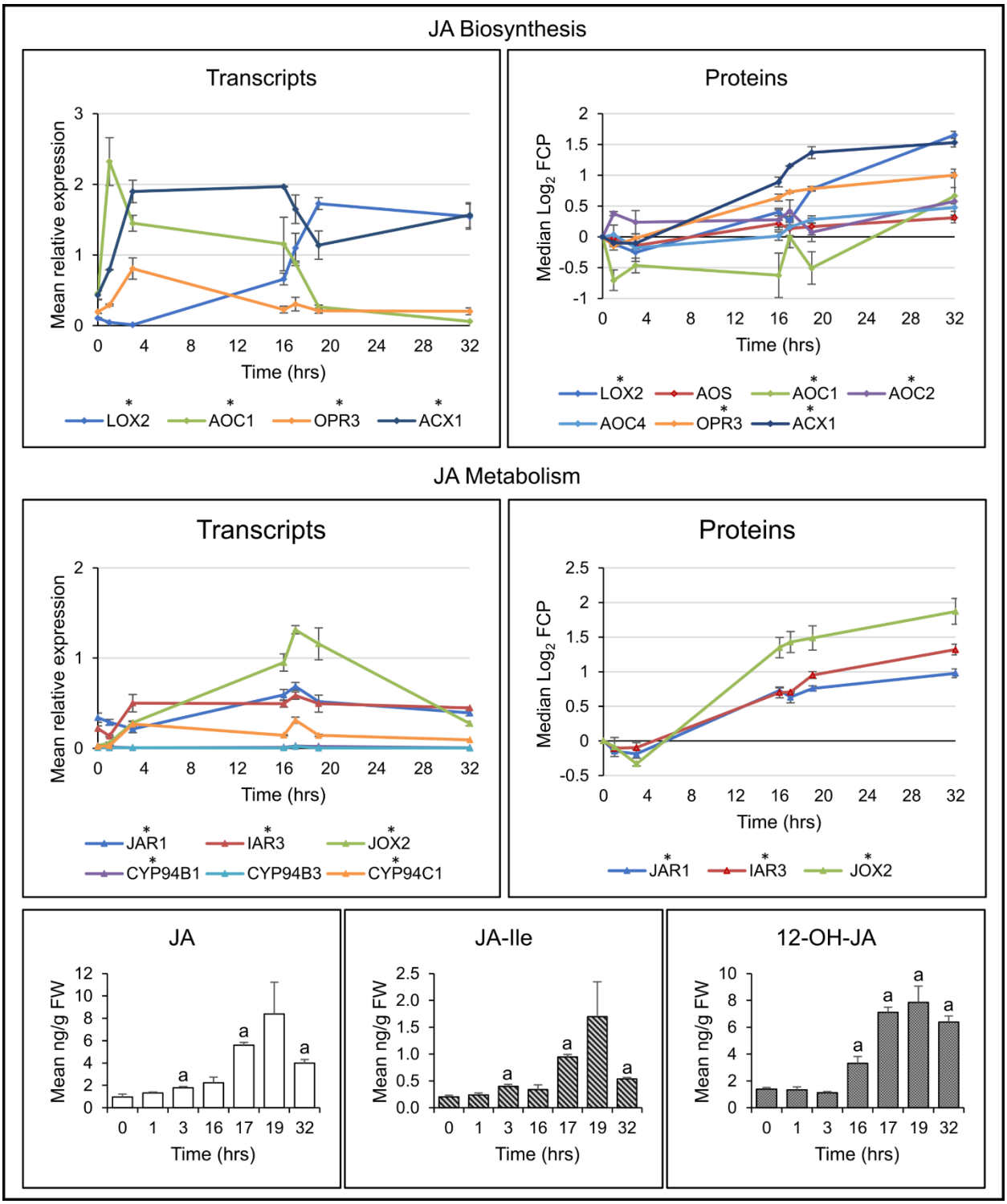

Figure 3-10: Flg22 effect on jasmonic acid (JA) biosynthesis and metabolism in *Arabidopsis thaliana myc234* (description on the next page).

Figure 3-10: Transcripts levels of the JA biosynthesis pathway increased early but to much lower levels in comparison with Col-0. Moreover, proteins in the JA biosynthesis did not increase until 16 hrs. JA and JA-Ile increased at 3 hrs and did not change afterwards until media exchange. JA metabolism transcript abundance increased after 3 hrs (1 hrs in Col-0) and to much lower levels in comparison to Col-0. Proteins of JA metabolism increased at 16 hrs and continued to increase up until 32 hrs. 12-OH-JA followed JOX2 and IAR3 increasing 16 hrs after PAMP exposure and to even higher levels after media exchange. Mean relative expression (n=3) to the mean of PP2A and UBC21 for transcripts, median $\log_2$ fold change (FCP) (to 0 hrs) (n=3) for proteins and mean ng/g fresh weight (FW) (n=3) for hormones are plotted. Error bars represent standard error. Asterisks (*) and (a) represent a statistically significant changes at 1, 3 or 16 hrs to 0 hrs and at each time point to 0 hrs, respectively (two-tailed t-test, $\alpha = 0.05$).

genes was lower than in Col-0 with and without flg22 treatment. JA levels also increased gradually to 2.2 ng/g at 16 hrs and elevated further to 8.4 ng/g at 19 hrs. They then decreased to 4 ng/g at 32 hrs. The JA precursor OPDA also increased to 109 ng/g at 16 hrs and then decreased to 51 ng/g at 32 hrs.

The abundance of proteins playing central roles in JA metabolism and conjugation proteins JAR1, IAR3 and JOX2 did not increase at 1 and 3 hrs, but rose significantly afterwards to 1.7, 1.6 and 2.5 FCP at 16 hrs, respectively. Moreover, they continued to increase to 2, 2.5 and 3.7 FCP at 32 hrs, respectively. Transcripts of CYP94B1 and B3 did not change significantly throughout the experiment. CYP94C1 transcript abundance increased to 13 fold at 3 hrs and then decreased to 4 fold (significant to the 0 hrs sampling time point) at 32 hrs. On the other hand, IAR3 increased to 2 fold at 3 hrs remaining at the same level up until 32 hrs. JOX2 transcript amounts elevated gradually to 31 fold at 16 hrs then decreased to 9 fold at 32 hrs (significant to the 16 hrs time point). The abundance of the bioactive conjugate JA-Ile followed the same trend as JA and was significantly increased after 3 hrs to 0.4 ng/g (2 fold). However, 12-OH-JA did not increase significantly until 16 hrs to 4 ng/g (4.4 fold). In general, the mean relative expression of most genes was much lower and increased later (at 3 hrs) in comparison to Col-0.

The abundance of proteins in the auxin biosynthesis pathways did not change substantially up until the 16 hrs time point such as in Col-0 (except for AAO1 which was elevated to 2 FCP), however, after media exchange AAO1, AAO3 and NIT1 increased to 2.3, 2.1 and 1.8 FCP at 32

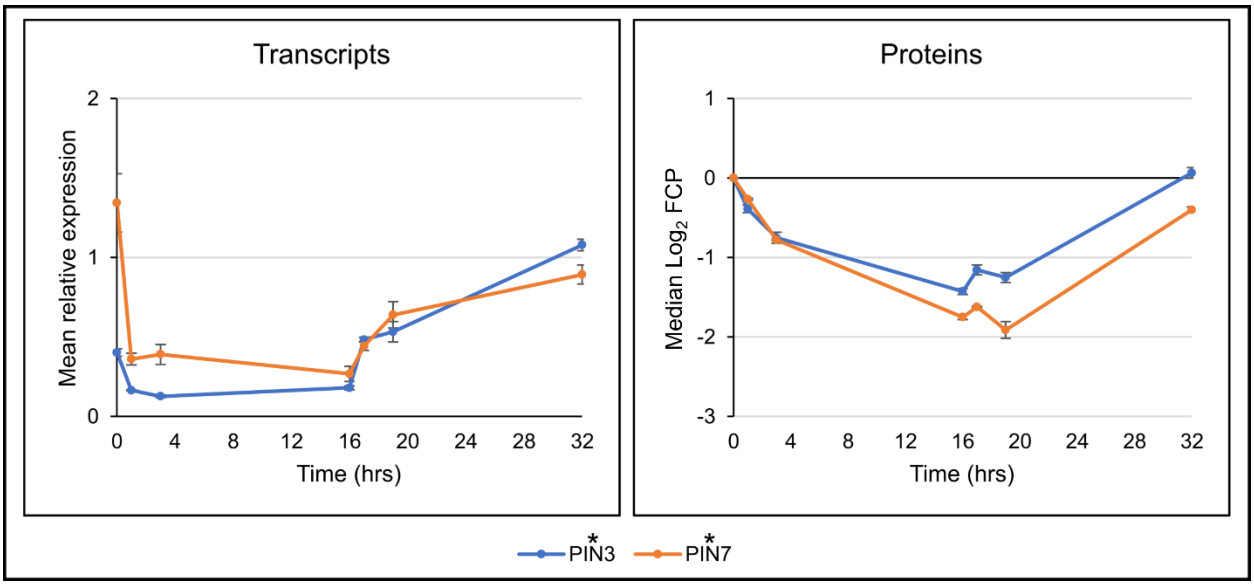

Figure 3-11: Flg22 effect on the auxin efflux transporters PIN3 and 7 in *Arabidopsis thaliana myc234*. Transcript and protein levels of these PINs decreased as early as 1 hrs and 3 hrs, respectively. However, the protein and transcript levels recovered after the media exchange returning to near basal levels for PIN7 and to basal levels or even higher for PIN3 after 32 hrs. Mean relative expression (n=3) to the mean of PP2A and UBC21 is plotted for transcripts. Median log_2 fold change (FCP) (to 0 hrs) (n=3) is plotted for proteins. Error bars represent standard error. Asterisks (*) represent a statistically significant change at 1, 3 or 16 hrs in respect to 0 hrs (two-tailed t-test, $\alpha = 0.05$).

hrs, respectively. AAO1 transcripts rose gradually to 4 fold at 16 hrs and then declined to 2 fold at 32 hrs. Nonetheless, IAA levels did not change throughout the experiment. The abundance of proteins of the Auxin/JA signaling did not change up until 16 hrs where they were elevated to a mean FCP of 1.2. They continued to increase to a mean of 1.6 FCP at 32 hrs. On the transcript level, the trend was different where SKP1 and CUL1 levels did not change throughout the experiment. Comparatively to Col-0, PIN3 and PIN7 protein abundance decreased gradually to a minimum of 0.4 and 0.3 FCP at 16 hrs, respectively, and then increased back to levels comparable to 0 hrs for the former and to 0.76 FCP for the later at 32 hrs (Figure 3-11). Transcripts followed almost the same trend as PIN3 levels reached 2.7 fold increase at 32 hrs and PIN7 returned to basal levels. As in Col-0, this return might be related to the importance of these transporters in the transition to growth.

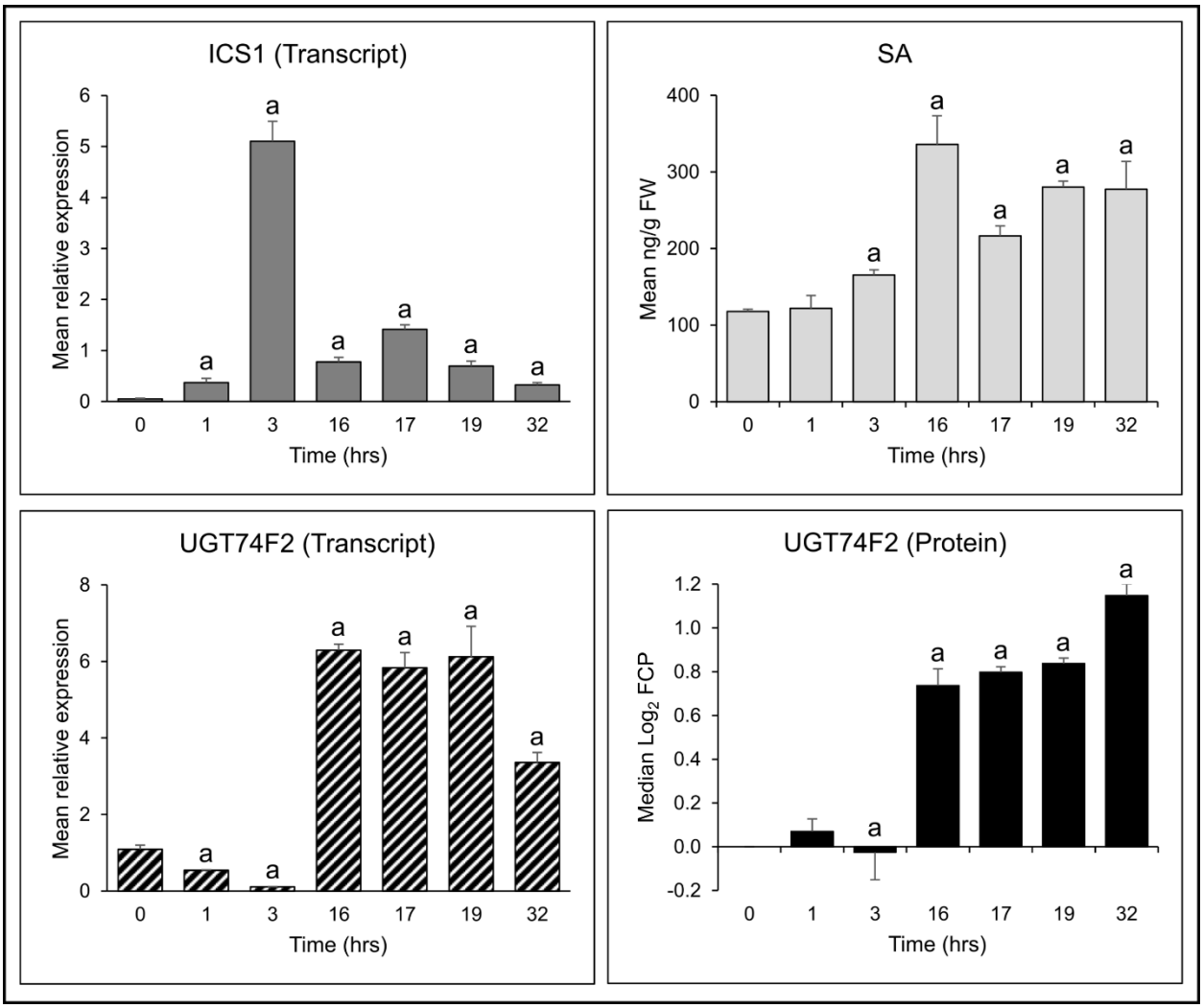

Figure 3-12: Flg22 effect on salicylic acid (SA) biosynthesis and metabolism in *Arabidopsis thaliana myc234*. Isochorismate synthase 1 (ICS1) transcripts increased as early as 1 hrs leading to SA increase at 3 hrs and to a higher level at 16 hrs. UDP-glucosyltransferase (UGT74F2) increased after 16 hrs on the transcript and protein levels to inactivate SA as SA levels remained high up until 32 hrs. Mean relative expression (n=3) to the mean of PP2A and UBC21 for transcripts, median $\log_2$ fold change (FCP) (to 0 hrs) (n=3) for proteins and mean ng/g fresh weight (FW) (n=3) for hormones are plotted. Error bars represent standard error. (a) indicates a statistically significant change at each time point to 0 hrs (two-tailed t-test, $\alpha = 0.05$).

The most important enzyme in SA biosynthesis, ICS1, increased on the transcript level to a maximum 95 fold at 3 hrs followed by a decline to 15 fold at 16 hrs (Figure 3-12). Afterwards, it increased to 26 fold at 17 hrs and decreased to 6 fold at 32 hrs. Moreover, NTL9 protein levels reached 1.6 FCP at 16 hrs and remained at the same level up until 32 hrs. On the other hand, TCP22 did not change at all throughout the experiment. The protein UGT74F2 reached 1.7 FCP

and a 6 fold change in transcript abundance at 16 hrs. Afterwards, it rose gradually to 2.2 FCP at 32 hrs while falling to 3 fold in change in the amount of transcripts. Furthermore, SA levels increased gradually to 336 ng/g at 16 hrs remaining constant up until 32 hrs.

As in Col-0, ACO2 transcripts reached a 3.3 fold increase in their abundance at 16 hrs declining afterwards to 1.7 fold at 32 hrs. Moreover, the abundance of the cognate protein was upregulated at 16 hrs to a 1.5 FCP lasting up until 32 hrs. NIT4 transcripts and proteins were comparable to Col-0 where the transcripts reached a maximum at 3 hrs and returned to basal levels at 32 hrs while protein levels reached a maximum at 16 hrs slightly declining afterwards until 32 hrs.

The same 23 photosynthesis proteins described before in Col-0, were quantified. Sixteen proteins, which were significantly changing at either 1,3 or 16 hrs in Col-0, showed a mean FCP ranging from 0.9 to 1 throughout the whole experiment (Figure 3-8). By comparison to Col-0, there was no visible decrease in the abundance of some photosynthesis related proteins. On the transcript levels, the trend was almost the same as in Col-0 with some minor differences. LHCB3 transcript abundance did not recover at 16 hrs (0.4 folds) and PDH-E1 alpha, TIM and FNR1 did not change at 1 hrs at all. On the other hand, 20 out of the 24 primary metabolism proteins were significantly increased at 16 hrs to a mean FCP of 1.7 and continued rising to 2.3 at 32 hrs.

3.4. Protein Turnover Rates Measurements

Throughout our experiment, it became generally evident that the abundance of transcripts changes at earlier time points than the abundance of their cognate proteins after flg22 treatment. To confirm this, a correlation analysis at different time points was done. Median protein abundance of biological replicates of the 34 target proteins of which cognate transcripts were quantified in Col-0 were $\log_{10}$ and then Z-score transformed in perseus v 1.6.6.0 (Tyanova et al., 2016). The mean relative expression (of biological replicates) of each gene was $\log_{10}$ and then Z-score transformed as well. All of the Z-scored data was increased by 5 (to keep it in the positive range) and then proteins were plotted against transcripts at each time point (Figure 3-13). The linear correlation had an R^2 of 0.36 at 0 hrs which was reported before to be in approximately the same range in experiments with human cell lines (Wilhelm et al., 2014, Schwanhausser et al., 2011). After treatment with flg22, the correlation diminished already at 1 hrs post exposure, becoming negative with an R^2 of 0.33. Then, it was with an R^2 of around zero at 16 hrs. After media exchange the correlation between protein and transcript abundance again became negative with an R^2 of 0.16 at 19 hrs. At the last sampling time point (32 hrs), the correlation was positive again with a low R^2 of 0.034. This analysis confirmed the observation that the abundance of transcripts and proteins changed at a different pace under the effect of flg22. To further

understand the connection between transcript and proteins, experiments to calculate protein turnover rates were conducted with and without flg22 treatment.

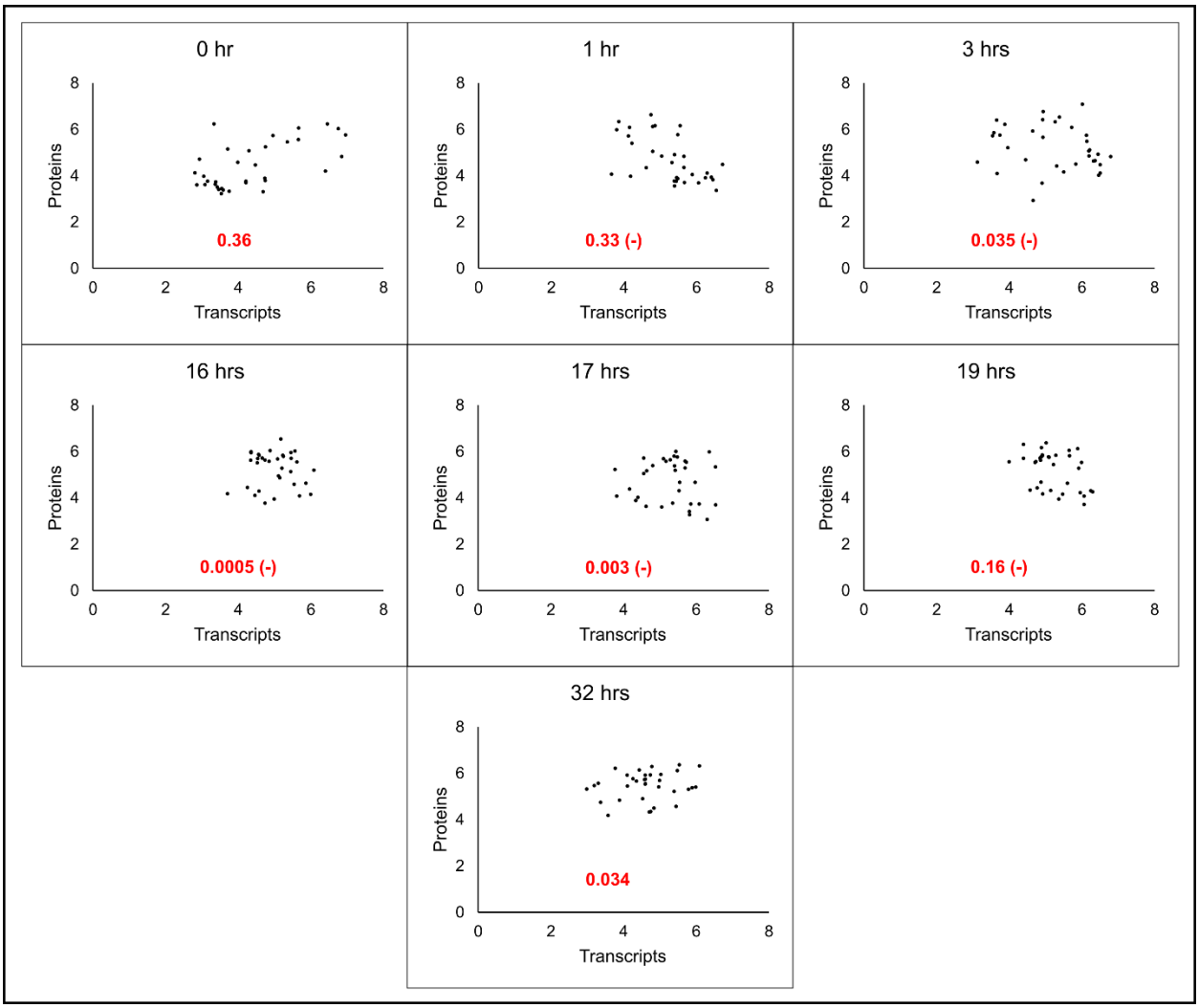

Figure 3-13: Loss of correlation between proteins and transcripts following exposure to flg22. Linear correlation between normalized protein and transcript abundance of 34 targets was affected by exposure to the PAMP flg22 over time as early as 1 hrs. Numbers in Red represent the coefficients of determination (R^2).

3.4.1. Target proteins turnover rates measurement under normal conditions (control)

To calculate the steady state turnover rates of our proteins, 10 days old Col-0 seedlings were transferred to ^{15}N media ($K^{15}NO_3$ and $^{15}NH_4{}^{15}NO_3$) and samples were taken at time points 0, 8, 9, 10, 12, 24, 36, 48, 72 and 96 hrs. A method described before using ^{15}N labeling of peptides was

used (Li et al., 2017; Nelson, Alexova, Jacoby, & Millar, 2014) where degradation rates (K_d) are calculated by measuring the decrease of naturally abundant proteins. A python-based code (protover) (Lyon et al., 2014) was used to calculate the ratios of the area of the peptide ion signal peak envelopes of the heavy peptides with increasing incorporation of ^{15}N over time to the total peptides' population i.e., naturally occurring and heavy labeled peptides; the relative isotopic abundance (RIA) (eq.2/ p.27). Measurements at early time points (8, 9, 10 and 12 hrs) were done to find out the point of measurable ^{15}N incorporation into target peptides (lag time). After analysis with protover, a mean RIA (of all peptides in 3 biological replicates) of 0.14, 0.15, 0.17 and 0.19 was observed at 8, 9, 10 and 12 hrs, respectively. This implied 14% ^{15}N incorporation at 8 hrs, and this was considered the starting point for the turnover calculations in the following experiments.

The apparent degradation rate (K_{loss}) was calculated as described in the methods (eq.3/ p.27). Moreover, the growth rate (K_{dil}), an index of protein increase in stable growth, was extracted by fitting an exponential model to the increase of weight over time (Figure 3-14) (eq.5/ p.27) (Nelson et al., 2014). From these, degradation and synthesis rates (K_d and K_s, respectively) were calculated as described in the methods in eq.4 and eq.7 (p.27). For a total of 69 proteins K_d and K_s were reported (Table 3.1). Then, proteins were classified on the basis of degradation rates as slow (<0.055 day^{-1}), intermediate (0.055-0.22 day^{-1}) and fast (>0.22 day^{-1}) as described before in (Li et al., 2017). In total, 32, 27 and 10 proteins were classified as slow, intermediate and fast,

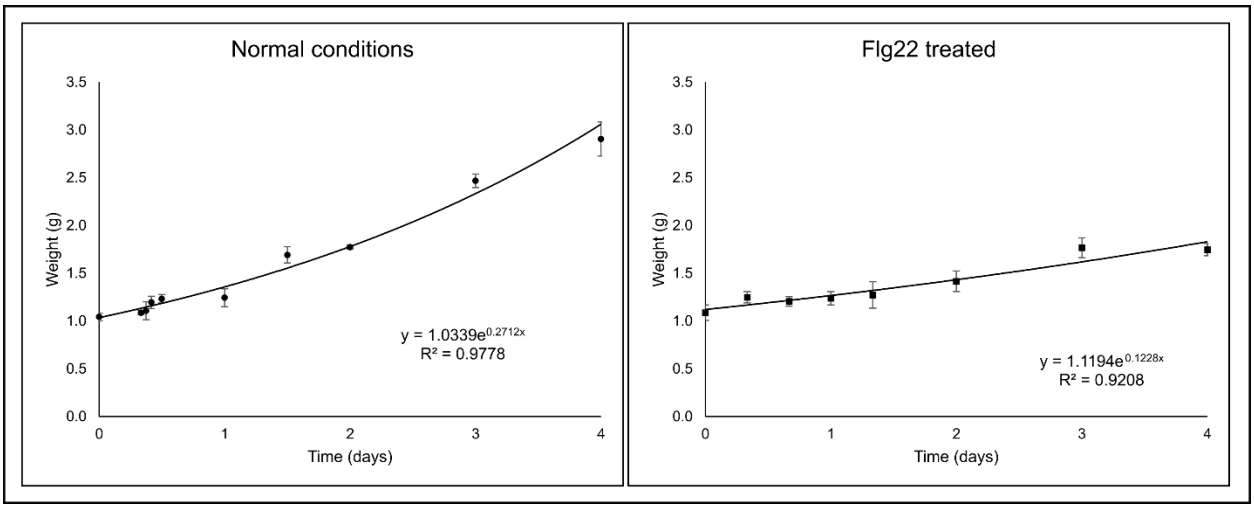

Figure 3-14: Growth rate of *Arabidopsis thaliana* Col-0 seedling with and without flg22. 10 days old *Arabidopsis thaliana* Col-0 seedlings weights were recorded at multiple time points with and without flg22 treatment. The plots were used to calculate the doubling constant (K_{dil}). Flg22 affected the growth of the seedlings leading to a lower K_{dil}. Mean weights are plotted and error bars represent standard deviation (n=3).

respectively. Interestingly, 12 out of the 17 photosynthesis proteins with calculated degradation rates were classified as degrading slowly.

Table 3.1. Turnover rates of target proteins in *Arabidopsis thaliana* Col-0 with and without flg22. K_d and K_s are degradation and synthesis rate constants, respectively. (C) and (F) represents Control and flg22 treated, respectively. Int: Intermediate. Asterisks (*) represent a statistically significant difference (two-tailed t-test, α = 0.05).

Protein Accession	Protein Name	K_d(C)	Index	K_d(F)	Index	K_s(C)	K_s(F)
AT2G29690	ASA2	0.191	Int	0.063	Int	0.624	0.212 (*)
AT2G04400	IGPS	0.081	Int	0.079	Int	0.471	0.229 (*)
AT3G54640	TSA1	-0.114	Slow	0.104 (*)	Int	0.207	0.258
AT5G54810	TSB1	0.156	Int	0.183	Int	0.576	0.350
AT5G20960	AAO1	-0.052	Slow	0.249	Fast	0.290	0.427
AT3G43600	AAO2	0.040	Slow	0.154	Int	0.416	0.316
AT2G27150	AAO3	0.088	Int			0.484	
AT1G08980	AMI1	0.040	Slow	0.153	Int	0.416	0.314
AT3G44310	NIT1	0.162	Int	0.342 (*)	Fast	0.583	0.534
AT3G44320	NIT3	0.067	Int			0.452	
AT4G31500	CYP83B1	0.286	Fast			0.762	
AT2G20610	SUR1			0.195	Int		0.363
AT1G24100	UGT74B1	0.241	Fast	0.415	Fast	0.699	0.620
AT1G74100	SOT16	-0.048	Slow			0.296	
AT5G57220	CYP81F2			0.461	Fast		0.676
AT4G30530	GGP1	0.046	Slow			0.423	
AT2G37040	PAL1	-0.026	Slow	0.105	Int	0.325	0.260
AT2G30490	C4H	0.017	Slow	0.283 (*)	Fast	0.385	0.465
AT3G21240	4CL2	0.065	Int	0.269	Fast	0.450	0.451
AT1G51680	4CL1	0.116	Int	0.314 (*)	Fast	0.520	0.502
AT5G13360	GH3	-0.092	Slow	0.180 (*)	Int	0.236	0.346
AT1G51760	IAR3	0.296	Fast	0.160	Int	0.777	0.323
AT5G05600	JOX2	0.219	Int			0.666	
AT3G45140	LOX2	-0.061	Slow	0.067	Int	0.279	0.216
AT5G42650	AOS	-0.070	Slow	0.237 (*)	Fast	0.267	0.412
AT3G25760	AOC1	-0.062	Slow	-0.025	Slow	0.278	0.111
AT3G25770	AOC2	0.222	Fast	0.258	Fast	0.669	0.437
AT1G13280	AOC4	-0.182	Slow	0.245 (*)	Fast	0.117	0.422 (*)
AT2G06050	OPR3	-0.040	Slow	0.033	Slow	0.307	0.177

AT4G16760	ACX1	0.181	Int	0.334 (*)	Fast	0.610	0.525
AT1G23080	PIN7	0.113	Int	0.126	Int	0.518	0.284
AT5G49980	AFB5	-0.083	Slow			0.249	
AT1G80490	TPR1			0.199	Int		0.368
AT3G16830	TPR2	0.159	Int			0.582	
AT5G27030	TPR3			0.500	Fast		0.720
AT1G75950	SKP1			0.163	Int		0.326
AT4G02570	CUL1	0.163	Int	0.161	Int	0.586	0.324 (*)
AT1G05180	AXR1	0.064	Int	0.037	Slow	0.447	0.181 (*)
AT1G72010	TCP22			0.243	Fast		0.420
AT2G43820	UGT74F2	0.094	Int	0.378	Fast	0.492	0.578
AT1G62380	ACO2			0.224	Fast		0.397
AT2G21370	XK-1			0.324	Fast		0.515
AT3G02870	VTC4	0.204	Int	0.311	Fast	0.643	0.498
AT5G58260	NDH-N	0.036	Slow	0.272	Fast	0.411	0.453
AT1G01090	PDH-E1 ALPHA	-0.169	Slow	0.057 (*)	Int	0.133	0.204
ATCG01090	NDHI	0.156	Int	0.266	Fast	0.576	0.446
AT5G35790	G6PD1	0.018	Slow	0.103	Int	0.385	0.257
AT4G02580	NADH dehydrogenase flavoprotein 2	0.045	Slow	0.267 (*)	Fast	0.422	0.447
AT4G20130	PTAC14	-0.046	Slow	0.104 (*)	Int	0.298	0.259
AT5G64380	Inositol monophosphatase	0.309	Fast	0.201	Int	0.792	0.370 (*)
AT1G12900	GAPA-2	0.050	Slow	0.067	Int	0.429	0.216
AT5G54270	LHCB3			0.192	Int		0.359
AT3G56650	PPD6	-0.136	Slow	0.243 (*)	Fast	0.177	0.419 (*)
AT1G12240	ATBETAFRUCT4	-0.044	Slow	0.073	Int	0.301	0.223
AT1G66430	FRK3	-0.058	Slow	0.064	Int	0.282	0.213
AT3G55800	SBPASE	-0.057	Slow			0.285	
AT2G21170	TIM	-0.011	Slow	0.168	Int	0.348	0.332
ATCG00350	PSAA	0.141	Int	0.075	Int	0.554	0.225 (*)
AT5G66190	FNR1	0.228	Fast	0.063	Int	0.678	0.211 (*)
AT2G39730	RCA	0.005	Slow	0.291 (*)	Fast	0.367	0.475 (*)
AT5G54960	PDC2	0.195	Int	-0.023 (*)	Slow	0.630	0.113 (*)
AT5G17380	2-hydroxyacyl-CoA lyase	0.034	Slow	0.248	Fast	0.409	0.425
AT5G40760	G6PD6			0.163	Int		0.327
AT5G11670	ATNADP-ME2	-0.026	Slow			0.327	
AT5G56350	pyruvate kinase	-0.037	Slow			0.310	
AT3G23920	BAM1	0.077	Int	0.014	Slow	0.467	0.155 (*)
AT5G20250	DIN10	0.178	Int	0.299	Fast	0.607	0.485

AT4G37870	PCK1	0.125	Int	0.276	Fast	0.532	0.458
AT4G26970	ACONITASE 2	0.016	Slow	0.319 (*)	Fast	0.382	0.507 (*)
AT3G24503	REF1	0.133	Int	0.179	Int	0.545	0.344
AT2G17130	IDH2			0.107	Int		0.262
AT4G04040	MEE51	0.093	Int	0.324	Fast	0.489	0.514
AT3G48000	ALDH2B4	-0.051	Slow	0.327 (*)	Fast	0.292	0.517
AT4G35260	IDH1	0.634	Fast			1.271	
AT1G23800	ALDH2B7	0.239	Fast	0.379	Fast	0.692	0.578
AT1G76450	PPD3	0.189	Int			0.622	
AT4G00570	malate oxidoreductase, putative			0.065	Int		0.214
AT4G25900	Glucose-6-phosphate 1-epimerase	0.845	Fast	0.458	Fast	1.594	0.673 (*)
AT2G36580	pyruvate kinase	0.096	Int	0.276 (*)	Fast	0.492	0.457
AT1G09430	ACLA-3	0.174	Int	0.238	Fast	0.601	0.414
AT3G52990	pyruvate kinase			0.132	Int		0.291
AT5G11770	NADH dehydrogenase iron-sulfur protein 7	0.258	Fast	0.269	Fast	0.719	0.450

3.4.2. Target proteins turnover measurements under flg22

The calculation of turnover rates following exposure to flg22 needed a different approach, as two situations needed to be differentiated: the early non-steady state situation where plant physiology shifted from growth to immunity (flg ns) hallmarked by pronounced changes in protein abundance and extensive proteome remodeling and the late steady state situation (flg ss) where immunity is fully induced and the proteome is again in a steady state. As it was already known that the lag time for ^{15}N incorporation is 8 hrs, the PTI elicitor flg22 was added at that time point, representing 0 hrs. Samples were taken 2, 4, 6, 8 and 16 hrs after flg22 treatment to calculate the non-steady state turnover rates in the shift from growth to fully induced immunity. On the other hand, 0, 8 and 16 hrs with later time points 24, 32, 48, 72 and 96 hrs were used to calculate the steady state turnover rates when PTI was considered to be fully induced. To calculate the non-steady state degradation rate (K_d), Fold Changes of Proteins (FCPs) should be factored in the equation (eq.8/ p.28). FCPs were calculated at 2, 4, 6, 8 hrs by using an equation from a fitted polynomial model to the PRM data of 0, 1, 3 and 16 hrs. Only proteins with FCPs with higher than 1.5 or lower than 0.75 were used in the calculation which amounted to a total of 52 proteins (Supplementary Table 10/ p.105). After the filtration, turnover rates (K_d and K_s) of 28 proteins were reported (Table 3.2). In general, it is evident that proteins which were increasing in their abundance had exceptionally low (negative) Kd and proteins which were decreasing in their abundance had high Kd. Moreover, synthesis rates (K_s) were calculated at each time point and the difference was considerable even between two-hour time points.

Table 3.2. Turnover rates of target proteins in *Arabidopsis thaliana* Col-0 under non-steady state flg22. K_d and K_s are degradation and synthesis rate constants, respectively.

Protein Accession	Protein Name	K_d	K_s				
			2 hrs	4 hrs	6 hrs	8 hrs	16 hrs
AT5G17990	TRP1	-1.46	1.36	1.12	0.99	0.87	0.49
AT2G04400	IGPS	-0.92	5.50	4.86	4.14	3.43	0.98
AT3G54640	TSA1	-1.96	3.17	3.00	2.42	1.81	-0.18
AT5G54810	TSB1	-2.70	-0.71	-0.80	-0.61	-0.44	-0.33
AT5G20960	AAO1	-0.90	1.22	0.67	0.58	0.60	0.84
AT4G31500	CYP83B1	-3.13	20.74	16.84	12.50	8.72	-0.77
AT1G24100	UGT74B1	-1.25	3.84	3.23	2.61	2.02	0.09
AT2G30490	C4H	-0.55	4.05	2.31	1.69	1.35	0.71
AT3G21240	4CL2	-0.83	1.89	1.89	1.69	1.46	0.53
AT1G51680	4CL1	-1.38	4.49	4.06	3.35	2.62	0.18
AT5G05600	JOX2	-2.24	3.46	2.94	2.42	1.93	0.45
AT3G25760	AOC1	-1.00	-0.22	0.05	0.11	0.12	0.03
AT1G23080	PIN7	1.85	0.40	0.15	0.07	0.04	0.19
AT5G49980	AFB5	0.72	0.87	0.74	0.66	0.57	0.22
AT1G75950	SKP1	0.72	1.90	1.65	1.43	1.20	0.15
AT5G18200	UTP	-0.51	-0.55	-0.78	-0.71	-0.56	0.12
AT3G02870	VTC4	0.76	2.16	1.57	1.26	1.01	0.07
ATCG00430	PSBG	1.50	1.27	1.36	1.28	1.14	0.29
AT1G01090	PDH-E1 ALPHA	0.82	0.12	0.04	0.03	0.04	0.15
ATCG01090	NDHI	1.33	2.06	1.74	1.54	1.36	0.56
AT4G02580	NADH dehydrogenase flavoprotein 2	1.03	1.20	1.03	0.92	0.81	0.34
AT4G20130	PTAC14	0.72	0.20	0.32	0.32	0.28	0.05
AT5G54270	LHCB3	1.52	6.62	4.64	3.76	3.12	0.76
AT1G66430	FRK3	0.61	1.57	1.18	0.96	0.78	0.13
AT5G66190	FNR1	0.80	2.04	1.64	1.38	1.14	0.15
AT2G39730	RCA	0.92	2.10	2.01	1.81	1.57	0.33
AT4G37870	PCK1	-0.45	-0.55	-0.39	-0.27	-0.16	0.24
AT3G24503	REF1	-0.79	1.00	0.94	0.81	0.66	0.09

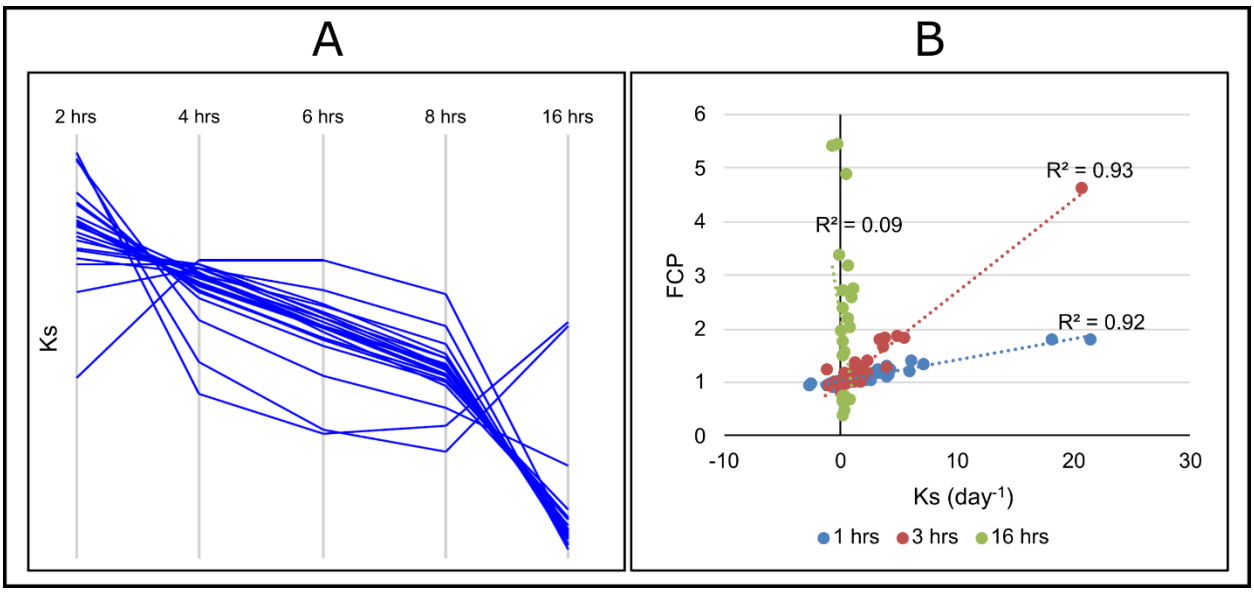

Figure 3-15. Analysis of the synthesis rates (K_s) in the non-steady state immune response. Z-scored K_s data formed a main cluster consisting of 23 out of 28 proteins, where K_s decreased over time (A). Correlations between Ks and Fold Change Protein (FCP) from original PRM data showed that the correlation was high at earlier time point 1 and 3 hrs then lost at 16 hrs.

So, in order to understand changes in synthesis rates, K_s values were Z-scored and then hierarchaly clustered using pearson and spearman correlation to produce row (proteins) and column (sampling time points) dendrograms, respectively. Twenty three out of the 28 proteins formed the main cluster (Figure 3-15 A). It was visible that synthesis rates were highest at 2 hrs then decreased gradually reaching their lowest at 16 hrs. Synthesis rates were also analyzed in relation to the original PRM data of 1, 3 and 16 hrs. FCPs of proteins were plotted against their K_s at the respective time point (Figure 3-15 B). Interestingly, K_s and FCP correlation at 1 and 3 hrs was high with R^2 values of 0.92 and 0.93, respectively, which means that the K_s is an important factor for the increase of protein abundance in addition to increase in mRNA levels. However, this correlation was lost at 16 hrs (R^2 = 0.09) meaning that the synthesis does not play a major role anymore at this time point presumably as proteome remodeling is complete. The second aspect was the steady state situation (flg ss), where K_d and K_s were calculated as in the previous section. However, the growth of the seedlings was affected by flg22 leading to a K_{dil} of 0.1228 day^{-1} (≈ 50% of the control) (Figure 3-14/ p.53). Here also, a total of 69 proteins K_d and K_s were determined (Table 3.1), where 5, 31 and 33 proteins were classified as slow, intermediate and fast based on their K_d, respectively. Comparison of flg22 ss to non-induced normally growing plants produced a set of 56 proteins, in which 26 proteins were significantly different in K_d or K_s or both. Pathway analysis yielded interesting results. For example, 16 photosynthesis related proteins (out of 23)

showed significantly higher degradation rates in the flg ss in comparison to control with a mean K_d of 0.16 day^{-1} in comparison to 0.05 day^{-1} (Figure 3-16). Synthesis rates on the other hand were higher in control with a mean K_s of 0.42 (0.33 in flg ss), however, this difference was not significant. This complements the previous observation of the decrease in photosynthesis proteins after the flg22 treatment as 12 proteins from this set were from the significantly decreasing set in Col-0. In general, these results highlight the role of protein turnover rates in immunity.

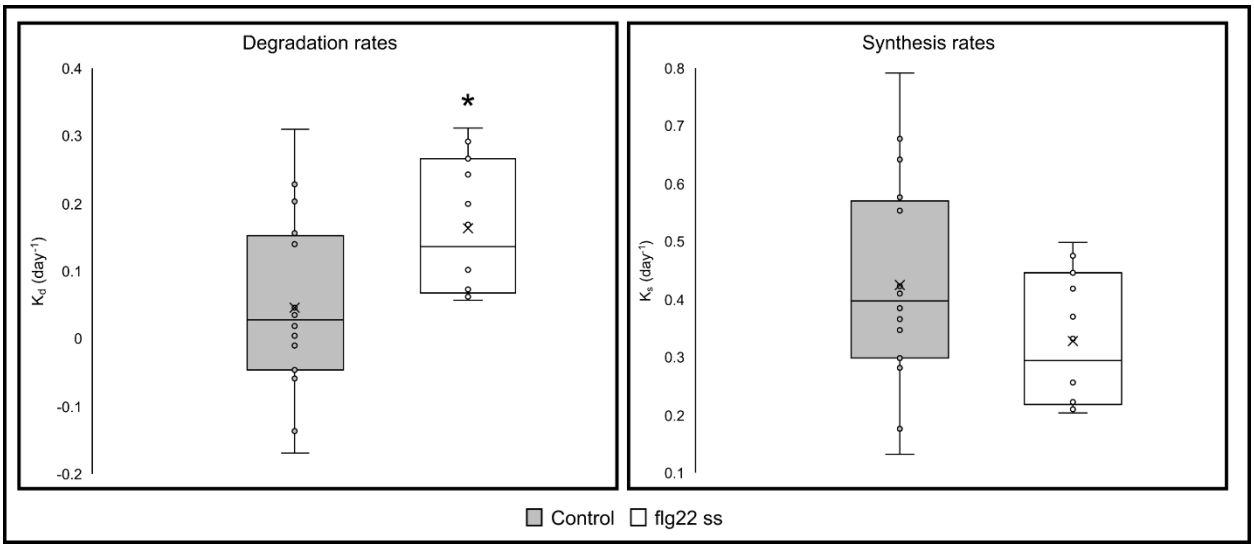

Figure 3-16. Change of turnover rates of photosynthesis proteins after flg22 treatment. Degradation rates (K_d) of photosynthesis proteins were significantly higher under flg22, on the other hand, synthesis rates (K_s) were lower but not significantly. flg ss: steady state flg22. Circles: are the data points and X is the mean. Asterisk (*) represents a statistically significant difference (n = 16, two-tailed t-test, α = 0.05)

4. Discussion

4.1. PRM coupled retention time (Rt) scheduling achieves sensitive and accurate quantification of hundreds of peptides

Targeted proteomics approaches have proven useful for the verification of quantification results of discovery proteomics experiments (Neilson et al., 2011). One of these approaches is parallel reaction monitoring (PRM) that records all fragment ions of a selected precursor ion providing sensitive and specific quantification (Peterson et al., 2012). However, this approach only allows a limited number of scans per chromatographic peak which requires the introduction of an additional dimension that can facilitate scanning of hundreds of peptide signal ion peaks per run (Rauniyar, 2015).

Rt scheduling has been shown to be able to expand the number of scans in the PRM experiment. A full scan followed by Rt scheduled PRM scanning was able to maximize the sensitivity (Majovsky et al., 2014). In this work, a total number of 224 proteotypic peptides, uniquely mapping to 99 cognate proteins, were quantified in a 180 min LC-MS run. In each run a list of around 250 mass to charge ratios (m/z) each in a 14 min Rt window was provided for the LC-MS machine. A label-free quantification approach using total integrated area under the curve (AUC) of the fragment ions was analyzed by Skyline v 19.1 (MacLean et al., 2010). Studies using the same approach with multiplexed selected reaction monitoring (SRM) achieved quantification of around 800 tryptic yeast peptides in a 60 min gradient (Gallien et al., 2012b). Furthermore, multiplexed PRM achieved a robust quantification of 856 peptides in a complex mouse bone marrow lysate over a 360 min gradient (Urisman et al., 2017). However, in comparison to SRM, PRM attains higher sensitivity and specificity and while multiplexing covers larger sets of target peptides, targeting low abundant peptides requires longer filling times that might exceed the transient length (Gallien et al., 2012a). Recently, a new method termed parallel accumulation–serial fragmentation (PASEF) (Meier et al., 2015) developed on a trapped ion mobility quadrupole time-of-flight mass spectrometer (timsTOF Pro), which adds a separation step in the MS itself, was coupled with PRM (prmPASEF) to quantify around 200 peptides in a 30 min run (Lesur et al., 2021).

New acquisition techniques have been developed in discovery proteomics to achieve robust identification and quantification with a large dynamic range. Data independent acquisition (DIA) has been shown to be a more sensitive and specific method than the common data dependent acquisition (DDA) scan strategy for quantitation and identification of proteins (Venable et al., 2004). In this acquisition method all precursor ions are fragmented leading to complex fragment

ion spectra that need spectral library data bases to be analyzed. Libraries are generated through DDA experiments which should be study specific due to lack of consistency (Krasny and Huang, 2021). To overcome this limitation, reference libraries of many organism have been published (http://www.swathatlas.org/) and newer algorithms that produce *in silico* libraries have been developed (Demichev et al., 2020, Tsou et al., 2015). Moreover, a global targeting approach using real-time recalibration of mass, intensity and Rt by MaxQuant.Live has shown robust targeting of 25,000 peptides in one LC-MS run (Wichmann et al., 2019).

Despite the availability of all of these techniques, the PRM targeting approach is still considered the method of choice for validation of changes in protein abundance which was applied in this study to calculate relative protein abundances as fold changes (FCPs) over time and to measure protein turnover of selected targets, a first in plant science.

4.2. Secondary metabolites pathways play a role in defense priming

Secondary metabolites such as glucosinolates (GS), camalexin and phenylpropanoids play an important role in plant defense (Piasecka et al., 2015, Yadav et al., 2020). Two main types of GSs are identified in *Arabidopsis thaliana*, aliphatic GS derived from methionine and indolic GS derived from tryptophan (Petersen et al., 2002). Moreover, GSs are recognized as phytoanticipins which are stored normally in plants and activated upon pathogen attack (Morant et al., 2008). On the other hand, the tryptophan derived phytoalexin, camalexin, is produced upon pathogen attack which possess antimicrobial properties (Bednarek, 2012b).

Transcripts and proteins of the tryptophan and GS biosynthesis pathways increased as early as 1 and 3 hrs, respectively, after the treatment with flg22 in Col-0 (Figure 3-4/ p.37). This was expected for tryptophan as it is needed for the synthesis of indole GS and camalexin that are known to be increased upon pathogen attack (Bednarek et al., 2011). Gene expression of these pathways were shown to be upregulated also in *Arabidopsis thaliana* seedlings after 1 and 3 hrs treatment with flg22 or oligogalacturonides (OGs) (Denoux et al., 2008). Moreover, methyl-jasmonate (MeJA) and 2,6-Dichloro-isonicotinic acid (INA), a salicylic acid (SA) homolog, demonstrated positive effects on GS production (Mikkelsen et al., 2003). Transcripts abundance decreased considerably after 16 hrs but the proteins reached even higher abundance at 16 hrs than at 3 hrs which suggested that the activity of these pathways is not necessarily correlated with transcript levels, explaining a previously observed increase in the end product 4-methoxy-indol-3-ylmethyl glucosinolate (4MOI3M) after 16 hrs of flg22 (Abukhalaf et al., 2020).

In the *myc234* triple mutant background (Figure 3-9/ p.46), the transcripts increased also but to lower levels than in Col-0 except for PEN2 and TSB1. Expression of GS biosynthesis genes has been shown to be considerably reduced in *myc234* mutants under normal conditions while PEN2 expression was comparable to Col-0 and tryptophan biosynthesis genes showed a fair reduction in the amount of cognate mRNAs (Schweizer et al., 2013). Genes of these pathways have also been identified as targets of MYC2 and 3 transcription factors recently (Zander et al., 2020). So, the increase in GS or tryptophan biosynthesis pathways could be caused by other transcription factors possibly regulated by ethylene (ET) or salicylic acid (SA) (Clay Nicole et al., 2009, Kiddle et al., 1994). On the other hand, protein fold changes (FCPs) increased to comparable levels as in Col-0, indicating comparable activation of these pathways which was reflected in transcript amounts by fold change comparison.

Interestingly, protein abundance did not decrease after removal of the elicitor until 32 hrs in all secondary metabolites and tryptophan biosynthesis pathways. This could be part of systemic acquired resistance (SAR) that is known to be activated by SA (Dempsey et al., 1999) which was elevated significantly 16 hrs after flg22 treatment. SAR has been related to the “priming” process which is identified as the induction of a faster and higher immune responses in plants (Conrath et al., 2001). *Arabidopsis* plants pretreated with Benzothiadiazole (BTH), an activator of SAR, showed enhanced PAL transcripts and callose deposition after subsequent inoculation with *Pseudomonas syringae* (Kohler et al., 2002). Moreover, wounding of Arabidopsis leaves caused resistance to *Botrytis* infection which was related to increased camalexin production (Chassot et al., 2008). Priming has also been shown to induce genes responsive to JA, SA or ET (Kohler et al., 2002, Verhagen et al., 2004).

The evaluation of priming depends on the costs and benefits of the process. Treatments with low doses of chemicals such as β-aminobutyric acid (BABA) or BTH did not affect growth and seed production of *Arabidopsis* plants, however, treatment with higher doses or infection with *P. syringae* affected them (van Hulten et al., 2006). Although these two priming events enhanced the plants fitness to consequent infections, the treatment with low doses of chemicals was the option where the benefits outweighed the costs. These states were described recently as the priming phase for the earlier and the post-challenge primed state for the later (Balmer et al., 2015).

Our data suggests a post-challenge primed stage where camalexin, GSs and phenylpropanoids pathways were upregulated due to continuous flg22 treatment and remained high to protect the plant from consequent infection.

4.3. Auxin efflux transporters PIN3 and PIN7 are important for growth-defense transition

Immune responses have been known to have a negative effect on growth in a phenomenon known as the growth – defense trade-off (Brown, 2003). It is believed that the costs of the activated immune response are the causes of hindered growth (Karasov et al., 2017). Moreover, the crosstalk between different hormones plays an important role in the regulation of growth and immunity (Chaiwanon et al., 2016). Auxin regulates cell elongation and development of different organs through polar auxin transport (PAT) which is regulated by different transporters where PINs have shown to play an important role (Adamowski and Friml, 2015).

In this study, PIN3 and 7 transcript and protein levels decreased significantly as early as 1 and 3 hrs after flg22 treatment, respectively, suggesting an effect on PAT (Figure 3-6/ p.41). Likewise, microarray data demonstrated a decrease in PIN3 and 7 gene expression after 1 and 3 hrs of flg22 treatment (Denoux et al., 2008). Furthermore, flg22 has been shown to inhibit growth of *A. thaliana* Col-0 seedlings after 2 weeks of treatment with 10 µM (Gómez-Gómez et al., 1999). PIN3 is known to be responsible for lateral auxin transport (Friml et al., 2002), whereas, PIN7 demonstrated an important role in auxin vertical transport (Friml et al., 2003). Moreover, flg22 treatment activated phosphorylation of PIN1 by MPK6 and changed its location to become intracellular, which was also expected to happen to other PINs (Dory et al., 2018). A co-expression network for *Arabidopsis* PIN proteins showed a direct significant correlation between PIN3, 4 and 7 (Zhou and Luo, 2018). So, it is plausible that down regulation of PIN3 and 7 by flg22 affects the auxin gradient and possibly leads to growth inhibition.

Interestingly, after the removal of the elicitor, PINs increased gradually returning to near normal levels at 32 hrs while there was no effect on auxin levels themselves. In comparison to other decreasing proteins such as proteins involved in photosynthesis, PINs recovery was fast implying their importance in attaining auxin gradients and regulation of growth. This could be a part of an important mechanism for the recovery from immunity to growth states.

In *myc234*, a similar trend of PIN3 and 7 protein and transcript levels was observed as in Col-0 (Figure 3-11/ p.49). In general, control (0 hrs) transcript levels were lower and recovery of PINs was faster in *myc234*. PIN3 and 7 were found to be targets to MYC2 and 3, yet JA did not have any significant effect on their gene expression (Zander et al., 2020). Moreover, microarray data did not show any difference in basic PIN3 and 7 expression between Col-0 and *myc234* (Schweizer et al., 2013). The master regulator of ethylene (ET) signaling Ethylene Insensitive 3

(EIN3) has been found to target PIN7 genes (Chang et al., 2013) while PIN3 genes were found to be a target for ERF1 and ORA59 which are also regulated by ET (Zander et al., 2020). Accordingly, PIN3 and 7 regulation is affected by multiple pathways and this regulation is expected to have a role in the growth-defense trade-off.

4.4. MYC controlled Jasmonic Acid Oxidase 2 (JOX2) and IAA-Alanine Resistant 3 (IAR3) inactivates JA and JA-Ile in PTI

Pathogens attack plants to feed on their nutrients and two types of feeding divide the pathogens into two categories; necrotrophs and biotrophs that feed on dead or living cells, respectively (Glazebrook, 2005). It is also widely accepted that biotrophic pathogens activate the SA pathway whereas necrotrophic pathogens and wounding activate the JA pathway, however, the reality is more complicated cross talk between these two signaling pathways (Spoel et al., 2007). Antagonism between JA and SA signaling has been widely demonstrated. Higher levels of JA and increased expression of JA responsive genes was observed in transgenic NahG *Arabidopsis* plants, that are unable to accumulate SA, after infection with *Pseudomonas syringae* pv *tomato* DC3000 (Spoel et al., 2003). Moreover, COR, which activates jasmonate signaling, was shown to be important for the suppression of SA induced defenses (Brooks et al., 2005).

JA is usually conjugated by JAR1 to form the active compound JA-Ile (Staswick et al., 2002). Catabolism of JA and JA-Ile is established in the wound response, where two main pathways are recognized (Smirnova et al., 2017). The first is composed of two ω-oxidation steps where JA-Ile is converted to 12-OH-JA-Ile then 12-COOH-JA-Ile by CYP94B1/3 and CYP94C1, respectively (Heitz et al., 2012, Koo et al., 2014), or 12-OH-JA-Ile is deconjugated back to 12-OH-JA by IAR3/ILL6 (Widemann et al., 2013, Zhang et al., 2016). The second pathway involves the direct oxidation of JA to 12-OH-JA by the JA Oxidases (JOXs), which was shown to be more prominent under necrotrophic pathogen attack (Caarls et al., 2017, Smirnova et al., 2017).

In this study, flg22 was used as an elicitor resembling *Pseudomonas syringae* flagella which is a known biotroph. JA and JA-Ile increased to their highest levels at 3 hrs post elicitation in Col-0 then there was no change for the former and a decrease for the later (Figure 3-5/ p.39). Moreover, the JA precursor OPDA increased to high levels 1 hrs after flg22 treatment and remained high until 32 hrs. At the same time, the abundance of JA biosynthesis genes transcripts increased significantly as early as 1 hrs, while on the protein level some reached a maximum at 16 hrs and remained high until 32 hrs. JAR1 did not show any significant changes throughout the experiment.

However, JOX2 and IAR3 transcripts increased significantly at 1 hrs and their protein levels followed at 3 and 16 hrs, respectively. Moreover, CYP94B1/3 transcripts did not increase in abundance while CYP94C1 increased significantly at 1 and 3 hrs and then returned to normal levels. 12-OH-JA showed a trend that follows JOX2 and IAR3 increase as it reached significance at 3 hrs and continued to be high whereas JA and JA-Ile stopped changing after this time point. This indicates that the catabolism of JA or JA-Ile follows the second previously mentioned pathway which involves mainly JOX2.

Interestingly in *myc234*, JA biosynthesis genes showed lower transcripts levels in comparison to Col-0 after flg22 treatment (Figure 3-10/ p.47). Moreover, components of the JA catabolic pathway JOX2, IAR3 and CYP94C1 transcripts were lower without elicitation and early response (1 and 3 hrs) was only seen on transcript and not at all on the protein level. The same was observed before in a microarray analysis of non-treated Col-0 and *myc234* plants (Schweizer et al., 2013). JA and JA-Ile levels increased until 16 hrs while 12-OH-JA and OPDA showed their first increase at 16 hrs. However, a different trend was seen previously on the levels of JA, JA-Ile in *myc234* as compared to Col-0 as JA and JA-Ile did not change until 16 hrs in Col-0 while JA increased significantly as early as 1 hrs and JA-Ile increased significantly only after 3 hrs in *myc234* (Abukhalaf et al., 2020). Regardless of that, this data suggests that the JA catabolic pathway is controlled in part by MYC transcription factors which was also recently underscored by MYC2/3 target genes analysis (Zander et al., 2020, Zhang et al., 2020).

A model describing MYC regulated JA catabolism in an early response to biotrophic pathogens was constructed (Figure 4-1). In Col-0, flg22 activates JA biosynthesis and downstream activation of JA responsive genes, by the release of MYCs, including JOX2, IAR3 and CYP94C1 which in turn converts JA and JA-Ile to the inactive 12-OH-JA. However, in *myc234*, flg22 slightly activates JA biosynthesis without affecting JOX2, IAR3 and CYP94C1, thus preventing JA and JA-Ile catabolism.

A network of incoherent type-4 feed-forward loop (I4-FFL) was identified in *Arabidopsis* before to explain SA-JA crosstalk which involves MYCs, PAD4 and EDS5 (Kim et al., 2014, Mine et al., 2017). Flg22 activates PAD4 and later EDS5 which in turn activates SA accumulation. Moreover, flg22 activates JA signaling through MYCs which have negative and positive effects on PAD4 and EDS5, respectively. This may explain the higher ICS1 transcripts and SA levels after flg22 elicitation (Figure 3-12/ p.50) in *myc234* as the negative effects on PAD4 are abolished.

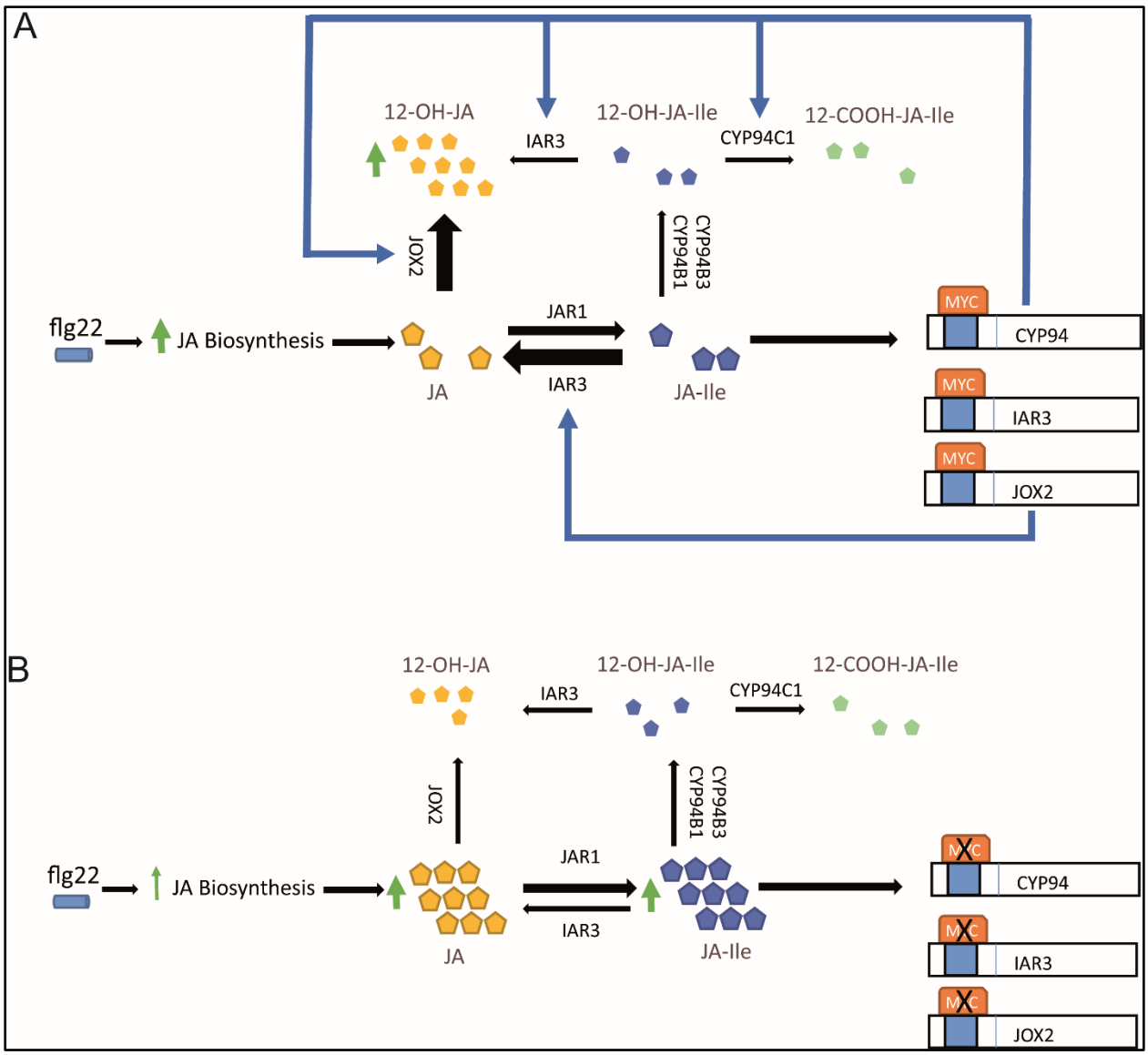

Figure 4-1. A model of jasmonic acid (JA) and JA-Isoleucine (JA-Ile) control by MYC transcription factors in the early response to biotrophic pathogens. Flg22 induce JA biosynthesis and later JA signaling through MYC2/3/4 which activates the expression of CYP94C1, JOX2 and IAR3. This leads to the catabolism of JA and JA-Ile by hydroxylation and deconjugation, respectively, to the inactive 12-OH-JA (A). In the absence of MYCs, expression of these catabolism proteins is blocked and JA and JA-Ile are not catabolized (B). Originally published (Abukhalaf et al., 2020).

4.5. Downregulation of photosynthesis in PTI and the involved MYC control

Increased production of defense compounds upon pathogen attack was expected to increase the demand on photosynthesis (Bekaert et al., 2012). However, activation of the PTI response have been shown to downregulate photosynthetic gene expression (Attaran et al., 2014, Denoux et al., 2008). A decrease in photosynthesis activity measured by chlorophyll fluorescence was observed upon bacterial infection (Bonfig et al., 2006). Moreover, early effects of flg22 treatment led to a rapid decrease in nonphotochemical quenching (Göhre et al., 2012) and long lasting activation of MPK3/6 caused downregulation of photosynthesis genes and ROS accumulation in the chloroplast (Su et al., 2018).

Fifteen photosynthesis proteins out of 23 decreased significantly after 16 hrs of flg22 treatment in Col-0 (Figure 3-8/ p.44). However, these proteins did not increase after flg22 removal and remained low until 32 hrs. Interestingly, the trend in *myc234* was different as the decrease was less pronounced and some proteins were not affected. Moreover, the removal of the elicitor in *myc234* achieved recovery in most of the proteins and even a marked increase in some. JA signaling has been shown before to cause suppression of growth and photosynthesis (Attaran et al., 2014). Moreover, MYC2 was shown to suppress blue light mediated photomorphogenic growth while enhancing lateral root formation (Yadav et al., 2005). It could be possible that the effects seen on photosynthesis are mainly JA regulated, however, they are not directly regulated by MYCs as these proteins were not found to be MYC targets (Zander et al., 2020).

Interestingly, turnover rates of photosynthesis proteins changed in the steady state PTI (Figure 3-16/ p.59). Degradation rates (K_d) were significantly higher and synthesis rates (K_s) were lower in flg22 steady state (flg ss). Twelve proteins out of the previously discussed where included in the calculations disclosing the decrease in protein levels in PTI. Moreover, the high K_d in flg ss could explain the prolonged effect observed after the removal of the elicitor. Accordingly, obtaining protein turnover rates expands the understanding of PTI effects and might provide explanations in *myc234*.

4.6. Transcriptional regulation is not a direct determinant of gene expression especially in PTI

Transcript levels have been used as a proxy for gene expression, however, this process involves also translation and mRNAs and proteins turnover. Correlations between transcripts and proteins

have been demonstrated for multiple organisms. Integrated proteomics and transcriptomics analysis in the yeast *Saccharomyces cerevisiae* showed correlation of 0.356 (Gygi Steven et al., 1999). Moreover, same approaches in mammalian and human cells showed also similar relations (Schwanhausser et al., 2011, Wilhelm et al., 2014) while variable correlations in plants were observed (Vélez-Bermúdez and Schmidt, 2014). Growth or perturbations in the system might lead to even lower correlations that can be explained by considering turnover rates of mRNA and proteins (Kristensen et al., 2013).

Although a limited number of targets were quantified on protein and transcript levels, similar correlations as reported in the literature were observed in comparison to global studies (Figure 3-13/ p.52). Moreover, the addition of the elicitor caused a considerable effect where transcripts increased or decreased much earlier than proteins leading to negative correlations at 1 and 3 hrs. At 16 hrs, a point of steady state immunity, a near zero correlation was detected. Decreased correlation between transcription and translation was previously reported in PTI (Xu et al., 2017).

Interestingly, further deterioration in the correlation was observed at 17 and 19 hrs after the elicitor removal while an extremely poor positive correlation was observed at 32 hrs due to the stability of the increased proteins. Thus, transitioning from growth to PTI and vice versa leads to considerable effects which could not be explained by transcripts alone.

To overcome this, synthesis and degradation of proteins should be considered which have previously shown to improve transcript to protein prediction (Kristensen et al., 2013, Schwanhausser et al., 2011).

4.7. ^{15}N metabolic labeling LC-MS protein turnover rates measurements and its application in steady state situations

In plants, measurements of turnover rates for a broad number of proteins was made possible by combining LC-MS with partial metabolic labeling such as ^{15}N (Nelson et al., 2014a) where relative isotopic abundance (RIA), a ratio of the remaining naturally abundant peptide (Zhang et al., 2011), was used to calculate degradation rates. However, extracting RIA of peptides from MS data needs special algorithms due to the increased complexity of the spectra. Protover is a program that has been shown to be more effective than other programs as it ensures high data quality by applying multiple filtration steps with reasonable computation times even with large Rt windows (Lyon et al., 2014). Using Protover, RIAs of around 200 peptides were calculated in *Arabidopsis thaliana* Col-0 seedlings with and without elicitation by flg22.

A biological system is considered to be in steady state when the protein abundance does not change over time (Christiano et al., 2014). However, this is not possible in long duration experiments as growth might lead to an increase in protein amount. Accordingly, a steady state was defined as a stable system where protein changes are governed only by the growth rate. In this state, RIAs are used for the calculations of the apparent degradation rate K_{loss} by a linear regression of their natural logarithm (eq.3/p.27) (Nelson et al., 2013). However, important factors have to be considered such as the time until the incorporation of the label in the amino acids (AAs) pool (lag time), which should be used as a starting point in the calculations, and the Coefficient of determination (R^2), which is used to assess the fitness of the linear correlation. The lag time was observed to be 8 hrs at an average of 14% ^{15}N incorporation which is in accordance with previous studies (Li et al., 2017, Nelson et al., 2014a). It was also used as a starting point for the flg22 experiment to ensure robust detection of newly synthesized peptides. Moreover, filtration of the results based on R^2, relative standard error (RSDTE) and discarding negative K_{loss} values was done to improve the quality of the data resulting in 69 proteins K_{loss} values.

The relative decrease in the naturally abundant peptides is not only due to degradation, but also caused by the increase in proteins. This dilution effect (K_{dil}) was calculated by plotting the increase of the seedlings weights over time (Figure 3-14/ p.53) which was also described before (Nelson et al., 2014a). It was apparent that the growth rate was remarkably lower in PTI reflecting the known growth-defense trade-off (Brown, 2003). Degradation rates (K_d), retrieved by subtracting K_{dil} from K_{loss}, showed to be in the same ranges as previously demonstrated (Li et al., 2017), thus the same classification system of the degradation velocity was used (Table 3.1). Negative K_d values were observed as a result of K_{dil} higher than K_{loss} meaning that they were not increasing as fast as the growth rate. However, they were included in the analysis and were considered to be near zero.

Fifty-six protein K_d values were calculated at steady state with and without flg22, yet only 16 proteins showed statistically significant differences. Comparisons of steady state K_d and K_s between flg22 treated and untreated seedlings demonstrated the previously discussed regulation of photosynthesis related proteins by changes in protein turnover. However, non-steady state measurements were more informative.

4.8. Protein turnover rates measurements in non-steady state PTI

A state where the abundance of proteins is rapidly changing is considered a non-steady state (Jayapal et al., 2010). Measurements of protein turnover rates for rapidly changing proteins is

more complex as changes in protein abundance should be considered (Li et al., 2012). However, mathematical models using protein fold changes (FCP) with RIA are able to calculate K_d and K_s in these states (Li et al., 2017).

The PRM data after flg22 treatment data was used to assess fold changes in abundance of rapidly changing proteins. Proteins considered in this state were either increasing or decreasing to 1.5 and 0.75 FCPs, respectively, at 1,3 or 16 hrs. Using a polynomial regression for FCPs of 52 proteins under the previous criteria to calculate their FCPs at 2, 4, 6, 8 hrs was effective as an average R^2 of 0.95 was observed (Supplementary Table 10/ p.105). Filtrations on turnover rates under the same criteria as in steady state resulted in 28 protein turnover rates (Table 3.2). Although K_d as a rate constant should not be negative, it was still observed in rapidly increasing proteins which could be due to the availability of naturally abundant amino acids coming from degradation of other proteins or incomplete labeling (Doherty et al., 2005, Jayapal et al., 2010). However, proteins with negative K_d values were considered for calculations of K_s values where most of the rapidly increasing proteins demonstrated high K_s values and decreasing proteins showed high and low K_d and K_s values, respectively, as expected.

Proteins were expected to reach their highest or lowest after 16 hrs. This was confirmed by the observed decrease in K_s reaching its lowest at 16 hrs (Figure 3-15/ p.58). Moreover, strong correlations between FCPs and calculated K_s were observed at 1 and 3 hrs while it was lost at 16 hrs. This further confirmed the expectation that 16 hrs represents steady state PTI. Together these measurements showed that post transcriptional regulation of protein abundance by way of flg22 induced changes in protein synthesis and degradation rates make an important contribution to remodeling the proteome in PTI in addition to the changes in gene expression, i.e., increase or decrease of cognate mRNA levels.

5. Summary

Plants protect themselves from multiple different pathogens by physical barriers. Some pathogens overcome these barriers leading to the activation of pattern triggered immunity (PTI). The PTI response starts when pattern recognition receptors (PRRs) recognize pathogen associated molecular patterns (PAMPs), thus leading to the activation of different signaling pathways on multiple levels including transcripts, proteins and hormones. Previous transcriptomic studies revealed regulations of jasmonic acid (JA), salicylic acid and secondary metabolites such as glucosinolates pathways while proteomic studies were limited. However, our recent deep proteomics study confirmed these findings with added insights on the defense-growth trade-off.

The aim was to study transitions from PTI to growth and vice versa in a multi-omics approach using the most sensitive and specific techniques. An experimental design using the elicitor flg22 was developed to cover early and late transition to PTI in *Arabidopsis thaliana* Col-0 seedlings while transferring the elicited seedlings into fresh PAMP free media modeled the transition to growth. A parallel reaction monitoring label free targeted proteomics approach coupled to retention time scheduling quantified 99 proteins at multiple experimental time points in addition to qPCR and LC-MS analysis of 38 genes and 7 metabolites, respectively. Moreover, the same was performed in the *myc234* mutant background to gain a closer insight into effects on the JA signaling pathway.

Pathways of tryptophan, glucosinolates, phenylpropanoids and camalexin biosynthesis increased gradually in the transition to PTI but did not decrease after the removal of the elicitor. Auxin efflux transporters PIN3 and 7 decreased gradually after elicitation and increased gradually in the transition to growth. Late PTI response led to the downregulation of photosynthesis proteins in Col-0 while the same effect was not observed in *myc234*. Moreover, JA Oxidase (JOX2) and IAA-Alanine Resistant 3 (IAR3) increased on transcript and protein levels early after flg22 treatment leading to production of 12-hydroxy JA (12-OH-JA) from JA and JA-Isoleucine (JA-Ile) in Col-0 in contrary to *myc234*. This introduced a MYC regulated model of JA catabolism in the early response to biotrophic pathogens.

Poor correlations between transcripts and their cognate proteins were observed throughout the experiment illuminating the importance of protein turnover rates. Accordingly, turnover rates of target proteins in normal and steady state and non-steady state PTI were measured using ^{15}N metabolic labeling with LC-MS proteomics. It was observed that the degradation rates of

photosynthesis proteins were higher in the steady state PTI. Moreover, synthesis rates were a major determinant of protein abundance in non-steady state PTI.

6. References

ABUKHALAF, M., BASSAL, M., MAJOVSKY, P., THIEME, D., HERR, T., AYASH, M., TABASSUM, N., AL SHWEIKI, M. R., PROKSCH, C., HMEDAT, A., ZIEGLER, J., LEE, J., NEUMANN, S. & HOEHENWARTER, W. 2020. Reshaping of the Arabidopsis thaliana Proteome Landscape and Co-regulation of Proteins in Development and Immunity. *Mol Plant,* 13**,** 1709-1732.

ADAMOWSKI, M. & FRIML, J. 2015. PIN-dependent auxin transport: action, regulation, and evolution. *The Plant cell,* 27**,** 20-32.

AHUJA, I., KISSEN, R. & BONES, A. M. 2012. Phytoalexins in defense against pathogens. *Trends Plant Sci,* 17**,** 73-90.

AL SHWEIKI, M. R., MÖNCHGESANG, S., MAJOVSKY, P., THIEME, D., TRUTSCHEL, D. & HOEHENWARTER, W. 2017. Assessment of Label-Free Quantification in Discovery Proteomics and Impact of Technological Factors and Natural Variability of Protein Abundance. *Journal of proteome research,* 16**,** 1410-1424.

ALTELAAR, A. F., MUNOZ, J. & HECK, A. J. 2013. Next-generation proteomics: towards an integrative view of proteome dynamics. *Nat Rev Genet,* 14**,** 35-48.

AMERICA, A. H. P. & CORDEWENER, J. H. G. 2008. Comparative LC-MS: A landscape of peaks and valleys. *PROTEOMICS,* 8**,** 731-749.

ANDERSON, L. & HUNTER, C. L. 2006. Quantitative mass spectrometric multiple reaction monitoring assays for major plasma proteins. *Mol Cell Proteomics,* 5**,** 573-88.

ASAI, T., TENA, G., PLOTNIKOVA, J., WILLMANN, M. R., CHIU, W.-L., GOMEZ-GOMEZ, L., BOLLER, T., AUSUBEL, F. M. & SHEEN, J. 2002. MAP kinase signalling cascade in Arabidopsis innate immunity. *Nature,* 415**,** 977-983.

ATTARAN, E., MAJOR, I. T., CRUZ, J. A., ROSA, B. A., KOO, A. J. K., CHEN, J., KRAMER, D. M., HE, S. Y. & HOWE, G. A. 2014. Temporal Dynamics of Growth and Photosynthesis Suppression in Response to Jasmonate Signaling *Plant Physiology,* 165**,** 1302-1314.

BALMER, A., PASTOR, V., GAMIR, J., FLORS, V. & MAUCH-MANI, B. 2015. The 'prime-ome': towards a holistic approach to priming. *Trends in Plant Science,* 20**,** 443-452.

BANTSCHEFF, M., LEMEER, S., SAVITSKI, M. M. & KUSTER, B. 2012. Quantitative mass spectrometry in proteomics: critical review update from 2007 to the present. *Anal Bioanal Chem,* 404**,** 939-65.

BATY, J. D. & ROBINSON, P. R. 1977. Single and multiple ion recording techniques for the analysis of diphenylhydantoin and its major metabolite in plasma. *Biomed Mass Spectrom,* 4**,** 36-41.

BEDNAREK, P. 2012a. Chemical warfare or modulators of defence responses – the function of secondary metabolites in plant immunity. *Current Opinion in Plant Biology,* 15**,** 407-414.

BEDNAREK, P. 2012b. Sulfur-Containing Secondary Metabolites from Arabidopsis thaliana and other Brassicaceae with Function in Plant Immunity. *ChemBioChem,* 13**,** 1846-1859.

BEDNAREK, P., PIŚLEWSKA-BEDNAREK, M., VER LOREN VAN THEMAAT, E., MADDULA, R. K., SVATOŠ, A. & SCHULZE-LEFERT, P. 2011. Conservation and

clade-specific diversification of pathogen-inducible tryptophan and indole glucosinolate metabolism in Arabidopsis thaliana relatives. *New Phytologist,* 192**,** 713-726.

BEKAERT, M., EDGER, P. P., HUDSON, C. M., PIRES, J. C. & CONANT, G. C. 2012. Metabolic and evolutionary costs of herbivory defense: systems biology of glucosinolate synthesis. *New Phytologist,* 196**,** 596-605.

BENKOVÁ, E., MICHNIEWICZ, M., SAUER, M., TEICHMANN, T., SEIFERTOVÁ, D., JÜRGENS, G. & FRIML, J. 2003. Local, Efflux-Dependent Auxin Gradients as a Common Module for Plant Organ Formation. *Cell,* 115**,** 591-602.

BENSIMON, A., HECK, A. J. & AEBERSOLD, R. 2012. Mass spectrometry-based proteomics and network biology. *Annu Rev Biochem,* 81**,** 379-405.

BONFIG, K. B., SCHREIBER, U., GABLER, A., ROITSCH, T. & BERGER, S. 2006. Infection with virulent and avirulent P. syringae strains differentially affects photosynthesis and sink metabolism in Arabidopsis leaves. *Planta,* 225**,** 1-12.

BOUDSOCQ, M., WILLMANN, M. R., MCCORMACK, M., LEE, H., SHAN, L., HE, P., BUSH, J., CHENG, S.-H. & SHEEN, J. 2010. Differential innate immune signalling via Ca(2+) sensor protein kinases. *Nature,* 464**,** 418-422.

BROOKS, D. M., BENDER, C. L. & KUNKEL, B. N. 2005. The Pseudomonas syringae phytotoxin coronatine promotes virulence by overcoming salicylic acid-dependent defences in Arabidopsis thaliana. *Molecular Plant Pathology,* 6**,** 629-639.

BROWN, J. K. M. 2003. A cost of disease resistance: paradigm or peculiarity? *Trends in Genetics,* 19**,** 667-671.

CAARLS, L., ELBERSE, J., AWWANAH, M., LUDWIG, N. R., DE VRIES, M., ZEILMAKER, T., VAN WEES, S. C. M., SCHUURINK, R. C. & VAN DEN ACKERVEKEN, G. 2017. Arabidopsis JASMONATE-INDUCED OXYGENASES down-regulate plant immunity by hydroxylation and inactivation of the hormone jasmonic acid. *Proc Natl Acad Sci U S A,* 114**,** 6388-6393.

CAMBRIDGE, S. B., GNAD, F., NGUYEN, C., BERMEJO, J. L., KRÜGER, M. & MANN, M. 2011. Systems-wide Proteomic Analysis in Mammalian Cells Reveals Conserved, Functional Protein Turnover. *Journal of Proteome Research,* 10**,** 5275-5284.

CHAHROUR, O., COBICE, D. & MALONE, J. 2015. Stable isotope labelling methods in mass spectrometry-based quantitative proteomics. *J Pharm Biomed Anal,* 113**,** 2-20.

CHAIWANON, J., WANG, W., ZHU, J. Y., OH, E. & WANG, Z. Y. 2016. Information Integration and Communication in Plant Growth Regulation. *Cell,* 164**,** 1257-1268.

CHAMBERS, M. C., MACLEAN, B., BURKE, R., AMODEI, D., RUDERMAN, D. L., NEUMANN, S., GATTO, L., FISCHER, B., PRATT, B., EGERTSON, J., HOFF, K., KESSNER, D., TASMAN, N., SHULMAN, N., FREWEN, B., BAKER, T. A., BRUSNIAK, M.-Y., PAULSE, C., CREASY, D., FLASHNER, L., KANI, K., MOULDING, C., SEYMOUR, S. L., NUWAYSIR, L. M., LEFEBVRE, B., KUHLMANN, F., ROARK, J., RAINER, P., DETLEV, S., HEMENWAY, T., HUHMER, A., LANGRIDGE, J., CONNOLLY, B., CHADICK, T., HOLLY, K., ECKELS, J., DEUTSCH, E. W., MORITZ, R. L., KATZ, J. E., AGUS, D. B., MACCOSS, M., TABB, D. L. & MALLICK, P. 2012. A cross-platform toolkit for mass spectrometry and proteomics. *Nature Biotechnology,* 30**,** 918-920.

CHANG, K. N., ZHONG, S., WEIRAUCH, M. T., HON, G., PELIZZOLA, M., LI, H., HUANG, S.-S. C., SCHMITZ, R. J., URICH, M. A., KUO, D., NERY, J. R., QIAO, H., YANG, A., JAMALI, A., CHEN, H., IDEKER, T., REN, B., BAR-JOSEPH, Z., HUGHES, T. R. & ECKER, J. R. 2013. Temporal transcriptional response to ethylene gas drives growth hormone cross-regulation in Arabidopsis. *eLife,* 2**,** e00675.

CHASSOT, C., BUCHALA, A., SCHOONBEEK, H.-J., MÉTRAUX, J.-P. & LAMOTTE, O. 2008. Wounding of Arabidopsis leaves causes a powerful but transient protection against Botrytis infection. *The Plant Journal,* 55**,** 555-567.

CHELIUS, D. & BONDARENKO, P. V. 2002. Quantitative Profiling of Proteins in Complex Mixtures Using Liquid Chromatography and Mass Spectrometry. *Journal of Proteome Research,* 1**,** 317-323.

CHEN, W. P., YANG, X. Y., HARMS, G. L., GRAY, W. M., HEGEMAN, A. D. & COHEN, J. D. 2011. An automated growth enclosure for metabolic labeling of Arabidopsis thaliana with 13C-carbon dioxide - an in vivo labeling system for proteomics and metabolomics research. *Proteome Sci,* 9**,** 9.

CHINCHILLA, D., ZIPFEL, C., ROBATZEK, S., KEMMERLING, B., NÜRNBERGER, T., JONES, J. D. G., FELIX, G. & BOLLER, T. 2007. A flagellin-induced complex of the receptor FLS2 and BAK1 initiates plant defence. *Nature,* 448**,** 497-500.

CHINI, A., FONSECA, S., FERNÁNDEZ, G., ADIE, B., CHICO, J. M., LORENZO, O., GARCÍA-CASADO, G., LÓPEZ-VIDRIERO, I., LOZANO, F. M., PONCE, M. R., MICOL, J. L. & SOLANO, R. 2007. The JAZ family of repressors is the missing link in jasmonate signalling. *Nature,* 448**,** 666-671.

CHISHOLM, S. T., COAKER, G., DAY, B. & STASKAWICZ, B. J. 2006. Host-Microbe Interactions: Shaping the Evolution of the Plant Immune Response. *Cell,* 124**,** 803-814.

CHOE, L., D'ASCENZO, M., RELKIN, N. R., PAPPIN, D., ROSS, P., WILLIAMSON, B., GUERTIN, S., PRIBIL, P. & LEE, K. H. 2007. 8-Plex quantitation of changes in cerebrospinal fluid protein expression in subjects undergoing intravenous immunoglobulin treatment for Alzheimer's disease. *PROTEOMICS,* 7**,** 3651-3660.

CHRISTIANO, R., NAGARAJ, N., FRÖHLICH, F. & WALTHER, TOBIAS C. 2014. Global Proteome Turnover Analyses of the Yeasts S. cerevisiae and S. pombe. *Cell Reports,* 9**,** 1959-1965.

CLAY NICOLE, K., ADIO ADEWALE, M., DENOUX, C., JANDER, G. & AUSUBEL FREDERICK, M. 2009. Glucosinolate Metabolites Required for an Arabidopsis Innate Immune Response. *Science,* 323**,** 95-101.

CONRATH, U., THULKE, O., KATZ, V., SCHWINDLING, S. & KOHLER, A. 2001. Priming as a Mechanism in Induced Systemic Resistance of Plants. *European Journal of Plant Pathology,* 107**,** 113-119.

COOK, D. E., MESARICH, C. H. & THOMMA, B. P. 2015. Understanding plant immunity as a surveillance system to detect invasion. *Annu Rev Phytopathol,* 53**,** 541-63.

COX, J., HEIN, M. Y., LUBER, C. A., PARON, I., NAGARAJ, N. & MANN, M. 2014. Accurate proteome-wide label-free quantification by delayed normalization and maximal peptide ratio extraction, termed MaxLFQ. *Molecular & cellular proteomics : MCP,* 13**,** 2513-2526.

COX, J. & MANN, M. 2011. Quantitative, high-resolution proteomics for data-driven systems biology. *Annu Rev Biochem,* 80**,** 273-99.

DANGL, J. L. & JONES, J. D. G. 2001. Plant pathogens and integrated defence responses to infection. *Nature,* 411**,** 826-833.

DEMICHEV, V., MESSNER, C. B., VERNARDIS, S. I., LILLEY, K. S. & RALSER, M. 2020. DIA-NN: neural networks and interference correction enable deep proteome coverage in high throughput. *Nature methods,* 17**,** 41-44.

DEMPSEY, D. M. A., SHAH, J. & KLESSIG, D. F. 1999. Salicylic Acid and Disease Resistance in Plants. *Critical Reviews in Plant Sciences,* 18**,** 547-575.

DENOUX, C., GALLETTI, R., MAMMARELLA, N., GOPALAN, S., WERCK, D., DE LORENZO, G., FERRARI, S., AUSUBEL, F. M. & DEWDNEY, J. 2008. Activation of defense response pathways by OGs and Flg22 elicitors in Arabidopsis seedlings. *Mol Plant,* 1**,** 423-45.

DING, P. & DING, Y. 2020. Stories of Salicylic Acid: A Plant Defense Hormone. *Trends Plant Sci,* 25**,** 549-565.

DOHERTY, M. K., WHITEHEAD, C., MCCORMACK, H., GASKELL, S. J. & BEYNON, R. J. 2005. Proteome dynamics in complex organisms: Using stable isotopes to monitor individual protein turnover rates. *PROTEOMICS,* 5**,** 522-533.

DORY, M., HATZIMASOURA, E., KÁLLAI, B. M., NAGY, S. K., JÄGER, K., DARULA, Z., NÁDAI, T. V., MÉSZÁROS, T., LÓPEZ-JUEZ, E., BARNABÁS, B., PALME, K., BÖGRE, L., DITENGOU, F. A. & DÓCZI, R. 2018. Coevolving MAPK and PID phosphosites indicate an ancient environmental control of PIN auxin transporters in land plants. *FEBS Lett,* 592**,** 89-102.

DU, C., LIU, H.-F., LIN, Y.-Z., WANG, X.-F., MA, J., LI, Y.-J., WANG, X. & ZHOU, J.-H. 2015. Proteomic alteration of equine monocyte-derived macrophages infected with equine infectious anemia virus. *PROTEOMICS,* 15**,** 1843-1858.

EDMAN, P. & BEGG, G. 1967. A Protein Sequenator. *European Journal of Biochemistry,* 1**,** 80-91.

ENG, J. K., MCCORMACK, A. L. & YATES, J. R. 1994. An approach to correlate tandem mass spectral data of peptides with amino acid sequences in a protein database. *J Am Soc Mass Spectrom,* 5**,** 976-89.

FENN, J. B., MANN, M., MENG, C. K., WONG, S. F. & WHITEHOUSE, C. M. 1989. Electrospray Ionization for Mass Spectrometry of Large Biomolecules. *Science,* 246**,** 64-71.

FERGUSON, P. L. & SMITH, R. D. 2003. Proteome analysis by mass spectrometry. *Annu Rev Biophys Biomol Struct,* 32**,** 399-424.

FEUSSNER, I. & WASTERNACK, C. 2002. THE LIPOXYGENASE PATHWAY. *Annual Review of Plant Biology,* 53**,** 275-297.

FRIML, J., VIETEN, A., SAUER, M., WEIJERS, D., SCHWARZ, H., HAMANN, T., OFFRINGA, R. & JÜRGENS, G. 2003. Efflux-dependent auxin gradients establish the apical–basal axis of Arabidopsis. *Nature,* 426**,** 147-153.

FRIML, J., WIŚNIEWSKA, J., BENKOVÁ, E., MENDGEN, K. & PALME, K. 2002. Lateral relocation of auxin efflux regulator PIN3 mediates tropism in Arabidopsis. *Nature,* 415**,** 806-809.

GALLIEN, S. & DOMON, B. 2015. Detection and quantification of proteins in clinical samples using high resolution mass spectrometry. *Methods,* 81**,** 15-23.

GALLIEN, S., DURIEZ, E., CRONE, C., KELLMANN, M., MOEHRING, T. & DOMON, B. 2012a. Targeted proteomic quantification on quadrupole-orbitrap mass spectrometer. *Molecular & cellular proteomics : MCP,* 11**,** 1709-1723.

GALLIEN, S., PETERMAN, S., KIYONAMI, R., SOUADY, J., DURIEZ, E., SCHOEN, A. & DOMON, B. 2012b. Highly multiplexed targeted proteomics using precise control of peptide retention time. *PROTEOMICS,* 12**,** 1122-1133.

GANGULY, A., PARK, M., KESAWAT, M. S. & CHO, H.-T. 2014. Functional Analysis of the Hydrophilic Loop in Intracellular Trafficking of Arabidopsis PIN-FORMED Proteins *The Plant Cell,* 26**,** 1570-1585.

GAO, M., LIU, J., BI, D., ZHANG, Z., CHENG, F., CHEN, S. & ZHANG, Y. 2008. MEKK1, MKK1/MKK2 and MPK4 function together in a mitogen-activated protein kinase cascade to regulate innate immunity in plants. *Cell Research,* 18**,** 1190-1198.

GEISLER, M., ARYAL, B., DI DONATO, M. & HAO, P. 2017. A Critical View on ABC Transporters and Their Interacting Partners in Auxin Transport. *Plant and Cell Physiology,* 58**,** 1601-1614.

GLAUSER, G., DUBUGNON, L., MOUSAVI, S. A., RUDAZ, S., WOLFENDER, J. L. & FARMER, E. E. 2009. Velocity estimates for signal propagation leading to systemic jasmonic acid accumulation in wounded Arabidopsis. *J Biol Chem,* 284**,** 34506-13.

GLAZEBROOK, J. 2005. Contrasting Mechanisms of Defense Against Biotrophic and Necrotrophic Pathogens. *Annual Review of Phytopathology,* 43**,** 205-227.

GÖHRE, V., JONES, A. M. E., SKLENÁŘ, J., ROBATZEK, S. & WEBER, A. P. M. 2012. Molecular Crosstalk Between PAMP-Triggered Immunity and Photosynthesis. *Molecular Plant-Microbe Interactions®,* 25**,** 1083-1092.

GÓMEZ-GÓMEZ, L. & BOLLER, T. 2000. FLS2: an LRR receptor-like kinase involved in the perception of the bacterial elicitor flagellin in Arabidopsis. *Mol Cell,* 5**,** 1003-11.

GÓMEZ-GÓMEZ, L., FELIX, G. & BOLLER, T. 1999. A single locus determines sensitivity to bacterial flagellin in Arabidopsis thaliana. *Plant J,* 18**,** 277-84.

GRUHLER, A., SCHULZE, W. X., MATTHIESEN, R., MANN, M. & JENSEN, O. N. 2005. Stable isotope labeling of Arabidopsis thaliana cells and quantitative proteomics by mass spectrometry. *Mol Cell Proteomics,* 4**,** 1697-709.

GYGI, S. P., RIST, B., GERBER, S. A., TURECEK, F., GELB, M. H. & AEBERSOLD, R. 1999. Quantitative analysis of complex protein mixtures using isotope-coded affinity tags. *Nature Biotechnology,* 17**,** 994-999.

GYGI STEVEN, P., ROCHON, Y., FRANZA, B. R. & AEBERSOLD, R. 1999. Correlation between Protein and mRNA Abundance in Yeast. *Molecular and Cellular Biology,* 19**,** 1720-1730.

HAMANN, T. 2012. Plant cell wall integrity maintenance as an essential component of biotic stress response mechanisms. *Frontiers in plant science,* 3**,** 77-77.

HEITZ, T., WIDEMANN, E., LUGAN, R., MIESCH, L., ULLMANN, P., DÉSAUBRY, L., HOLDER, E., GRAUSEM, B., KANDEL, S., MIESCH, M., WERCK-REICHHART, D. & PINOT, F. 2012. Cytochromes P450 CYP94C1 and CYP94B3 Catalyze Two Successive Oxidation Steps of Plant Hormone Jasmonoyl-isoleucine for Catabolic Turnover. *Journal of Biological Chemistry,* 287**,** 6296-6306.

HELLEBUST, J. A. & BIDWELL, R. G. S. 1964. PROTEIN TURNOVER IN ATTACHED WHEAT AND TOBACCO LEAVES. *Canadian Journal of Botany,* 42**,** 1-12.

HENZEL, W. J., BILLECI, T. M., STULTS, J. T., WONG, S. C., GRIMLEY, C. & WATANABE, C. 1993. Identifying proteins from two-dimensional gels by molecular mass searching of peptide fragments in protein sequence databases. *Proceedings of the National Academy of Sciences of the United States of America,* 90**,** 5011-5015.

HILLMER, R. A., TSUDA, K., RALLAPALLI, G., ASAI, S., TRUMAN, W., PAPKE, M. D., SAKAKIBARA, H., JONES, J. D. G., MYERS, C. L. & KATAGIRI, F. 2017. The highly buffered Arabidopsis immune signaling network conceals the functions of its components. *PLOS Genetics,* 13**,** e1006639.

HINKSON, I. V. & ELIAS, J. E. 2011. The dynamic state of protein turnover: It's about time. *Trends in Cell Biology,* 21**,** 293-303.

ISHIGA, Y., UPPALAPATI, S. R., ISHIGA, T., ELAVARTHI, S., MARTIN, B. & BENDER, C. L. 2009. The phytotoxin coronatine induces light-dependent reactive oxygen species in tomato seedlings. *New Phytologist,* 181**,** 147-160.

JAYAPAL, K. P., SUI, S., PHILP, R. J., KOK, Y.-J., YAP, M. G. S., GRIFFIN, T. J. & HU, W.-S. 2010. Multitagging Proteomic Strategy to Estimate Protein Turnover Rates in Dynamic Systems. *Journal of Proteome Research,* 9**,** 2087-2097.

JEWORUTZKI, E., ROELFSEMA, M. R. G., ANSCHÜTZ, U., KROL, E., ELZENGA, J. T. M., FELIX, G., BOLLER, T., HEDRICH, R. & BECKER, D. 2010. Early signaling through the Arabidopsis pattern recognition receptors FLS2 and EFR involves Ca2+-associated opening of plasma membrane anion channels. *The Plant Journal,* 62**,** 367-378.

JONES, J. D. G. & DANGL, J. L. 2006. The plant immune system. *Nature,* 444**,** 323-329.

JUN, L. & XIU-JIE, W. 2006. An Integrative Analysis of the Effects of Auxin on Jasmonic Acid Biosynthesis in Arabidopsis thaliana. *Journal of Integrative Plant Biology,* 48**,** 99-103.

KADOTA, Y., SKLENAR, J., DERBYSHIRE, P., STRANSFELD, L., ASAI, S., NTOUKAKIS, V., JONES, JONATHAN D., SHIRASU, K., MENKE, F., JONES, A. & ZIPFEL, C. 2014. Direct Regulation of the NADPH Oxidase RBOHD by the PRR-Associated Kinase BIK1 during Plant Immunity. *Molecular Cell,* 54**,** 43-55.

KARASOV, T. L., CHAE, E., HERMAN, J. J. & BERGELSON, J. 2017. Mechanisms to Mitigate the Trade-Off between Growth and Defense. *The Plant Cell,* 29**,** 666-680.

KAZAN, K. & MANNERS, J. M. 2009. Linking development to defense: auxin in plant–pathogen interactions. *Trends in Plant Science,* 14**,** 373-382.

KAZAN, K. & MANNERS, J. M. 2013. MYC2: the master in action. *Mol Plant,* 6**,** 686-703.

KELLER, A., NESVIZHSKII, A. I., KOLKER, E. & AEBERSOLD, R. 2002. Empirical Statistical Model To Estimate the Accuracy of Peptide Identifications Made by MS/MS and Database Search. *Analytical Chemistry,* 74**,** 5383-5392.

KELLIE, J. F., TRAN, J. C., LEE, J. E., AHLF, D. R., THOMAS, H. M., NTAI, I., CATHERMAN, A. D., DURBIN, K. R., ZAMDBORG, L., VELLAICHAMY, A., THOMAS, P. M. & KELLEHER, N. L. 2010. The emerging process of Top Down mass spectrometry for protein analysis: biomarkers, protein-therapeutics, and achieving high throughput. *Molecular bioSystems,* 6**,** 1532-1539.

KEMP, J. D. & SUTTON, D. W. 1971. Protein metabolism in cultured plant tissues. Calculation of an absolute rate of protein synthesis, accumulation, and degradation in tobacco callus in vivo. *Biochemistry,* 10**,** 81-88.

KESHISHIAN, H., BURGESS, M. W., GILLETTE, M. A., MERTINS, P., CLAUSER, K. R., MANI, D. R., KUHN, E. W., FARRELL, L. A., GERSZTEN, R. E. & CARR, S. A. 2015. Multiplexed, Quantitative Workflow for Sensitive Biomarker Discovery in Plasma Yields Novel Candidates for Early Myocardial Injury*. *Molecular & Cellular Proteomics,* 14**,** 2375-2393.

KIDDLE, G. A., DOUGHTY, K. J. & WALLSGROVE, R. M. 1994. Salicylic acid-induced accumulation of glucosinolates in oilseed rape (Brassica napus L.) leaves. *Journal of Experimental Botany,* 45**,** 1343-1346.

KIM, Y., TSUDA, K., IGARASHI, D., HILLMER, R. A., SAKAKIBARA, H., MYERS, C. L. & KATAGIRI, F. 2014. Mechanisms underlying robustness and tunability in a plant immune signaling network. *Cell host & microbe,* 15**,** 84-94.

KOBS, G. 1998. Isolation of RNA from plant, yeast and bacteria. *Promega Notes,* 68**,** 28.

KOHLER, A., SCHWINDLING, S. & CONRATH, U. 2002. Benzothiadiazole-induced priming for potentiated responses to pathogen infection, wounding, and infiltration of water into leaves requires the NPR1/NIM1 gene in Arabidopsis. *Plant physiology,* 128**,** 1046-1056.

KOO, A. J., THIREAULT, C., ZEMELIS, S., POUDEL, A. N., ZHANG, T., KITAOKA, N., BRANDIZZI, F., MATSUURA, H. & HOWE, G. A. 2014. Endoplasmic Reticulum-associated Inactivation of the Hormone Jasmonoyl-l-Isoleucine by Multiple Members of the Cytochrome P450 94 Family in Arabidopsis*. *Journal of Biological Chemistry,* 289**,** 29728-29738.

KRASNY, L. & HUANG, P. H. 2021. Data-independent acquisition mass spectrometry (DIA-MS) for proteomic applications in oncology. *Molecular Omics,* 17**,** 29-42.

KRECEK, P., SKUPA, P., LIBUS, J., NARAMOTO, S., TEJOS, R., FRIML, J. & ZAZÍMALOVÁ, E. 2009. The PIN-FORMED (PIN) protein family of auxin transporters. *Genome Biol,* 10**,** 249.

KRISTENSEN, A. R., GSPONER, J. & FOSTER, L. J. 2013. Protein synthesis rate is the predominant regulator of protein expression during differentiation. *Molecular systems biology,* 9**,** 689-689.

LANGE, V., PICOTTI, P., DOMON, B. & AEBERSOLD, R. 2008. Selected reaction monitoring for quantitative proteomics: a tutorial. *Molecular systems biology,* 4**,** 222-222.

LESUR, A., SCHMIT, P.-O., BERNARDIN, F., LETELLIER, E., BREHMER, S., DECKER, J. & DITTMAR, G. 2021. Highly Multiplexed Targeted Proteomics Acquisition on a TIMS-QTOF. *Analytical Chemistry,* 93**,** 1383-1392.

LI, L., LI, M., YU, L., ZHOU, Z., LIANG, X., LIU, Z., CAI, G., GAO, L., ZHANG, X., WANG, Y., CHEN, S. & ZHOU, J.-M. 2014. The FLS2-Associated Kinase BIK1 Directly Phosphorylates the NADPH Oxidase RbohD to Control Plant Immunity. *Cell Host & Microbe,* 15**,** 329-338.

LI, L., NELSON, C. J., SOLHEIM, C., WHELAN, J. & MILLAR, A. H. 2012. Determining degradation and synthesis rates of arabidopsis proteins using the kinetics of progressive 15N labeling of two-dimensional gel-separated protein spots. *Molecular & cellular proteomics : MCP,* 11**,** M111.010025-M111.010025.

LI, L., NELSON, C. J., TROSCH, J., CASTLEDEN, I., HUANG, S. & MILLAR, A. H. 2017. Protein Degradation Rate in Arabidopsis thaliana Leaf Growth and Development. *Plant Cell,* 29**,** 207-228.

LI, X.-J., ZHANG, H., RANISH, J. A. & AEBERSOLD, R. 2003. Automated Statistical Analysis of Protein Abundance Ratios from Data Generated by Stable-Isotope Dilution and Tandem Mass Spectrometry. *Analytical Chemistry,* 75**,** 6648-6657.

LIU, H., SADYGOV, R. G. & YATES, J. R. 2004. A Model for Random Sampling and Estimation of Relative Protein Abundance in Shotgun Proteomics. *Analytical Chemistry,* 76**,** 4193-4201.

LU, D., WU, S., GAO, X., ZHANG, Y., SHAN, L. & HE, P. 2010. A receptor-like cytoplasmic kinase, BIK1, associates with a flagellin receptor complex to initiate plant innate immunity. *Proceedings of the National Academy of Sciences,* 107**,** 496.

LYON, D., CASTILLEJO, M. A., STAUDINGER, C., WECKWERTH, W., WIENKOOP, S. & EGELHOFER, V. 2014. Automated protein turnover calculations from 15N partial metabolic labeling LC/MS shotgun proteomics data. *PLoS One,* 9**,** e94692.

MACHO, A. P. & ZIPFEL, C. 2014. Plant PRRs and the activation of innate immune signaling. *Mol Cell,* 54**,** 263-72.

MACLEAN, B., TOMAZELA, D. M., SHULMAN, N., CHAMBERS, M., FINNEY, G. L., FREWEN, B., KERN, R., TABB, D. L., LIEBLER, D. C. & MACCOSS, M. J. 2010. Skyline: an open source document editor for creating and analyzing targeted proteomics experiments. *Bioinformatics (Oxford, England),* 26**,** 966-968.

MAERKENS, A., KLEY, R. A., OLIVÉ, M., THEIS, V., VAN DER VEN, P. F. M., REIMANN, J., MILTING, H., SCHREINER, A., USZKOREIT, J., EISENACHER, M., BARKOVITS, K., GÜTTSCHES, A. K., TONILLO, J., KUHLMANN, K., MEYER, H. E., SCHRÖDER, R., TEGENTHOFF, M., FÜRST, D. O., MÜLLER, T., GOLDFARB, L. G., VORGERD, M. & MARCUS, K. 2013. Differential proteomic analysis of abnormal intramyoplasmic aggregates in desminopathy. *Journal of proteomics,* 90**,** 14-27.

MAJOVSKY, P., NAUMANN, C., LEE, C. W., LASSOWSKAT, I., TRUJILLO, M., DISSMEYER, N. & HOEHENWARTER, W. 2014. Targeted proteomics analysis of protein degradation in plant signaling on an LTQ-Orbitrap mass spectrometer. *J Proteome Res,* 13**,** 4246-58.

MAKAROV, A. 2000. Electrostatic Axially Harmonic Orbital Trapping: A High-Performance Technique of Mass Analysis. *Analytical Chemistry,* 72**,** 1156-1162.

MAKAROV, A., DENISOV, E., KHOLOMEEV, A., BALSCHUN, W., LANGE, O., STRUPAT, K. & HORNING, S. 2006. Performance Evaluation of a Hybrid Linear Ion Trap/Orbitrap Mass Spectrometer. *Analytical Chemistry,* 78**,** 2113-2120.

MALLICK, P., SCHIRLE, M., CHEN, S. S., FLORY, M. R., LEE, H., MARTIN, D., RANISH, J., RAUGHT, B., SCHMITT, R., WERNER, T., KUSTER, B. & AEBERSOLD, R. 2007. Computational prediction of proteotypic peptides for quantitative proteomics. *Nature Biotechnology,* 25**,** 125-131.

MARTIN, S. F., MUNAGAPATI, V. S., SALVO-CHIRNSIDE, E., KERR, L. E. & LE BIHAN, T. 2012. Proteome Turnover in the Green Alga Ostreococcus tauri by Time Course 15N Metabolic Labeling Mass Spectrometry. *Journal of Proteome Research,* 11**,** 476-486.

MCLAFFERTY, F. W. 1981. Tandem Mass Spectrometry. *Science,* 214**,** 280-287.

MCLAFFERTY, F. W., BREUKER, K., JIN, M., HAN, X., INFUSINI, G., JIANG, H., KONG, X. & BEGLEY, T. P. 2007. Top-down MS, a powerful complement to the high capabilities of proteolysis proteomics. *Febs j,* 274**,** 6256-68.

MEIER, F., BECK, S., GRASSL, N., LUBECK, M., PARK, M. A., RAETHER, O. & MANN, M. 2015. Parallel Accumulation–Serial Fragmentation (PASEF): Multiplying Sequencing Speed and Sensitivity by Synchronized Scans in a Trapped Ion Mobility Device. *Journal of Proteome Research,* 14**,** 5378-5387.

MEINDL, T., BOLLER, T. & FELIX, G. 2000. The bacterial elicitor flagellin activates its receptor in tomato cells according to the address-message concept. *Plant Cell,* 12**,** 1783-94.

MELOTTO, M., UNDERWOOD, W. & HE, S. Y. 2008. Role of stomata in plant innate immunity and foliar bacterial diseases. *Annual review of phytopathology,* 46**,** 101-122.

METEIGNIER, L. V., EL OIRDI, M., COHEN, M., BARFF, T., MATTEAU, D., LUCIER, J. F., RODRIGUE, S., JACQUES, P. E., YOSHIOKA, K. & MOFFETT, P. 2017. Translatome analysis of an NB-LRR immune response identifies important contributors to plant immunity in Arabidopsis. *J Exp Bot,* 68**,** 2333-2344.

MIERSCH, O., NEUMERKEL, J., DIPPE, M., STENZEL, I. & WASTERNACK, C. 2008. Hydroxylated jasmonates are commonly occurring metabolites of jasmonic acid and contribute to a partial switch-off in jasmonate signaling. *New Phytol,* 177**,** 114-127.

MIKKELSEN, M. D., PETERSEN, B. L., GLAWISCHNIG, E., JENSEN, A. B., ANDREASSON, E. & HALKIER, B. A. 2003. Modulation of CYP79 Genes and Glucosinolate Profiles in Arabidopsis by Defense Signaling Pathways. *Plant Physiology,* 131**,** 298-308.

MINE, A., NOBORI, T., SALAZAR-RONDON, M. C., WINKELMÜLLER, T. M., ANVER, S., BECKER, D. & TSUDA, K. 2017. An incoherent feed-forward loop mediates robustness and tunability in a plant immune network. *EMBO reports,* 18**,** 464-476.

MORANT, A. V., JØRGENSEN, K., JØRGENSEN, C., PAQUETTE, S. M., SÁNCHEZ-PÉREZ, R., MØLLER, B. L. & BAK, S. 2008. β-Glucosidases as detonators of plant chemical defense. *Phytochemistry,* 69**,** 1795-1813.

MUELLER, L. N., BRUSNIAK, M.-Y., MANI, D. R. & AEBERSOLD, R. 2008. An Assessment of Software Solutions for the Analysis of Mass Spectrometry Based Quantitative Proteomics Data. *Journal of Proteome Research,* 7**,** 51-61.

MUTZ, K.-O., HEILKENBRINKER, A., LÖNNE, M., WALTER, J.-G. & STAHL, F. 2013. Transcriptome analysis using next-generation sequencing. *Current Opinion in Biotechnology,* 24**,** 22-30.

NEILSON, K. A., ALI, N. A., MURALIDHARAN, S., MIRZAEI, M., MARIANI, M., ASSADOURIAN, G., LEE, A., VAN SLUYTER, S. C. & HAYNES, P. A. 2011. Less label, more free: approaches in label-free quantitative mass spectrometry. *Proteomics,* 11**,** 535-53.

NELSON, C. J., ALEXOVA, R., JACOBY, R. P. & MILLAR, A. H. 2014a. Proteins with high turnover rate in barley leaves estimated by proteome analysis combined with in planta isotope labeling. *Plant Physiol,* 166**,** 91-108.

NELSON, C. J., LI, L., JACOBY, R. P. & MILLAR, A. H. 2013. Degradation Rate of Mitochondrial Proteins in Arabidopsis thaliana Cells. *Journal of Proteome Research,* 12**,** 3449-3459.

NELSON, C. J., LI, L. & MILLAR, A. H. 2014b. Quantitative analysis of protein turnover in plants. *Proteomics,* 14**,** 579-92.

NICKSTADT, A., THOMMA, B. P., FEUSSNER, I., KANGASJÄRVI, J., ZEIER, J., LOEFFLER, C., SCHEEL, D. & BERGER, S. 2004. The jasmonate-insensitive mutant jin1 shows increased resistance to biotrophic as well as necrotrophic pathogens. *Mol Plant Pathol,* 5**,** 425-34.

O'BRIEN, J. A., DAUDI, A., BUTT, V. S. & PAUL BOLWELL, G. 2012. Reactive oxygen species and their role in plant defence and cell wall metabolism. *Planta,* 236**,** 765-779.

OLD, W. M., MEYER-ARENDT, K., AVELINE-WOLF, L., PIERCE, K. G., MENDOZA, A., SEVINSKY, J. R., RESING, K. A. & AHN, N. G. 2005. Comparison of label-free methods for quantifying human proteins by shotgun proteomics. *Mol Cell Proteomics,* 4**,** 1487-502.

ONG, S.-E., BLAGOEV, B., KRATCHMAROVA, I., KRISTENSEN, D. B., STEEN, H., PANDEY, A. & MANN, M. 2002. Stable Isotope Labeling by Amino Acids in Cell Culture, SILAC, as a Simple and Accurate Approach to Expression Proteomics*. *Molecular & Cellular Proteomics,* 1**,** 376-386.

OSBOURN, A. E. 1996. Preformed Antimicrobial Compounds and Plant Defense against Fungal Attack. *The Plant cell,* 8**,** 1821-1831.

PAUWELS, L., BARBERO, G. F., GEERINCK, J., TILLEMAN, S., GRUNEWALD, W., PÉREZ, A. C., CHICO, J. M., BOSSCHE, R. V., SEWELL, J., GIL, E., GARCÍA-CASADO, G., WITTERS, E., INZÉ, D., LONG, J. A., DE JAEGER, G., SOLANO, R. & GOOSSENS, A. 2010. NINJA connects the co-repressor TOPLESS to jasmonate signalling. *Nature,* 464**,** 788-791.

PAUWELS, L. & GOOSSENS, A. 2011. The JAZ Proteins: A Crucial Interface in the Jasmonate Signaling Cascade. *The Plant Cell,* 23**,** 3089-3100.

PÉRET, B., SWARUP, K., FERGUSON, A., SETH, M., YANG, Y., DHONDT, S., JAMES, N., CASIMIRO, I., PERRY, P., SYED, A., YANG, H., REEMMER, J., VENISON, E., HOWELLS, C., PEREZ-AMADOR, M. A., YUN, J., ALONSO, J., BEEMSTER, G. T., LAPLAZE, L., MURPHY, A., BENNETT, M. J., NIELSEN, E. & SWARUP, R. 2012. AUX/LAX genes encode a family of auxin influx transporters that perform distinct functions during Arabidopsis development. *Plant Cell,* 24**,** 2874-85.

PERKINS, D. N., PAPPIN, D. J. C., CREASY, D. M. & COTTRELL, J. S. 1999. Probability-based protein identification by searching sequence databases using mass spectrometry data. *ELECTROPHORESIS,* 20**,** 3551-3567.

PETERSEN, B., CHEN, S., HANSEN, C., OLSEN, C. & HALKIER, B. 2002. Composition and content of glucosinolates in developing Arabidopsis thaliana. *Planta,* 214**,** 562-571.

PETERSON, A. C., RUSSELL, J. D., BAILEY, D. J., WESTPHALL, M. S. & COON, J. J. 2012. Parallel reaction monitoring for high resolution and high mass accuracy quantitative, targeted proteomics. *Molecular & cellular proteomics : MCP,* 11**,** 1475-1488.

PIASECKA, A., JEDRZEJCZAK-REY, N. & BEDNAREK, P. 2015. Secondary metabolites in plant innate immunity: conserved function of divergent chemicals. *New Phytologist,* 206**,** 948-964.

PICOTTI, P. & AEBERSOLD, R. 2012. Selected reaction monitoring-based proteomics: workflows, potential, pitfalls and future directions. *Nat Methods,* 9**,** 555-66.

PIERSMA, S. R., FIEDLER, U., SPAN, S., LINGNAU, A., PHAM, T. V., HOFFMANN, S., KUBBUTAT, M. H. G. & JIMÉNEZ, C. R. 2010. Workflow Comparison for Label-Free, Quantitative Secretome Proteomics for Cancer Biomarker Discovery: Method Evaluation, Differential Analysis, and Verification in Serum. *Journal of Proteome Research,* 9**,** 1913-1922.

PINEDA, M., SAJNANI, C. & BARÓN, M. 2010. Changes induced by the Pepper mild mottle tobamovirus on the chloroplast proteome of Nicotiana benthamiana. *Photosynth Res,* 103**,** 31-45.

PINO, L. K., SEARLE, B. C., BOLLINGER, J. G., NUNN, B., MACLEAN, B. & MACCOSS, M. J. 2020. The Skyline ecosystem: Informatics for quantitative mass spectrometry proteomics. *Mass Spectrometry Reviews,* 39**,** 229-244.

PIOTROWSKI, M., SCHONFELDER, S. & WEILER, E. W. 2001. The Arabidopsis thaliana isogene NIT4 and its orthologs in tobacco encode beta-cyano-L-alanine hydratase/nitrilase. *J Biol Chem,* 276**,** 2616-21.

PRATT, J. M., PETTY, J., RIBA-GARCIA, I., ROBERTSON, D. H. L., GASKELL, S. J., OLIVER, S. G. & BEYNON, R. J. 2002. Dynamics of Protein Turnover, a Missing Dimension in Proteomics*. *Molecular & Cellular Proteomics,* 1**,** 579-591.

QI, L., YAN, J., LI, Y., JIANG, H., SUN, J., CHEN, Q., LI, H., CHU, J., YAN, C., SUN, X., YU, Y., LI, C. & LI, C. 2012. Arabidopsis thaliana plants differentially modulate auxin biosynthesis and transport during defense responses to the necrotrophic pathogen Alternaria brassicicola. *New Phytologist,* 195**,** 872-882.

QIU, J.-L., FIIL, B. K., PETERSEN, K., NIELSEN, H. B., BOTANGA, C. J., THORGRIMSEN, S., PALMA, K., SUAREZ-RODRIGUEZ, M. C., SANDBECH-CLAUSEN, S., LICHOTA, J., BRODERSEN, P., GRASSER, K. D., MATTSSON, O., GLAZEBROOK, J., MUNDY, J. & PETERSEN, M. 2008. Arabidopsis MAP kinase 4 regulates gene expression through transcription factor release in the nucleus. *The EMBO journal,* 27**,** 2214-2221.

RABANI, M., LEVIN, J. Z., FAN, L., ADICONIS, X., RAYCHOWDHURY, R., GARBER, M., GNIRKE, A., NUSBAUM, C., HACOHEN, N., FRIEDMAN, N., AMIT, I. & REGEV, A. 2011. Metabolic labeling of RNA uncovers principles of RNA production and degradation dynamics in mammalian cells. *Nature Biotechnology,* 29**,** 436-442.

RAUNIYAR, N. 2015. Parallel Reaction Monitoring: A Targeted Experiment Performed Using High Resolution and High Mass Accuracy Mass Spectrometry. *Int J Mol Sci,* 16**,** 28566-81.

RODRÍGUEZ-MORENO, L., PINEDA, M., SOUKUPOVÁ, J., MACHO, A. P., BEUZÓN, C. R., BARÓN, M. & RAMOS, C. 2008. Early detection of bean infection by Pseudomonas syringae in asymptomatic leaf areas using chlorophyll fluorescence imaging. *Photosynthesis Research,* 96**,** 27-35.

RONSEIN, G. E., PAMIR, N., VON HALLER, P. D., KIM, D. S., ODA, M. N., JARVIK, G. P., VAISAR, T. & HEINECKE, J. W. 2015. Parallel reaction monitoring (PRM) and

selected reaction monitoring (SRM) exhibit comparable linearity, dynamic range and precision for targeted quantitative HDL proteomics. *Journal of proteomics,* 113**,** 388-399.

ROSS, P. L., HUANG, Y. N., MARCHESE, J. N., WILLIAMSON, B., PARKER, K., HATTAN, S., KHAINOVSKI, N., PILLAI, S., DEY, S., DANIELS, S., PURKAYASTHA, S., JUHASZ, P., MARTIN, S., BARTLET-JONES, M., HE, F., JACOBSON, A. & PAPPIN, D. J. 2004. Multiplexed Protein Quantitation in Saccharomyces cerevisiae Using Amine-reactive Isobaric Tagging Reagents*. *Molecular & Cellular Proteomics,* 3**,** 1154-1169.

SCHIFFMANN, C., HANSEN, R., BAUMANN, S., KUBLIK, A., NIELSEN, P. H., ADRIAN, L., VON BERGEN, M., JEHMLICH, N. & SEIFERT, J. 2014. Comparison of targeted peptide quantification assays for reductive dehalogenases by selective reaction monitoring (SRM) and precursor reaction monitoring (PRM). *Analytical and Bioanalytical Chemistry,* 406**,** 283-291.

SCHILMILLER, A. L., KOO, A. J. & HOWE, G. A. 2007. Functional diversification of acyl-coenzyme A oxidases in jasmonic acid biosynthesis and action. *Plant Physiol,* 143**,** 812-24.

SCHMITTGEN, T. D. & LIVAK, K. J. 2008. Analyzing real-time PCR data by the comparative C(T) method. *Nat Protoc,* 3**,** 1101-8.

SCHOENHEIMER, R., RATNER, S. & RITTENBERG, D. 1939. The Process of Continuous Deamination and Reamination of Amino Acids in the Proteins of Normal Animals. *Science,* 89**,** 272-273.

SCHULZE, B., MENTZEL, T., JEHLE, A. K., MUELLER, K., BEELER, S., BOLLER, T., FELIX, G. & CHINCHILLA, D. 2010. Rapid heteromerization and phosphorylation of ligand-activated plant transmembrane receptors and their associated kinase BAK1. *The Journal of biological chemistry,* 285**,** 9444-9451.

SCHWANHAUSSER, B., BUSSE, D., LI, N., DITTMAR, G., SCHUCHHARDT, J., WOLF, J., CHEN, W. & SELBACH, M. 2011. Global quantification of mammalian gene expression control. *Nature,* 473**,** 337-42.

SCHWEIZER, F., FERNÁNDEZ-CALVO, P., ZANDER, M., DIEZ-DIAZ, M., FONSECA, S., GLAUSER, G., LEWSEY, M. G., ECKER, J. R., SOLANO, R. & REYMOND, P. 2013. Arabidopsis Basic Helix-Loop-Helix Transcription Factors MYC2, MYC3, and MYC4 Regulate Glucosinolate Biosynthesis, Insect Performance, and Feeding Behavior *The Plant Cell,* 25**,** 3117-3132.

SETHI, V., RAGHURAM, B., SINHA, A. K. & CHATTOPADHYAY, S. 2014. A Mitogen-Activated Protein Kinase Cascade Module, MKK3-MPK6 and MYC2, Is Involved in Blue Light-Mediated Seedling Development in Arabidopsis *The Plant Cell,* 26**,** 3343-3357.

SHEVCHENKO, A., JENSEN, O. N., PODTELEJNIKOV, A. V., SAGLIOCCO, F., WILM, M., VORM, O., MORTENSEN, P., SHEVCHENKO, A., BOUCHERIE, H. & MANN, M. 1996. Linking genome and proteome by mass spectrometry: large-scale identification of yeast proteins from two dimensional gels. *Proceedings of the National Academy of Sciences of the United States of America,* 93**,** 14440-14445.

SMIRNOVA, E., MARQUIS, V., POIRIER, L., AUBERT, Y., ZUMSTEG, J., MÉNARD, R., MIESCH, L. & HEITZ, T. 2017. Jasmonic Acid Oxidase 2 Hydroxylates Jasmonic

Acid and Represses Basal Defense and Resistance Responses against Botrytis cinerea Infection. *Molecular Plant,* 10**,** 1159-1173.

SONG, G., HSU, P. Y. & WALLEY, J. W. 2018. Assessment and Refinement of Sample Preparation Methods for Deep and Quantitative Plant Proteome Profiling. *Proteomics,* 18**,** e1800220.

SPOEL, S. H., JOHNSON, J. S. & DONG, X. 2007. Regulation of tradeoffs between plant defenses against pathogens with different lifestyles. *Proceedings of the National Academy of Sciences,* 104**,** 18842.

SPOEL, S. H., KOORNNEEF, A., CLAESSENS, S. M. C., KORZELIUS, J. M. P., VAN PELT, J. A., MUELLER, M. J., BUCHALA, A. J., MÉTRAUX, J.-P., BROWN, R., KAZAN, K., VAN LOON, L. C., DONG, X. & PIETERSE, C. M. J. 2003. NPR1 Modulates Cross-Talk between Salicylate- and Jasmonate-Dependent Defense Pathways through a Novel Function in the Cytosol. *The Plant Cell,* 15**,** 760-770.

STASWICK, P. E. & TIRYAKI, I. 2004. The oxylipin signal jasmonic acid is activated by an enzyme that conjugates it to isoleucine in Arabidopsis. *The Plant cell,* 16**,** 2117-2127.

STASWICK, P. E., TIRYAKI, I. & ROWE, M. L. 2002. Jasmonate response locus JAR1 and several related Arabidopsis genes encode enzymes of the firefly luciferase superfamily that show activity on jasmonic, salicylic, and indole-3-acetic acids in an assay for adenylation. *Plant Cell,* 14**,** 1405-15.

STEEN, H. & MANN, M. 2004. The ABC's (and XYZ's) of peptide sequencing. *Nat Rev Mol Cell Biol,* 5**,** 699-711.

SU, J., YANG, L., ZHU, Q., WU, H., HE, Y., LIU, Y., XU, J., JIANG, D. & ZHANG, S. 2018. Active photosynthetic inhibition mediated by MPK3/MPK6 is critical to effector-triggered immunity. *PLoS Biol,* 16**,** e2004122.

SWARUP, R. & BENNETT, M. 2003. Auxin Transport: The Fountain of Life in Plants? *Developmental Cell,* 5**,** 824-826.

SWARUP, R. & PÉRET, B. 2012. AUX/LAX family of auxin influx carriers-an overview. *Frontiers in plant science,* 3**,** 225-225.

TABASSUM, N., ESCHEN-LIPPOLD, L., ATHMER, B., BARUAH, M., BRODE, M., MALDONADO-BONILLA, L. D., HOEHENWARTER, W., HAUSE, G., SCHEEL, D. & LEE, J. 2020. Phosphorylation-dependent control of an RNA granule-localized protein that fine-tunes defence gene expression at a post-transcriptional level. *Plant J,* 101**,** 1023-1039.

TAN, S., ABAS, M., VERSTRAETEN, I., GLANC, M., MOLNÁR, G., HAJNÝ, J., LASÁK, P., PETŘÍK, I., RUSSINOVA, E., PETRÁŠEK, J., NOVÁK, O., POSPÍŠIL, J. & FRIML, J. 2020. Salicylic Acid Targets Protein Phosphatase 2A to Attenuate Growth in Plants. *Current Biology,* 30**,** 381-395.e8.

TREWAVAS, A. 1972. Control of the Protein Turnover Rates in Lemna minor. *Plant physiology,* 49**,** 47-51.

TSOU, C.-C., AVTONOMOV, D., LARSEN, B., TUCHOLSKA, M., CHOI, H., GINGRAS, A.-C. & NESVIZHSKII, A. I. 2015. DIA-Umpire: comprehensive computational framework for data-independent acquisition proteomics. *Nature Methods,* 12**,** 258-264.

TURCK, C. W., FALICK, A. M., KOWALAK, J. A., LANE, W. S., LILLEY, K. S., PHINNEY, B. S., WEINTRAUB, S. T., WITKOWSKA, H. E. & YATES, N. A. 2007. The

Association of Biomolecular Resource Facilities Proteomics Research Group 2006 Study: Relative Protein Quantitation*. *Molecular & Cellular Proteomics,* 6**,** 1291-1298.

TYANOVA, S., TEMU, T., SINITCYN, P., CARLSON, A., HEIN, M. Y., GEIGER, T., MANN, M. & COX, J. 2016. The Perseus computational platform for comprehensive analysis of (prote)omics data. *Nature Methods,* 13**,** 731.

TYERS, M. & MANN, M. 2003. From genomics to proteomics. *Nature,* 422**,** 193-197.

URISMAN, A., LEVIN, R. S., GORDAN, J. D., WEBBER, J. T., HERNANDEZ, H., ISHIHAMA, Y., SHOKAT, K. M. & BURLINGAME, A. L. 2017. An Optimized Chromatographic Strategy for Multiplexing In Parallel Reaction Monitoring Mass Spectrometry: Insights from Quantitation of Activated Kinases*. *Molecular & Cellular Proteomics,* 16**,** 265-277.

VAN HULTEN, M., PELSER, M., VAN LOON, L. C., PIETERSE, C. M. J. & TON, J. 2006. Costs and benefits of priming for defense in Arabidopsis. *Proceedings of the National Academy of Sciences of the United States of America,* 103**,** 5602-5607.

VÉLEZ-BERMÚDEZ, I. C. & SCHMIDT, W. 2014. The conundrum of discordant protein and mRNA expression. Are plants special? *Frontiers in Plant Science,* 5.

VENABLE, J. D., DONG, M.-Q., WOHLSCHLEGEL, J., DILLIN, A. & YATES, J. R. 2004. Automated approach for quantitative analysis of complex peptide mixtures from tandem mass spectra. *Nature Methods,* 1**,** 39-45.

VERHAGEN, B. W. M., GLAZEBROOK, J., ZHU, T., CHANG, H.-S., VAN LOON, L. C. & PIETERSE, C. M. J. 2004. The Transcriptome of Rhizobacteria-Induced Systemic Resistance in Arabidopsis. *Molecular Plant-Microbe Interactions®,* 17**,** 895-908.

VICKERY, H. B., PUCHER, G. W., SCHOENHEIMER, R. & RITTENBERG, D. 1940. THE ASSIMILATION OF AMMONIA NITROGEN BY THE TOBACCO PLANT: A PRELIMINARY STUDY WITH ISOTOPIC NITROGEN. *Journal of Biological Chemistry,* 135**,** 531-539.

WANG, D., PAJEROWSKA-MUKHTAR, K., CULLER, A. H. & DONG, X. 2007. Salicylic Acid Inhibits Pathogen Growth in Plants through Repression of the Auxin Signaling Pathway. *Current Biology,* 17**,** 1784-1790.

WASTERNACK, C. & HAUSE, B. 2013. Jasmonates: biosynthesis, perception, signal transduction and action in plant stress response, growth and development. An update to the 2007 review in Annals of Botany. *Ann Bot,* 111**,** 1021-58.

WICHMANN, C., MEIER, F., VIRREIRA WINTER, S., BRUNNER, A.-D., COX, J. & MANN, M. 2019. MaxQuant.Live Enables Global Targeting of More Than 25,000 Peptides. *Molecular & Cellular Proteomics,* 18**,** 982-994.

WIDEMANN, E., MIESCH, L., LUGAN, R., HOLDER, E., HEINRICH, C., AUBERT, Y., MIESCH, M., PINOT, F. & HEITZ, T. 2013. The Amidohydrolases IAR3 and ILL6 Contribute to Jasmonoyl-Isoleucine Hormone Turnover and Generate 12-Hydroxyjasmonic Acid Upon Wounding in Arabidopsis Leaves*. *Journal of Biological Chemistry,* 288**,** 31701-31714.

WILHELM, M., SCHLEGL, J., HAHNE, H., GHOLAMI, A. M., LIEBERENZ, M., SAVITSKI, M. M., ZIEGLER, E., BUTZMANN, L., GESSULAT, S., MARX, H., MATHIESON, T., LEMEER, S., SCHNATBAUM, K., REIMER, U., WENSCHUH, H., MOLLENHAUER, M., SLOTTA-HUSPENINA, J., BOESE, J. H., BANTSCHEFF,

M., GERSTMAIR, A., FAERBER, F. & KUSTER, B. 2014. Mass-spectrometry-based draft of the human proteome. *Nature,* 509**,** 582-7.

WILKINS, M. R., PASQUALI, C., APPEL, R. D., OU, K., GOLAZ, O., SANCHEZ, J.-C., YAN, J. X., GOOLEY, A. A., HUGHES, G., HUMPHERY-SMITH, I., WILLIAMS, K. L. & HOCHSTRASSER, D. F. 1996. From Proteins to Proteomes: Large Scale Protein Identification by Two-Dimensional Electrophoresis and Arnino Acid Analysis. *Bio/Technology,* 14**,** 61-65.

WISNIEWSKI, J. R., ZOUGMAN, A., NAGARAJ, N. & MANN, M. 2009. Universal sample preparation method for proteome analysis. *Nat Methods,* 6**,** 359-62.

XIE, X., FENG, S., VUONG, H., LIU, Y., GOODISON, S. & LUBMAN, D. M. 2010. A comparative phosphoproteomic analysis of a human tumor metastasis model using a label-free quantitative approach. *Electrophoresis,* 31**,** 1842-52.

XU, G., GREENE, G. H., YOO, H., LIU, L., MARQUES, J., MOTLEY, J. & DONG, X. 2017. Global translational reprogramming is a fundamental layer of immune regulation in plants. *Nature,* 545**,** 487-490.

YADAV, V., MALLAPPA, C., GANGAPPA, S. N., BHATIA, S. & CHATTOPADHYAY, S. 2005. A Basic Helix-Loop-Helix Transcription Factor in Arabidopsis, MYC2, Acts as a Repressor of Blue Light–Mediated Photomorphogenic Growth. *The Plant Cell,* 17**,** 1953-1966.

YADAV, V., WANG, Z., WEI, C., AMO, A., AHMED, B., YANG, X. & ZHANG, X. 2020. Phenylpropanoid Pathway Engineering: An Emerging Approach towards Plant Defense. *Pathogens (Basel, Switzerland),* 9**,** 312.

YEATS, T. H. & ROSE, J. K. C. 2013. The formation and function of plant cuticles. *Plant physiology,* 163**,** 5-20.

YOO, S. D., CHO, Y. H., TENA, G., XIONG, Y. & SHEEN, J. 2008. Dual control of nuclear EIN3 by bifurcate MAPK cascades in C2H4 signalling. *Nature,* 451**,** 789-95.

ZANDER, M., LEWSEY, M. G., CLARK, N. M., YIN, L., BARTLETT, A., SALDIERNA GUZMAN, J. P., HANN, E., LANGFORD, A. E., JOW, B., WISE, A., NERY, J. R., CHEN, H., BAR-JOSEPH, Z., WALLEY, J. W., SOLANO, R. & ECKER, J. R. 2020. Integrated multi-omics framework of the plant response to jasmonic acid. *Nat Plants,* 6**,** 290-302.

ZHANG, C., LEI, Y., LU, C., WANG, L. & WU, J. 2020. MYC2, MYC3, and MYC4 function additively in wounding-induced jasmonic acid biosynthesis and catabolism. *Journal of Integrative Plant Biology,* 62**,** 1159-1175.

ZHANG, T., POUDEL, A. N., JEWELL, J. B., KITAOKA, N., STASWICK, P., MATSUURA, H. & KOO, A. J. 2016. Hormone crosstalk in wound stress response: wound-inducible amidohydrolases can simultaneously regulate jasmonate and auxin homeostasis in Arabidopsis thaliana. *Journal of Experimental Botany,* 67**,** 2107-2120.

ZHANG, Y., RECKOW, S., WEBHOFER, C., BOEHME, M., GORMANNS, P., EGGE-JACOBSEN, W. M. & TURCK, C. W. 2011. Proteome Scale Turnover Analysis in Live Animals Using Stable Isotope Metabolic Labeling. *Analytical Chemistry,* 83**,** 1665-1672.

ZHOU, J.-J. & LUO, J. 2018. The PIN-FORMED Auxin Efflux Carriers in Plants. *International Journal of Molecular Sciences,* 19.

ZHOU, W., EUDES, F. & LAROCHE, A. 2006. Identification of differentially regulated proteins in response to a compatible interaction between the pathogen Fusarium graminearum and its host, Triticum aestivum. *PROTEOMICS,* 6**,** 4599-4609.

ZIEGLER, J., QWEGWER, J., SCHUBERT, M., ERICKSON, J. L., SCHATTAT, M., BURSTENBINDER, K., GRUBB, C. D. & ABEL, S. 2014. Simultaneous analysis of apolar phytohormones and 1-aminocyclopropan-1-carboxylic acid by high performance liquid chromatography/electrospray negative ion tandem mass spectrometry via 9-fluorenylmethoxycarbonyl chloride derivatization. *J Chromatogr A,* 1362**,** 102-9.

ZIMMER, D., SCHNEIDER, K., SOMMER, F., SCHRODA, M. & MÜHLHAUS, T. 2018. Artificial Intelligence Understands Peptide Observability and Assists With Absolute Protein Quantification. *Frontiers in plant science,* 9**,** 1559-1559.

ZIPFEL, C., KUNZE, G., CHINCHILLA, D., CANIARD, A., JONES, J. D., BOLLER, T. & FELIX, G. 2006. Perception of the bacterial PAMP EF-Tu by the receptor EFR restricts Agrobacterium-mediated transformation. *Cell,* 125**,** 749-60.

ZOU, J., RODRIGUEZ-ZAS, S., ALDEA, M., LI, M., ZHU, J., GONZALEZ, D. O., VODKIN, L. O., DELUCIA, E. & CLOUGH, S. J. 2005. Expression Profiling Soybean Response to Pseudomonas syringae Reveals New Defense-Related Genes and Rapid HR-Specific Downregulation of Photosynthesis. *Molecular Plant-Microbe Interactions®,* 18**,** 1161-1174.

7. Appendix

Supplementary Table 1: Proteins and their proteotypic peptides sequences

Protein Accession	Peptide Sequence
AT1G01090.1	EEGLELYEDMILGR
AT1G01090.1	SDSVVSTYR
AT1G01090.1	RGEGPTLVECETYR
AT1G01090.1	KIDELVEEAVEFADASPQPGR
AT1G05180.1	VQFGDLGNNFMVDAK
AT1G08980.1	VTGFGNPDWLR
AT1G08980.1	VPGGSSSGSAVAVAAR
AT1G09430.1	LANIDLQIR
AT1G09430.1	LDLAEVADFVK
AT1G09430.1	VVIDCATTDPDGR
AT1G12240.1	DFRDPTTAWK
AT1G12240.1	NLVQWPVEEIK
AT1G12240.1	ILVDHSIVEAFGQGGR
AT1G12900.1	KDSPLDVVVINDTGGVK
AT1G12900.1	DSPLDVVVINDTGGVK
AT1G12900.1	YDSTLGIFDADVKPSGDSALSVDGK
AT1G13280.1	GVAADLPVELTGK
AT1G15750.1	LTEVSEPSQCR
AT1G23080.1	AGLQVDNGANEQVGK
AT1G23800.1	SGIEQGPQVDSEQFNK
AT1G24100.1	FSNGDFPLPADPNSAPFR
AT1G24100.1	GLPSLSYDELPSFVGR
AT1G24100.1	LPEGFVESTK
AT1G26380.1	DIDIGSNPSGETDVDEAK
AT1G51680.1	YDLSSIR
AT1G51680.1	IVDPDTGDSLSR
AT1G51680.1	GYLNNPAATAETIDK
AT1G51760.1	EGPMLAGSGFFK
AT1G51760.1	EADPLDSQVVTVAK

AT1G51760.1	FEGGGAFNVIPDSVTIGGTFR
AT1G54990.1	AIELGSEETAR
AT1G62380.1	VSNYPPCPKPEMIK
AT1G62380.1	AHTDAGGIILLFQDDK
AT1G62380.1	NASAVTELNPTAAVETF
AT1G66430.1	LGGSSAFIGK
AT1G66430.1	VGEDEFGYMLANILK
AT1G66430.1	GEDPYDDNVVR
AT1G70940.1	DVNTNQQTTLPTGGK
AT1G72010.1	ASQFQEQELAQGR
AT1G74100.1	TTQNGSEVVELTEFEK
AT1G74100.1	ALTYAIVNR
AT1G75950.1	AEAVEGAATSDDDLK
AT1G75950.1	NLLDLTCQTVADMIK
AT1G75950.1	NDFTPEEEEEVRR
AT1G76450.1	VEAFAETLVSGLDR
AT1G80490.1	EITQLLTLENFR
AT1G80490.1	LIEANPLFR
AT1G80490.1	YLAAGDDFSIK
AT2G04400.1	ESLAVSSSSVEDK
AT2G04400.1	NILEEITWYK
AT2G04400.1	ELNPLDVLK
AT2G06050.1	ALNGVPNAALAEYYAQR
AT2G17130.1	TEDLGGNSTTQEVVDAVIANLD
AT2G20610.1	QNLDVTPDPATIIQAALPAILEK
AT2G20610.1	KPESCTYLLTK
AT2G20610.1	EENLVFLPGDALGLK
AT2G21170.1	AFADAVPSWDNIVVAYEPVWAIGTGK
AT2G21170.1	VASPQQAQEVHVAVR
AT2G21170.1	GPEFATIVNSVTSK
AT2G21370.1	ATLFSLLEDIPVTVR
AT2G27150.1	TLFGPGPLFADELTR
AT2G27150.1	IALVVADTQK
AT2G29690.1	EDDRDAPSFLFESVEPGSQSSNIGR

AT2G29690.1	YSVVGAQPTIEIVAK
AT2G30490.1	NLVVVSSPDLTK
AT2G30490.1	RFESEDDPLFLR
AT2G30490.1	QIASSKPTGSEGLK
AT2G36580.1	FDFSWCDADYHQETLENLK
AT2G36580.1	IENEEGLTHFDEILQEADGIILSR
AT2G36580.1	AEATDVANAVLDGSDAILLGAETLR
AT2G36580.1	VFNQDLFFK
AT2G36580.1	SVEVIAGCLK
AT2G37040.1	AGVNASSDWVMESMNK
AT2G37040.1	ATGPNGEALTAEEAFK
AT2G37040.1	AAYDNGTSAIPNR
AT2G39470.1	SYSPFVDREDGYSYYYPSDWR
AT2G39470.1	TPIYATTSFATVAVGNNR
AT2G39470.1	YYTLIVGANER
AT2G39730.1	VPIICTGNDFSTLYAPLIR
AT2G39730.1	IKDEDIVTLVDQFPGQSIDFFGALR
AT2G39730.1	EGPPVFEQPEMTYEK
AT2G39940.1	GADEQGMEDEEGLVSQR
AT2G43820.1	SDTGYDLNLFESK
AT2G43820.1	SSEEEKLPSGFLETVNK
AT2G43820.1	SLNEGGSTDTNIDTFVSR
AT2G44490.1	ISDSSDGNVAVDFYHR
AT2G44490.1	DINMDSFR
AT2G44490.1	LSIAWPR
AT2G46370.1	LLTPNPELAETIR
AT3G02870.1	VPVVGVVYNPIMEELFTGVQGK
AT3G02870.1	VSAQSELLTALLVTEAGTK
AT3G16830.1	LAFPSFK
AT3G16830.1	DGNLLAVTTADNGFK
AT3G16830.1	VIEPSELSR
AT3G16830.1	AGTENGRPSSSSAANNSSSDQIQR
AT3G17770.1	VGDGDCGSTMYR
AT3G21240.1	ILDPDTGDSLPR

AT3G23920.1	YPSYPEQEGTWK
AT3G23920.1	LVNQVALATLAAEVPLAGENALPR
AT3G24503.1	FADLIEENIEELAK
AT3G24503.1	VSFTGSTDVGR
AT3G24503.1	GYFIQPTIFADVTEDMK
AT3G25760.1	FGLGDLVPFTNK
AT3G25760.1	LYTGDLK
AT3G25770.1	ALSQNGNIENPRPSK
AT3G25770.1	VQELSVYEINELDR
AT3G25770.1	GLANDLPLELTGTPVPPSK
AT3G43600.1	SQYSDLTVVEAEK
AT3G43600.1	LTLEEFLER
AT3G43600.1	IPTVDTIPK
AT3G44310.1	VTIVQSSTVYNDTPATIDK
AT3G44310.1	CIWGQGDGSTIPVYDTPIGK
AT3G44310.1	LGAAICWENR
AT3G44320.1	FIVEAASK
AT3G45140.1	GLDDIADIR
AT3G45140.1	SLLVELISAK
AT3G45140.1	LDPAVYGDPTSLITWEIVER
AT3G48000.1	TGEVIAHVAEGDAEDINR
AT3G48000.1	TAEQTPLTAFYAGK
AT3G48000.1	VYDEFVEK
AT3G48000.1	SGIESNATLECGGDQIGDK
AT3G52990.1	ADGLVTLTPNQDQEASSEVLPINFNGLAK
AT3G52990.1	LGDLSQTQIFAK
AT3G54640.1	VAFIPYITAGDPDLSTTAEALK
AT3G54640.1	VLDACGSDIIELGVPYSDPLADGPVIQAAATR
AT3G54640.1	AVGVQGLVVPDVPLEETEMLR
AT3G55800.1	LTGITGGDQVAAAMGIYGPR
AT3G55800.1	TTYVLAVK
AT3G55800.1	LLFEVAPLGLLIENAGGFSSDGHK
AT3G55800.1	GFPGTHEFLLLDEGK
AT3G56650.1	IANILSGNYCQPK

AT3G56650.1	LTNKPNATIEDLGEPEK
AT3G56650.1	VIASLGPFVTGNSYDSDELLK
AT3G56650.1	TLEAILDSFQL
AT4G00570.1	GEPENVVALAK
AT4G00570.1	ILGLGDLGVQGIGIPIGK
AT4G00570.1	LDMYVAAAGINPQR
AT4G02570.1	ASSWIQEDSCPDYMLK
AT4G02570.1	TVSQNDAFEFNSK
AT4G02580.1	VIEVAPIR
AT4G02580.1	DIESALLDHLGVK
AT4G04040.1	IIDGPPSSSAGHPEEIEK
AT4G04040.1	LFPNLFGQPSALLVPNQSNEVSSDQK
AT4G04040.1	NVTDNIVDVIYK
AT4G13770.1	TMVVISSAELAK
AT4G13770.1	GTDYEFIPFGSGR
AT4G16760.1	SLEDHSPLPNITVGDIGTK
AT4G16760.1	SLTTTATADGIEECR
AT4G16760.1	AEDWLNPDVVLEAFEAR
AT4G20130.1	EGPDGFGVYASK
AT4G20130.1	ILDFWEK
AT4G20130.1	MLAEYPTTAEQDQK
AT4G25900.1	VITFNAQLDR
AT4G26970.1	ILLESAIR
AT4G26970.1	EGVTATDLVLTVTQILR
AT4G26970.1	VSDIRPGQDVTVTTDSGK
AT4G30530.1	DAITPGSYFGNEIPDSIAIIK
AT4G30530.1	CHQDEVLVLPETAK
AT4G30530.1	EILFEIVDR
AT4G31500.1	ELGFGQYTAYYR
AT4G31500.1	LEPVIPILLHR
AT4G31500.1	DTAAWGDNPNEFIPER
AT4G31500.1	GQDFELLPFGSGR
AT4G34860.1	GQPVGTIAAVDNSEEK
AT4G34860.1	STGDSSLADMPECQK

AT4G35260.1	TPVGGGVSSLNVQLR
AT4G35260.1	DLGGTSTTQEVVDAVIAK
AT4G35260.1	DLGGTSTTQEVVDAVIAKLD
AT4G35580.1	FADDEVQVQSR
AT4G37870.1	FTHVLYNLSPAELYEQAIK
AT4G37870.1	GSFITSNGALATLSGAK
AT4G37870.1	DATTEDELWWGK
AT5G05600.1	VQSLAESNLSSLPDR
AT5G11670.1	LLIDNVEELLPVVYTPTVGEACQK
AT5G11670.1	AIFGSGSPFDPVVYDGK
AT5G11670.1	TYDLGLASNLPR
AT5G11670.1	VLVQFEDFANHNAFDLLSK
AT5G11770.1	QSDCMIVAGTLTNK
AT5G11770.1	VDDLMNWAR
AT5G13360.3	QIQDSVLEAILSR
AT5G13360.3	ESETASGILVR
AT5G17380.1	SEIESAVSLLR
AT5G17380.1	LNWLLHFGESPK
AT5G17380.1	KPAVVNVIIDPFAGAESGR
AT5G17990.1	VLSGESGAIADSLILNAAAALLVSNR
AT5G17990.1	VQTLAEGVTVAR
AT5G18200.1	NLETQSTQPETGTSR
AT5G20250.4	VYTVFLPLIEGSFR
AT5G20250.4	TDVMTLQGLGLVSPK
AT5G20250.4	VDVQCVLETLGGGLGGR
AT5G20960.1	DLKPPILSLEEAVENFSLFEVPPPLR
AT5G20960.1	AGEFSEYTLPLLWDR
AT5G20960.1	ICCDGLVER
AT5G22300.1	ATVVQASTVFYDTPATLDK
AT5G27030.2	VFSTFNEELYK
AT5G27030.2	QLCVITCGDDK
AT5G35790.1	WDGVPFLMK
AT5G35790.1	VQPDEGIYLR
AT5G35790.1	EIPDAYER

AT5G40760.1	YVSGPYDAEEGFQR
AT5G40760.1	DLESAEQLSSQIGELFDESQIYR
AT5G40760.1	DVPGDIFR
AT5G42650.1	DLFTGTYMPSTELTGGYR
AT5G42650.1	IFPEFQATYSELFDSLEK
AT5G42650.1	ADFGGSSDGTAFNFLAR
AT5G49980.1	DSPFGDVALR
AT5G51830.1	LPLWPSEEAAR
AT5G54270.1	INGLDGVGEGNDLYPGGQYFDPLGLADDPVTFAELK
AT5G54270.1	GPLENLLDHLDNPVANNAWAFATK
AT5G54270.1	WAMLGAFGCITPEVLQK
AT5G54810.1	QALNVFR
AT5G54810.1	MIGVEAAGFGLDSGK
AT5G54810.1	AEYYSITDEEALEAFK
AT5G54960.1	VSNQIGLDAAVEAAAEFLNK
AT5G54960.1	DFLSELAK
AT5G54960.1	VSAANSRPPNPQ
AT5G56350.1	NVNLPGVVVDLPTLTEK
AT5G56350.1	AEATDVANAVLDGTDCVMLSGETAAGAYPELAVR
AT5G56350.1	VENQEGVANFDDILVNSDAFMIAR
AT5G57220.1	LVDEPDIANLPYLQNIVSETFR
AT5G58260.1	GLGDPETTLLK
AT5G64380.1	LVYEGNPLAFLVEQAGGK
AT5G66190.1	GVCSNFLCDLKPGDEAK
AT5G66190.1	MAEYAEELWELLK
AT5G66190.1	GIDDIMVSLAAK
ATCG00350.1	FSNYEAWLSDPTHIGPSAQVVWPIVGQEILNGDVGGGFR
ATCG00350.1	YNDLLDR
ATCG00350.1	FPCDGPGR
ATCG00430.1	SPHIGNYDQELLYPPSSTSEISTETFFK
ATCG01090.1	LPVTIQYPYEK
ATCG01090.1	LPMSVIDDYTIR

Supplementary Table 2: Statistical testing for target proteins changes in media exchange experiment.

Protein Accession	Log_2 FCP																q-value
	0 hrs-1	0 hrs-2	0 hrs-3	0 hrs-4	16 hsr-1	16 hrs-2	16 hsr-3	16 hrs-4	17 hrs-1	17 hrs-2	17 hrs-3	17 hrs-4	19 hrs-1	19 hrs-2	19 hrs-3	19 hrs-4	
AT2G29690.1	0.00	0.00	0.00	0.00	0.46	0.60	0.61	0.50	0.00	0.18	0.34	-0.23	0.11	0.21	0.08	-0.04	0.12
AT5G17990.1	0.00	0.00	0.00	0.00	0.03	0.16	0.36	-0.19	0.56	0.03	-0.34	-0.33	-0.42	0.08	-0.13	-0.25	0.79
AT2G04400.1	0.00	0.00	0.00	0.00	-0.12	0.26	0.31	0.06	0.73	0.24	-0.29	-0.22	-0.14	0.20	-0.01	-0.28	0.71
AT3G54640.1	0.00	0.00	0.00	0.00	0.06	-0.05	-0.21	0.18	0.32	0.17	-0.25	-0.23	0.14	0.36	0.00	0.03	0.69
AT5G54810.1	0.00	0.00	0.00	0.00	0.04	0.41	0.60	0.00	0.70	0.44	0.75	0.12	0.76	0.86	0.87	0.49	0.02
AT5G20960.1	0.00	0.00	0.00	0.00	-0.07	-0.03	0.17	-0.24	0.39	0.20	-0.04	-1.91	-0.95	0.03	0.12	0.01	0.55
AT3G43600.1	0.00	0.00	0.00	0.00	-0.03	-0.50	0.21	0.37	0.84	-0.06	-0.20	-0.21	0.07	0.05	-0.25	0.20	0.79
AT2G27150.1	0.00	0.00	0.00	0.00	-0.30	0.50	0.34	-0.20	0.72	0.06	0.23	0.22	0.62	0.09	0.38	0.01	0.17
AT1G08980.1	0.00	0.00	0.00	0.00	-0.33	0.43	0.10	0.25	0.76	0.16	-0.01	0.03	-0.16	0.32	-0.10	0.47	0.33
AT3G44310.1	0.00	0.00	0.00	0.00	0.17	0.06	0.61	0.30	0.78	0.00	-0.01	-0.42	-0.01	0.23	0.01	-0.70	0.69
AT3G44320.1	0.00	0.00	0.00	0.00	-2.71	-3.11	-0.85	-5.22	-2.95	-0.53	-0.96	-0.02	1.74	-0.26	-3.19	0.09	0.13
AT5G22300.1	0.00	0.00	0.00	0.00	0.29	0.12	-0.89	0.88	1.21	0.30	-0.54	0.30	0.23	0.06	-0.30	0.49	0.54
AT4G31500.1	0.00	0.00	0.00	0.00	0.14	0.09	0.10	0.27	0.85	0.44	0.05	0.19	0.60	0.91	0.79	0.73	0.04
AT2G20610.1	0.00	0.00	0.00	0.00	0.22	0.43	0.03	0.03	0.36	0.18	-0.06	-0.23	0.19	0.54	0.30	-0.04	0.17
AT1G24100.1	0.00	0.00	0.00	0.00	-0.15	0.29	0.36	0.29	0.71	0.20	-0.02	-0.12	0.12	0.24	0.17	0.23	0.13
AT1G74100.1	0.00	0.00	0.00	0.00	0.75	0.42	0.27	0.20	-0.39	-0.13	0.02	-1.12	0.67	0.21	0.04	0.21	0.71
AT5G57220.1	0.00	0.00	0.00	0.00	0.22	2.69	2.79	1.68	3.90	4.51	5.29	2.93	-1.12	4.94	5.56	2.93	0.02
AT2G44490.1	0.00	0.00	0.00	0.00	-0.08	0.14	-1.48	0.66	1.08	0.20	-0.34	-0.03	-4.84	0.18	0.01	0.26	0.69
AT4G13770.1	0.00	0.00	0.00	0.00	-0.58	0.21	0.50	1.07	1.19	-1.25	0.44	-0.03	-0.18	-0.80	-0.04	0.99	0.74
AT1G26380.1	0.00	0.00	0.00	0.00	0.37	0.24	-0.49	1.04	0.96	0.35	-1.44	-4.93	-0.08	0.08	-1.18	-4.49	0.45
AT4G30530.1	0.00	0.00	0.00	0.00	0.13	0.37	0.14	0.00	0.86	0.24	-0.10	-0.31	0.05	0.35	0.12	-0.11	0.37
AT2G37040.1	0.00	0.00	0.00	0.00	1.08	1.01	1.41	1.69	1.48	1.04	0.64	0.84	1.14	1.41	1.10	1.43	0.00 *
AT2G30490.1	0.00	0.00	0.00	0.00	-0.24	0.01	0.47	0.19	0.78	-0.35	-0.53	0.08	-4.94	0.23	1.37	0.93	0.81
AT3G21240.1	0.00	0.00	0.00	0.00	0.15	0.10	0.07	0.49	1.23	-0.12	-0.36	0.35	0.52	0.06	0.24	0.40	0.20
AT1G51680.1	0.00	0.00	0.00	0.00	0.36	0.55	0.53	0.71	0.94	0.51	0.22	0.09	0.03	0.63	0.30	0.50	0.02
AT5G13360.3	0.00	0.00	0.00	0.00	-0.47	1.16	-0.14	-0.71	-0.03	1.09	-0.05	-0.77	0.44	0.45	-0.95	-0.33	0.92
AT2G46370.1	0.00	0.00	0.00	0.00	-0.42	0.46	0.02	0.08	0.50	0.19	-0.30	-0.21	0.48	0.63	0.21	0.31	0.37
AT1G51760.1	0.00	0.00	0.00	0.00	-0.04	0.14	0.03	0.38	0.37	0.05	-0.20	0.02	-0.04	0.32	0.07	0.43	0.21
AT5G05600.1	0.00	0.00	0.00	0.00	0.01	0.26	-0.43	0.56	1.23	0.42	0.21	0.57	-0.68	0.70	1.60	0.96	0.18
AT3G45140.1	0.00	0.00	0.00	0.00	0.03	0.00	0.21	0.10	0.43	0.06	-0.19	-0.10	-0.18	0.34	-0.06	-0.36	0.81
AT5G42650.1	0.00	0.00	0.00	0.00	-0.28	0.07	-0.02	0.17	0.42	0.20	-0.11	0.03	0.40	0.27	0.15	0.60	0.20
AT3G25760.1	0.00	0.00	0.00	0.00	0.00	0.25	0.14	0.10	0.84	0.10	0.74	0.51	0.93	0.38	0.91	1.75	0.07
AT3G25770.1	0.00	0.00	0.00	0.00	-0.16	0.24	0.44	0.20	0.54	0.38	0.18	-0.02	-0.16	0.26	0.39	0.47	0.11
AT1G13280.1	0.00	0.00	0.00	0.00	-0.12	0.42	0.21	-0.04	0.84	0.22	0.23	-0.05	-4.75	0.23	0.31	-0.10	0.76
AT2G06050.1	0.00	0.00	0.00	0.00	3.76	1.22	0.12	0.60	1.53	1.78	-0.25	-0.88	4.37	1.80	2.98	0.11	0.12
AT4G16760.1	0.00	0.00	0.00	0.00	-0.35	0.50	0.33	0.11	0.67	0.25	-0.09	-0.19	-1.05	0.36	0.08	0.13	0.77
AT1G54990.1	0.00	0.00	0.00	0.00	-0.29	0.36	0.25	0.09	0.65	0.06	-0.14	-0.19	-0.36	0.17	-0.09	-0.03	0.77
AT1G70940.1	0.00	0.00	0.00	0.00	0.06	0.74	0.42	0.22	0.93	0.42	-0.17	-7.12	-9.20	0.50	-0.07	0.01	0.53
AT1G23080.1	0.00	0.00	0.00	0.00	0.39	-0.82	-2.77	0.77	0.46	-0.56	-0.58	1.27	0.96	-0.26	-3.08	-0.09	0.61
AT5G49980.1	0.00	0.00	0.00	0.00	-0.05	0.18	-0.16	0.28	0.58	0.08	-0.17	0.18	0.24	0.40	-0.09	0.26	0.22
AT2G39940.1	0.00	0.00	0.00	0.00	-0.03	-0.01	0.75	0.32	0.71	0.18	0.37	0.09	-0.11	0.24	0.40	-1.77	0.76
AT1G80490.1	0.00	0.00	0.00	0.00	-0.31	0.37	-0.19	0.05	0.30	0.19	-0.47	-0.12	-0.35	0.30	-0.53	-0.28	0.61
AT3G16830.1	0.00	0.00	0.00	0.00	-0.14	0.60	0.37	0.39	0.53	0.16	-0.12	-0.27	-1.53	0.34	0.17	0.53	0.76
AT5G27030.2	0.00	0.00	0.00	0.00	-0.25	0.88	0.68	0.61	0.83	0.65	0.85	-0.61	-2.18	0.95	1.36	0.72	0.46
AT1G15750.1	0.00	0.00	0.00	0.00	-0.38	0.59	0.49	0.29	0.48	0.25	0.21	0.01	0.13	0.26	0.33	-3.94	0.82
AT1G75950.1	0.00	0.00	0.00	0.00	-0.13	0.35	0.15	-0.08	0.84	0.21	-0.38	-0.30	0.03	0.39	-0.20	-0.09	0.71
AT4G02570.1	0.00	0.00	0.00	0.00	-0.03	-0.06	0.32	0.09	0.34	0.25	-0.12	0.10	0.12	0.46	-1.40	0.28	0.87
AT1G05180.1	0.00	0.00	0.00	0.00	0.12	0.39	0.02	0.67	0.88	0.12	-0.35	0.44	-0.13	-0.11	-0.23	0.50	0.35
AT4G35580.1	0.00	0.00	0.00	0.00	-0.45	-0.03	0.23	0.29	0.46	-0.09	0.08	-1.04	-2.76	0.28	0.49	0.64	0.74
AT1G72010.1	0.00	0.00	0.00	0.00	-0.07	1.04	0.06	0.16	0.52	0.79	-0.08	-0.92	-1.03	0.88	0.10	0.20	0.69
AT2G43820.1	0.00	0.00	0.00	0.00	0.11	0.38	0.38	0.18	1.01	0.14	0.04	0.01	-4.28	0.25	0.26	0.10	0.82
AT1G62380.1	0.00	0.00	0.00	0.00	-0.20	-0.09	1.51	-0.52	-1.40	-0.09	-1.43	-1.50	-0.93	0.36	0.16	0.56	0.53
AT4G34860.1	0.00	0.00	0.00	0.00	0.80	-2.82	1.38	1.67	1.03	-3.16	0.80	2.60	2.02	-3.22	1.01	1.38	0.77
AT5G18200.1	0.00	0.00	0.00	0.00	-0.21	0.66	0.41	0.28	0.55	0.27	0.02	0.08	0.10	0.30	0.25	-1.50	0.72
AT2G21370.1	0.00	0.00	0.00	0.00	-0.52	-4.25	-1.48	-1.48	0.24	-2.40	-4.84	1.50	0.70	-1.76	-0.02	2.51	0.40
AT3G02870.1	0.00	0.00	0.00	0.00	-0.32	0.14	0.09	-0.39	0.08	0.33	-0.07	-0.53	0.41	-0.85	-0.34	-0.09	0.50
AT5G58260.1	0.00	0.00	0.00	0.00	-0.33	0.10	-0.01	0.01	0.81	-0.03	0.20	-0.15	-8.85	0.02	0.05	0.24	0.62
ATCG00430.1	0.00	0.00	0.00	0.00	0.03	0.12	0.61	-0.36	0.19	0.33	0.21	-0.14	0.06	0.51	0.16	-0.33	0.46
AT1G01090.1	0.00	0.00	0.00	0.00	-0.31	0.39	0.23	0.16	0.52	0.44	-0.21	-0.01	0.00	0.39	-0.26	-0.03	0.46
ATCG01090.1	0.00	0.00	0.00	0.00	-0.19	0.38	0.20	-0.16	0.89	0.47	0.12	0.00	-1.56	0.43	0.04	-0.15	0.86
AT2G39470.1	0.00	0.00	0.00	0.00	-0.08	0.43	0.27	-0.26	0.26	0.47	-0.06	-0.19	-0.35	0.25	-0.22	-0.43	0.94
AT5G35790.1	0.00	0.00	0.00	0.00	0.04	0.55	0.16	0.27	-1.15	0.32	0.00	-0.06	0.30	0.28	-0.01	0.44	0.69
AT4G02580.1	0.00	0.00	0.00	0.00	-0.23	0.04	0.17	-0.57	0.66	0.41	0.05	-0.42	-1.27	0.31	0.22	0.09	0.82
AT4G20130.1	0.00	0.00	0.00	0.00	-0.11	0.29	0.13	0.18	0.81	0.28	-0.27	-0.40	-0.15	0.22	-0.19	-0.05	0.71

AT5G64380.1	0.00	0.00	0.00	0.00	-0.22	0.59	0.42	-0.01	-0.19	0.67	0.14	-0.64	0.74	0.26	0.24	0.06	0.43
AT1G12900.1	0.00	0.00	0.00	0.00	-0.26	0.06	0.34	1.12	1.24	0.40	0.38	0.07	-0.38	0.46	-0.01	0.02	0.25
AT5G54270.1	0.00	0.00	0.00	0.00	0.29	-0.35	0.64	-1.68	0.81	-0.30	-0.93	-0.52	0.25	-0.59	-0.51	-1.46	0.37
AT3G56650.1	0.00	0.00	0.00	0.00	0.36	0.20	0.40	0.03	1.27	0.45	0.07	-0.22	0.29	0.07	-0.06	0.15	0.20
AT1G12240.1	0.00	0.00	0.00	0.00	-0.21	0.05	0.17	-0.03	0.23	-0.02	0.10	-0.13	-0.07	0.25	0.17	0.41	0.43
AT1G66430.1	0.00	0.00	0.00	0.00	-0.23	1.48	-0.26	-6.32	0.47	0.73	-0.62	-1.44	-0.56	-0.50	-1.25	-0.23	0.46
AT3G55800.1	0.00	0.00	0.00	0.00	-0.43	0.06	0.13	0.03	1.37	0.23	0.37	-0.11	1.02	0.31	0.23	0.27	0.23
AT2G21170.1	0.00	0.00	0.00	0.00	-0.15	0.46	-0.02	0.36	0.93	0.50	-0.08	0.31	-0.06	0.69	0.03	0.45	0.13
ATCG00350.1	0.00	0.00	0.00	0.00	-0.26	0.48	0.66	0.11	1.25	0.20	-0.07	0.05	0.02	-0.35	1.52	-0.26	0.37
AT5G66190.1	0.00	0.00	0.00	0.00	-0.03	-1.25	0.16	-0.18	0.87	0.30	-0.37	-0.45	0.21	-0.51	-0.13	-0.25	0.61
AT2G39730.1	0.00	0.00	0.00	0.00	0.18	-0.20	0.53	-0.56	0.22	-0.32	-0.05	-0.32	-0.36	-0.01	-0.17	-0.29	0.46
AT5G54960.1	0.00	0.00	0.00	0.00	0.04	0.22	0.51	0.22	0.72	0.03	1.11	-0.15	1.13	0.04	1.23	-0.12	0.13
AT5G17380.1	0.00	0.00	0.00	0.00	0.80	-1.31	-0.46	-0.05	0.58	-0.89	-0.13	0.53	-1.34	-1.19	0.03	0.47	0.54
AT5G40760.1	0.00	0.00	0.00	0.00	-0.11	0.23	0.11	0.55	0.76	0.07	-0.11	-0.24	-0.37	0.39	0.12	0.35	0.42
AT5G11670.1	0.00	0.00	0.00	0.00	-0.25	0.30	-0.27	0.00	-0.39	0.21	-0.71	0.02	-0.04	0.84	0.10	1.05	0.76
AT5G51830.1	0.00	0.00	0.00	0.00	2.20	0.29	-0.38	0.48	3.37	0.59	-0.43	0.14	-0.68	0.66	0.03	0.70	0.35
AT5G56350.1	0.00	0.00	0.00	0.00	-0.51	-0.85	1.13	-2.54	1.17	-0.16	1.01	-1.98	-3.67	2.47	-0.07	-2.67	0.56
AT3G23920.1	0.00	0.00	0.00	0.00	-0.02	0.45	0.46	0.30	0.08	0.00	0.34	-0.26	0.32	0.28	0.38	0.14	0.11
AT5G20250.4	0.00	0.00	0.00	0.00	-0.33	-0.79	-0.28	-1.62	0.14	-0.05	-1.35	-1.44	0.29	-0.67	-1.51	-1.19	0.07
AT4G37870.1	0.00	0.00	0.00	0.00	-0.16	0.13	0.09	0.25	0.60	0.20	-0.31	-0.04	0.13	0.19	-0.23	0.34	0.46
AT4G26970.1	0.00	0.00	0.00	0.00	-0.28	0.51	0.02	0.03	1.07	-0.01	-0.13	0.04	-0.21	0.33	-0.11	-0.37	0.71
AT3G24503.1	0.00	0.00	0.00	0.00	-0.39	-0.16	-0.04	0.01	0.35	0.32	-0.22	-0.10	0.12	0.50	-0.11	0.09	0.79
AT3G17770.1	0.00	0.00	0.00	0.00	0.00	0.20	0.44	0.10	1.47	0.54	0.39	0.17	0.64	0.54	0.59	-3.75	0.82
AT2G17130.1	0.00	0.00	0.00	0.00	-0.35	0.09	-0.04	0.29	-0.21	0.02	-0.42	0.15	-0.88	0.13	-0.25	0.11	0.48
AT4G04040.1	0.00	0.00	0.00	0.00	-0.05	0.52	0.39	0.03	0.83	0.27	0.07	-0.03	0.07	0.38	0.07	-0.02	0.13
AT3G48000.1	0.00	0.00	0.00	0.00	-0.35	0.47	0.28	-0.21	0.76	0.41	0.19	-0.07	-0.17	0.41	0.36	-0.30	0.43
AT4G35260.1	0.00	0.00	0.00	0.00	-0.31	0.38	0.07	-0.22	0.32	-0.01	-0.28	-0.14	-0.51	0.22	-0.27	-0.19	0.59
AT1G23800.1	0.00	0.00	0.00	0.00	0.14	0.35	0.19	0.15	1.14	0.02	-0.27	-0.10	-0.32	0.25	0.03	0.14	0.46
AT1G76450.1	0.00	0.00	0.00	0.00	0.08	-0.23	-0.16	0.76	0.64	0.00	0.12	0.85	0.27	0.53	0.29	0.91	0.12
AT4G00570.1	0.00	0.00	0.00	0.00	-0.14	0.49	0.06	-0.21	0.65	0.33	0.06	-0.23	-0.84	0.44	0.11	0.22	0.71
AT4G25900.1	0.00	0.00	0.00	0.00	-0.07	-0.64	1.21	-0.27	1.45	1.44	1.12	1.15	1.46	0.37	0.29	-0.25	0.13
AT2G36580.1	0.00	0.00	0.00	0.00	-0.34	0.29	0.06	0.20	0.42	-0.22	-0.27	0.01	-0.18	0.09	-0.18	0.10	0.98
AT1G09430.1	0.00	0.00	0.00	0.00	-0.06	0.23	-0.37	-0.32	1.04	0.46	-0.16	-0.29	-0.41	0.39	-0.11	-0.35	0.98
AT3G52990.1	0.00	0.00	0.00	0.00	-0.14	0.50	0.21	0.32	0.44	0.21	0.02	-0.04	-2.98	0.21	-0.09	0.08	0.80
AT5G11770.1	0.00	0.00	0.00	0.00	0.32	-0.36	0.14	0.28	1.21	0.44	0.01	-0.20	-0.83	0.44	0.10	0.14	0.59

Supplementary Table 3: Target proteins levels change overtime in *Arabidopsis thaliana* Col-0. White to red gradient represents values from lowest to highest in each row.

Biological Function	Protein Accession	Log_2 FCP							Significance to 0 hrs					
		0	1	3	16	17	19	32	1	3	16	17	19	32
Tryptophan Biosynthesis	AT2G29690	0	0.02	0.10	-0.03	-0.28	-0.33	-0.32						
	AT5G17990	0	0.24	0.43	1.67	1.49	1.73	2.12			*	*	*	*
	AT2G04400	0	0.27	0.87	1.45	1.36	1.47	1.48		*	*	*	*	*
	AT3G54640	0	-0.04	0.85	1.75	1.66	1.58	1.44		*	*	*	*	*
	AT5G54810	0	0.37	0.28	2.44	2.33	2.30	2.27		*	*	*	*	*
Auxin Biosynthesis	AT5G20960	0	0.38	0.21	1.37	1.17	1.06	0.81			*	*	*	*
	AT3G43600	0	0.05	0.11	0.08	-0.18	-0.16	0.03				*		
	AT2G27150	0	-0.05	-0.60	0.19	-0.20	-0.12	0.07						
	AT1G08980	0	0.01	0.11	-0.07	-0.08	-0.27	-0.19						
	AT3G44310	0	-0.40	-0.15	0.44	0.08	-0.16	0.05				*	*	*
	AT3G44320	0	0.08	-0.03	0.36	0.15	0.08	0.49						
	AT5G22300	0	-0.62	2.61	5.61	5.50	5.05	4.81	*	*	*	*	*	*
Glucosinolate Biosynthesis	AT4G31500	0	0.47	2.20	2.43	2.23	2.11	2.00	*	*	*	*	*	*
	AT2G20610	0	0.07	0.57	0.64	0.39	0.30	0.72		*	*	*		*
	AT1G24100	0	0.23	0.72	1.26	1.16	1.11	1.03		*	*	*	*	*
	AT1G74100	0	0.43	1.50	1.99	1.99	1.63	1.73		*	*	*	*	*
	AT5G57220	0	4.53	5.17	3.99	3.63	3.56	2.59	*	*	*	*	*	*
	AT2G44490	0	0.26	0.90	0.59	0.19	0.27	0.19	*	*	*		*	*
	AT4G13770	0	0.004	-0.24	-0.28	-0.93	-0.86	-0.05			*	*	*	*
4-OH-ICN Biosynthesis	AT1G26380	0	2.29	3.51	4.03	4.11	3.46	3.24	*	*	*	*	*	*

	AT4G30530	0	0.42	1.36	1.32	1.05	1.25	1.19		*	*	*	*	*
Phenylpropanoid Metabolite Synthesis	AT2G37040	0	0.34	2.26	2.52	2.26	2.33	1.61		*	*	*	*	*
	AT2G30490	0	0.83	0.35	1.01	0.92	0.74	1.28		*	*	*	*	*
	AT3G21240	0	-0.02	0.48	1.14	0.94	0.96	1.04		*	*	*	*	*
	AT1G51680	0	0.08	0.88	1.42	1.38	1.32	0.69		*	*	*	*	*
JA Metabolism and Conjugation	AT5G13360	0	-0.14	-0.19	0.06	-0.09	0.10	0.14						
	AT2G46370	0	0.21	-0.05	0.30	0.27	0.23	0.38						
	AT1G51760	0	0.05	0.49	0.52	0.44	0.69	0.24			*	*	*	*
	AT5G05600	0	0.30	0.84	2.28	2.13	2.27	2.34		*	*	*	*	*
JA Biosynthesis	AT3G45140	0	0.41	0.21	0.00	-0.26	-0.10	0.61						*
	AT5G42650	0	0.24	0.33	0.08	-0.01	0.29	0.12						
	AT3G25760	0	-0.19	0.20	0.80	0.96	1.06	0.87						
	AT3G25770	0	0.02	0.10	0.18	-0.21	-0.02	-0.21				*		*
	AT1G13280	0	0.22	0.09	-0.49	-0.54	-0.55	-0.45				*		
	AT2G06050	0	0.23	0.52	0.70	0.56	0.46	0.63			*			*
	AT4G16760	0	0.25	0.25	0.59	0.27	0.47	0.60			*			*
Auxin / JA Signaling	AT1G54990	0	-0.003	-0.05	-0.08	-0.31	-0.38	-0.16						
	AT1G70940	0	-0.12	-0.50	-1.06	-1.28	-0.95	-0.56		*	*	*	*	
	AT1G23080	0	0.01	-0.35	-1.45	-1.88	-1.61	-0.75		*	*	*	*	*
	AT5G49980	0	0.03	-0.01	-0.44	-0.44	-0.83	-0.64				*		
	AT2G39940	0	-0.42	0.08	-0.19	-0.25	-0.64	-0.37						
	AT1G80490	0	0.04	-0.08	-0.07	-0.16	-0.02	0.01						
	AT3G16830	0	0.05	0.14	0.21	-0.05	-0.03	-0.01				*		
	AT5G27030	0	-0.01	0.07	0.46	0.24	0.26	0.52			*			*
	AT1G15750	0	0.05	-0.29	0.59	0.04	0.23	0.02						
	AT1G75950	0	0.09	0.16	-0.52	-0.49	-0.44	-0.62			*	*	*	*
	AT4G02570	0	-0.05	0.00	0.07	-0.28	-0.15	-0.11			*	*		*
	AT1G05180	0	0.18	-0.18	-0.24	-0.52	-0.53	-0.52			*	*		*
SA Biosynthesis	AT4G35580	0	-0.15	-0.54	0.09	-0.03	-0.19	-0.87						
	AT1G72010	0	-0.08	0.29	0.40	0.02	-0.14	-0.53						
	AT2G43820	0	0.001	0.17	0.63	0.62	0.64	0.89			*	*	*	*
ET Biosynthesis	AT1G62380	0	0.03	0.10	-0.33	-0.54	-0.58	0.03				*		
Photosynthesis	AT4G34860	0	-0.33	-0.06	-0.13	-0.26	-0.59	-0.04					*	
	AT5G18200	0	0.20	-0.12	0.59	0.08	0.41	0.26						
	AT2G21370	0	0.19	0.13	-0.76	-0.71	-0.34	0.01						
	AT3G02870	0	0.27	0.09	-0.66	-0.58	-0.50	-0.23						
	AT5G58260	0	0.08	0.02	-0.50	-0.81	-0.97	-0.96			*	*	*	*
	ATCG00430	0	-0.13	0.00	-1.06	-1.23	-1.12	-1.53			*	*	*	*
	AT1G01090	0	-0.01	-0.16	-0.58	-0.73	-0.41	-0.46			*	*	*	*
	ATCG01090	0	0.14	0.00	-0.61	-0.66	-0.65	-0.88	*		*	*	*	*
	AT2G39470	0	0.36	0.05	0.06	0.06	0.11	-0.06	*					
	AT5G35790	0	-0.10	-0.14	-0.05	-0.39	-0.47	-0.54			*	*	*	*
	AT4G02580	0	0.06	-0.01	-0.57	-0.55	-0.68	-0.31			*	*	*	*
	AT4G20130	0	-0.12	-0.08	-0.63	-0.96	-0.90	-0.80			*	*	*	*
	AT5G64380	0	0.15	0.02	-0.16	-0.13	0.03	-0.02	*					
	AT1G12900	0	0.13	0.17	-0.34	-0.47	-0.57	-0.71			*	*	*	*
	AT5G54270	0	0.69	0.32	-0.56	-0.50	-0.31	-0.20		*		*		
	AT3G56650	0	0.23	0.19	-0.13	-0.16	-0.58	-0.31						
	AT1G12240	0	0.03	0.25	-0.34	-0.47	-0.66	-0.68			*	*	*	*
	AT1G66430	0	0.18	0.08	-0.47	-0.89	-0.62	-0.60			*	*	*	*
	AT3G55800	0	0.08	0.00	-0.13	-0.06	-0.16	-0.31			*	*		*
	AT2G21170	0	0.53	0.45	0.03	-0.12	-0.01	0.06						
	ATCG00350	0	0.34	0.12	0.00	-0.01	-0.10	0.07				*	*	*
	AT5G66190	0	0.18	0.13	-0.59	-0.55	-0.96	-0.78			*	*	*	*

	AT2G39730	0	0.01	0.20	-0.52	-0.38	-0.46	-0.60			*	*	*	*
Primary Metabolism	AT5G54960	0	0.02	0.09	0.54	0.35	0.44	1.08			*	*	*	*
	AT5G17380	0	0.36	0.38	0.71	0.51	0.82	0.73			*	*	*	*
	AT5G40760	0	0.12	0.31	0.81	0.55	0.76	0.94		*	*	*	*	*
	AT5G11670	0	0.35	1.04	1.35	1.25	1.18	1.26		*	*	*	*	*
	AT5G51830	0	0.22	0.53	1.14	0.95	0.86	0.91		*	*	*	*	*
	AT5G56350	0	-0.17	0.10	0.11	0.07	0.38	0.47			*	*	*	*
	AT3G23920	0	0.13	0.01	0.20	0.09	0.07	0.15	*		*			*
	AT5G20250	0	0.16	0.30	0.04	0.05	-0.13	-0.08	*		*	*		*
	AT4G37870	0	-0.03	-0.01	0.62	0.38	0.50	1.13			*	*	*	*
	AT4G26970	0	0.19	0.14	0.31	0.42	0.20	0.49			*			*
	AT3G24503	0	0.04	0.31	0.81	0.54	0.57	1.01		*	*	*	*	*
	AT3G17770	0	0.19	-0.12	0.21	-0.03	-0.12	-0.14						
	AT2G17130	0	-0.15	0.55	0.31	0.13	0.13	0.64						*
	AT4G04040	0	0.08	0.19	-0.18	-0.17	-0.07	0.02			*	*		*
	AT3G48000	0	0.06	0.14	0.23	0.25	0.18	0.21			*	*	*	*
	AT4G35260	0	-0.10	0.00	-0.03	-0.06	-0.03	-0.02				*		
	AT1G23800	0	0.08	0.08	0.25	0.17	0.07	0.39						*
	AT1G76450	0	0.15	0.25	-0.33	-0.54	-0.40	-0.27						
	AT4G00570	0	0.17	0.12	0.19	0.03	0.06	0.31			*			*
	AT4G25900	0	0.37	0.33	0.84	0.64	0.42	0.51			*	*		
	AT2G36580	0	0.04	0.28	0.06	0.09	0.05	0.46	*	*	*			*
	AT1G09430	0	0.08	0.32	0.10	-0.03	0.03	0.08						
	AT3G52990	0	-0.07	-0.04	-0.21	-0.35	-0.34	0.03			*	*		*
	AT5G11770	0	0.04	0.26	-0.50	-0.95	-0.90	-0.92			*	*	*	*

Supplementary Table 4: Target proteins levels change overtime in *Arabidopsis thaliana myc234*. White to red gradient represents values from lowest to highest in each row.

Biological Function	Protein Accession	Log_2 FCP							Significance to 0 hrs					
		0	1	3	16	17	19	32	1	3	16	17	19	32
Tryptophan Biosynthesis	AT2G29690	0	-0.02	0.04	-0.58	-0.43	-0.36	0.54	*	*	*	*	*	
	AT5G17990	0	-0.08	0.16	1.55	1.12	1.20	1.10	*		*	*	*	*
	AT2G04400	0	0.00	0.36	1.63	1.51	1.64	1.61		*	*	*	*	*
	AT3G54640	0	-0.12	0.47	2.09	2.10	2.09	2.18		*	*	*	*	*
	AT5G54810	0	0.66	0.71	2.12	1.77	1.48	1.64		*	*	*	*	*
Auxin Biosynthesis	AT5G20960	0	-0.25	-0.10	1.03	1.14	1.32	1.19			*	*	*	*
	AT3G43600	0	-0.18	-0.08	0.23	0.08	0.10	0.31	*		*	*	*	*
	AT2G27150	0	0.28	0.37	0.70	0.58	0.79	1.09		*	*	*	*	*
	AT1G08980	0	0.00	-0.10	-0.06	0.12	-0.08	0.14					*	*
	AT3G44310	0	-0.07	-0.26	0.31	0.43	0.60	0.88		*	*	*	*	*
	AT3G44320	0	-0.11	-0.22	-0.08	0.08	-0.56	0.29		*				
	AT5G22300	0	-0.23	2.91	6.07	6.19	5.94	5.74		*	*	*	*	*
Glucosinolate Biosynthesis	AT4G31500	0	0.72	3.73	4.89	5.00	5.06	4.89	*	*	*	*	*	*
	AT2G20610	0	-0.07	0.17	1.23	1.18	1.17	1.52	*	*	*	*	*	*
	AT1G24100	0	-0.07	0.28	1.23	1.18	1.27	1.30		*	*	*	*	*
	AT1G74100	0	-0.35	1.22	2.33	2.98	2.98	2.85	*	*	*	*	*	*
	AT5G57220	0	2.86	4.45	3.34	3.21	3.25	2.28	*	*	*	*	*	*
	AT2G44490	0	0.51	0.67	1.55	2.22	2.20	2.34	*	*	*	*	*	*
	AT4G13770	0	0.220	0.35	0.78	0.06	1.03	1.46				*	*	*
4-OH-ICN Biosynthesis	AT1G26380	0	1.56	4.49	4.89	5.18	5.07	4.64	*	*	*	*	*	*
	AT4G30530	0	0.05	1.20	2.52	2.30	2.31	2.30		*	*	*	*	*
Phenylpropanoid Metabolite Synthesis	AT2G37040	0	-0.12	3.20	4.51	4.46	4.33	2.66		*	*	*	*	*
	AT2G30490	0	1.45	1.00	1.98	2.25	2.39	2.54		*	*	*	*	*
	AT3G21240	0	-0.31	0.29	2.12	2.03	2.06	1.72	*	*	*	*	*	*
	AT1G51680	0	-0.25	1.34	2.86	2.73	2.65	1.42	*	*	*	*	*	*
JA Metabolism and Conjugation	AT5G13360	0	0.98	2.11	1.28	0.23	1.75	1.18		*	*			*
	AT2G46370	0	-0.15	-0.19	0.73	0.63	0.76	0.98		*	*	*	*	*
	AT1G51760	0	-0.11	-0.10	0.70	0.70	0.95	1.32	*		*	*	*	*

	AT5G05600	0	-0.09	-0.33	1.35	1.43	1.49	1.87			*	*	*	*
JA Biosynthesis	AT3G45140	0	-0.11	-0.25	0.40	0.27	0.78	1.66			*	*	*	*
	AT5G42650	0	-0.02	-0.14	0.22	0.13	0.17	0.31				*	*	*
	AT3G25760	0	-0.70	-0.46	-0.62	0.00	-0.51	0.66	*	*	*	*	*	*
	AT3G25770	0	0.38	0.24	0.28	0.42	0.07	0.58	*	*	*	*	*	*
	AT1G13280	0	0.04	-0.18	0.01	0.16	0.28	0.48					*	*
	AT2G06050	0	-0.15	-0.02	0.64	0.73	0.78	1.00			*	*	*	*
	AT4G16760	0	-0.10	-0.10	0.89	1.15	1.37	1.53		*	*	*	*	*
Auxin / JA Signaling	AT1G54990	0	-0.127	-0.28	-0.10	-0.03	0.01	0.55		*				*
	AT1G70940	0	-0.39	-0.75	-1.43	-1.16	-1.25	0.07	*	*	*	*	*	
	AT1G23080	0	-0.27	-0.78	-1.75	-1.62	-1.91	-0.40	*	*	*	*	*	*
	AT5G49980	0	-0.14	-0.20	-0.04	-0.06	0.07	0.20						
	AT2G39940	0	0.03	-0.14	0.26	0.61	0.63	0.90			*	*	*	*
	AT1G80490	0	-0.02	-0.20	0.11	0.06	0.25	0.37		*			*	*
	AT3G16830	0	-0.06	-0.13	0.22	0.27	-0.01	0.55			*	*	*	*
	AT5G27030	0	0.05	-0.18	0.67	0.58	0.79	0.74		*	*	*	*	*
	AT1G15750	0	0.04	-0.20	0.22	0.50	-0.05	0.57				*		*
	AT1G75950	0	0.02	-0.20	0.14	0.30	0.25	0.59			*	*	*	*
	AT4G02570	0	-0.22	-0.13	0.31	0.86	0.77	1.15			*	*	*	*
	AT1G05180	0	-0.33	-0.38	0.36	0.28	0.42	0.85				*	*	*
SA Biosynthesis and Metabolism	AT4G35580	0	0.03	-0.03	0.64	0.29	0.36	0.79			*	*		*
	AT1G72010	0	-0.05	0.00	0.12	0.13	0.05	0.08						
	AT2G43820	0	0.069	-0.03	0.74	0.80	0.84	1.15		*	*	*	*	*
ET Biosynthesis	AT1G62380	0	-0.04	-0.31	0.59	0.68	0.57	0.87			*	*	*	*
Photosynthesis	AT4G34860	0	0.01	-0.36	-0.06	0.31	0.26	0.73	*	*		*	*	*
	AT5G18200	0	0.00	-0.25	0.11	0.09	-0.35	0.40					*	
	AT2G21370	0	0.24	0.43	0.59	-0.57	-0.33	0.30						
	AT3G02870	0	0.06	0.12	0.26	0.42	0.16	0.72				*		*
	AT5G58260	0	0.14	-0.17	-0.16	-0.01	-0.21	0.14						
	ATCG00430	0	0.23	0.04	-0.39	0.25	-0.05	0.09	*		*			
	AT1G01090	0	-0.01	-0.28	-0.51	-0.51	-0.65	-0.23		*	*	*	*	*
	ATCG01090	0	0.23	0.09	-0.23	0.38	0.24	0.27	*		*	*	*	*
	AT2G39470	0	0.17	0.03	-0.09	-0.03	-0.02	0.10	*					
	AT5G35790	0	0.06	-0.27	-0.04	0.00	-0.12	0.60		*	*	*	*	*
	AT4G02580	0	-0.10	-0.11	0.23	0.31	0.40	0.55			*	*	*	*
	AT4G20130	0	-0.06	-0.27	-0.28	-0.30	-0.32	0.01		*	*	*	*	
	AT5G64380	0	-0.01	0.12	-0.03	0.07	-0.11	-0.02						
	AT1G12900	0	0.04	-0.11	-0.21	-0.19	-0.36	-0.56			*	*	*	*
	AT5G54270	0	-0.15	0.02	0.00	0.06	0.28	-0.32				*	*	*
	AT3G56650	0	0.09	0.32	0.32	0.28	-0.02	0.56				*	*	*
	AT1G12240	0	-0.06	-0.08	-0.17	0.15	0.11	-0.04		*	*			*
	AT1G66430	0	-0.05	-0.17	0.16	0.17	0.22	0.66	*	*		*	*	*
	AT3G55800	0	0.24	0.00	0.02	0.23	0.48	0.10	*			*	*	*
	AT2G21170	0	-0.02	0.04	0.09	0.35	0.37	0.38				*	*	*
	ATCG00350	0	0.11	-0.09	0.00	0.21	-0.30	-0.09	*			*	*	
	AT5G66190	0	0.18	-0.14	-0.12	0.24	0.45	0.04				*	*	
	AT2G39730	0	-0.01	0.21	0.02	-0.37	-0.10	-0.89				*		*
Primary Metabolism	AT5G54960	0	-0.04	-0.09	-2.42	0.15	-0.19	0.86			*	*	*	*
	AT5G17380	0	-0.11	0.20	1.43	1.71	1.90	1.70			*	*	*	*
	AT5G40760	0	-0.03	0.30	1.52	1.41	1.55	1.69		*	*	*	*	*
	AT5G11670	0	-0.15	0.87	1.76	1.67	1.84	1.97		*	*	*	*	*
	AT5G51830	0	0.00	0.22	1.76	1.95	1.95	2.01		*	*	*	*	*
	AT5G56350	0	-0.21	-0.05	0.78	1.01	1.13	1.36	*		*	*	*	*
	AT3G23920	0	-0.06	-0.13	0.16	0.37	0.49	0.50			*	*	*	*

	AT5G20250	0	-0.06	0.37	0.94	0.58	0.64	0.41	*	*	*	*	*	*
	AT4G37870	0	-0.15	-0.22	1.11	1.53	1.81	2.49	*	*	*	*	*	*
	AT4G26970	0	-0.05	0.03	1.01	0.51	0.60	0.90			*	*	*	*
	AT3G24503	0	-0.09	0.10	1.25	1.22	1.35	1.67			*	*	*	*
	AT3G17770	0	0.38	0.40	0.05	0.77	0.54	1.19				*	*	*
	AT2G17130	0	-0.18	-0.09	0.70	0.84	0.86	1.22			*	*	*	*
	AT4G04040	0	-0.02	-0.20	0.20	0.30	0.24	0.11			*	*	*	*
	AT3G48000	0	0.16	-0.07	0.88	1.07	0.85	1.23	*		*	*	*	*
	AT4G35260	0	-0.11	-0.14	0.05	-0.01	0.04	0.21			*		*	*
	AT1G23800	0	-0.30	-0.26	0.02	0.07	0.11	0.59	*	*			*	*
	AT1G76450	0	-0.15	-0.25	0.09	-0.07	0.09	-0.07						
	AT4G00570	0	-0.01	-0.11	0.35	0.51	0.43	1.10			*	*	*	*
	AT4G25900	0	0.10	-0.37	0.48	0.64	0.67	1.33			*	*	*	*
	AT2G36580	0	-0.09	-0.03	0.64	0.59	0.66	0.96	*		*	*	*	*
	AT1G09430	0	0.03	0.09	0.67	0.75	0.89	0.94		*	*	*	*	*
	AT3G52990	0	-0.13	-0.22	0.22	0.26	0.34	0.68	*	*	*	*	*	*
	AT5G11770	0	0.34	-0.14	0.17	1.30	1.36	1.62			*	*	*	*

Supplementary Table 5: Targets expression change overtime in *Arabidopsis thaliana* Col-0. White to red gradient represents values from lowest to highest in each row.

Biological Function	Gene Accession	Mean Relative Expression							Significance to 0 hrs					
		0	1	3	16	17	19	32	1	3	16	17	19	32
Tryptophan Biosynthesis	AT2G29690	0.45	0.39	0.43	0.42	0.69	0.36	0.15				*		
	AT5G17990	0.84	10.18	18.09	2.73	5.61	3.61	2.82	*	*	*	*	*	*
	AT3G54640	0.89	37.44	57.12	4.81	10.92	7.55	4.77	*	*	*	*	*	*
	AT5G54810	2.82	49.07	55.53	3.40	4.41	3.54	4.69	*	*		*		
Auxin Biosynthesis	AT5G20960	0.51	0.73	0.85	1.56	2.67	2.14	1.18	*	*	*	*	*	*
	AT5G22300	0.02	1.00	4.75	0.76	1.17	0.61	0.17	*	*	*	*	*	*
Glucosinolate Biosynthesis	AT4G31500	0.29	29.41	24.07	2.25	7.07	2.80	0.77	*	*	*	*		
	AT1G74100	0.79	53.73	37.13	2.71	6.47	3.51	1.75	*	*	*	*	*	*
	AT2G44490	2.14	32.30	16.06	3.66	2.55	4.65	4.99	*	*	*		*	
	AT4G13770	1.88	0.62	0.41	0.68	1.50	2.51	2.38	*	*	*	*		
Phenylpropanoid Biosynthesis	AT2G37040	0.49	8.62	23.08	10.24	12.30	3.87	0.94	*	*	*	*		
	AT1G51680	0.31	4.58	7.90	2.02	3.44	3.06	1.39	*	*	*	*	*	*
JA Metabolism and Conjugation	AT2G46370	0.25	0.35	0.28	0.38	0.71	0.27	0.10	*		*	*		
	AT1G51760	0.36	5.39	2.36	0.79	2.03	1.03	0.69	*	*	*	*	*	*
	AT5G05600	0.29	3.10	2.63	2.50	3.87	3.64	1.58	*	*	*	*	*	*
	AT5G63450	0.05	0.06	0.05	0.02	0.05	0.07	0.01						*
	AT3G48520	0.02	0.02	0.02	0.02	0.03	0.02	0.01			*			*
	AT2G27690	0.17	2.69	1.97	0.17	0.29	0.21	0.12	*	*				
JA Biosynthesis	AT3G45140	0.35	0.32	0.15	0.84	1.80	2.08	2.42		*	*	*	*	*
	AT3G25760	0.62	6.84	2.04	0.96	1.90	1.03	0.16	*	*		*		*
	AT2G06050	0.64	4.58	4.06	0.62	1.58	0.28	0.21	*	*		*	*	
	AT4G16760	0.73	2.16	2.15	2.21	2.58	2.01	1.81	*	*	*	*	*	*
Auxin / JA Signaling	AT1G70940	1.42	0.26	0.29	0.55	1.11	0.61	0.43	*	*	*		*	*
	AT1G23080	2.93	0.51	0.85	0.37	0.70	1.23	1.17	*	*	*	*	*	*
	AT2G39940	0.53	0.47	0.52	0.95	1.45	0.41	0.19			*	*		*
	AT1G80490	0.28	0.28	0.17	0.28	0.40	0.40	0.40						
	AT5G27030	0.15	0.24	0.34	0.28	0.35	0.31	0.25	*	*	*	*	*	*
	AT1G75950	18.99	24.99	25.75	21.93	21.59	27.54	24.88					*	*
	AT4G02570	2.24	2.59	2.48	2.63	2.54	2.67	2.61						
SA Biosynthesis	AT2G43820	1.37	0.29	0.29	9.75	5.56	5.16	4.40	*	*	*	*	*	*

	AT1G74710	0.06	0.27	1.38	0.22	0.49	0.20	0.04	*	*	*	*	*	
ET Biosynthesis	AT1G62380	20.67	22.37	39.57	70.70	55.01	83.15	35.29		*	*	*	*	*
Photosynthesis	AT1G01090	4.65	3.37	2.58	2.37	2.03	2.63	2.85		*	*	*	*	*
	AT5G54270	16.58	4.37	1.00	17.36	14.10	29.78	0.79	*	*			*	*
	AT2G21170	10.89	6.81	4.72	7.43	4.95	7.93	9.03		*				
	AT5G66190	15.86	8.75	4.32	5.79	5.38	6.71	6.24		*	*			*
Primary Metabolism	AT5G40760	0.54	1.52	3.16	1.25	0.98	1.24	0.87	*	*	*		*	*
	AT4G26970	3.25	10.95	17.01	10.29	6.84	7.69	4.62	*	*	*		*	*

Supplementary Table 6: Targets expression change overtime in *Arabidopsis thaliana myc234*. White to red gradient represents values from lowest to highest in each row.

Biological Function	Gene Accession	Mean Relative Expression							Significance to 0 hrs					
		0	1	3	16	17	19	32	1	3	16	17	19	32
Tryptophan Biosynthesis	AT2G29690	0.41	0.30	0.13	0.34	0.36	0.38	0.38	*	*				
	AT5G17990	0.36	1.07	6.73	1.66	1.48	1.29	1.03	*	*	*	*	*	*
	AT3G54640	0.44	3.61	30.75	4.30	3.31	3.08	2.25	*	*	*	*	*	*
	AT5G54810	3.95	37.99	62.34	7.01	6.82	4.75	6.26	*	*	*	*		*
Auxin Biosynthesis	AT5G20960	0.38	0.70	1.29	1.58	1.51	0.85	0.85	*	*	*	*	*	*
	AT5G22300	0.04	0.21	5.73	2.04	1.30	0.47	0.14	*	*	*	*	*	*
Glucosinolate Biosynthesis	AT4G31500	0.06	3.91	11.94	1.80	1.82	0.96	0.87	*	*	*	*	*	*
	AT1G74100	0.22	4.23	19.56	1.19	1.43	0.92	0.63	*	*	*	*	*	*
	AT2G44490	2.28	37.95	18.21	5.63	3.57	3.17	3.71	*	*	*	*	*	*
	AT4G13770	0.00	0.00	0.00	0.00	0.00	0.00	0.00					*	*
Phenylpropanoid Biosynthesis	AT2G37040	0.67	7.04	46.60	30.07	22.59	11.78	7.44	*	*	*	*	*	*
	AT1G51680	0.47	4.35	10.88	4.21	4.01	2.36	3.27	*	*	*	*	*	*
JA Metabolism and Conjugation	AT2G46370	0.34	0.29	0.22	0.59	0.69	0.52	0.39			*	*	*	
	AT1G51760	0.22	0.14	0.50	0.49	0.58	0.50	0.45		*	*	*	*	*
	AT5G05600	0.03	0.06	0.28	0.95	1.31	1.16	0.27	*	*	*	*	*	*
	AT5G63450	0.03	0.02	0.01	0.01	0.03	0.02	0.01	*	*	*			*
	AT3G48520	0.01	0.01	0.01	0.00	0.02	0.00	0.00				*	*	*
	AT2G27690	0.02	0.03	0.27	0.14	0.31	0.14	0.09		*	*	*	*	*
JA Biosynthesis	AT3G45140	0.11	0.05	0.01	0.66	1.10	1.73	1.54	*	*	*	*	*	*
	AT3G25760	0.46	2.32	1.45	1.16	0.88	0.26	0.06	*	*		*		*
	AT2G06050	0.20	0.29	0.81	0.23	0.31	0.21	0.20	*	*				
	AT4G16760	0.44	0.79	1.90	1.97	1.65	1.14	1.57	*	*	*	*	*	*
Auxin / JA Signaling	AT1G70940	0.40	0.16	0.13	0.18	0.48	0.53	1.08	*	*	*	*		*
	AT1G23080	1.34	0.36	0.39	0.27	0.44	0.64	0.89	*	*	*	*	*	
	AT2G39940	0.42	0.26	0.41	0.75	0.77	0.65	0.66	*		*	*	*	*
	AT1G80490	0.56	0.61	0.44	0.80	1.05	0.97	0.92			*	*	*	*
	AT5G27030	0.07	0.16	0.20	0.21	0.25	0.23	0.22	*	*	*	*	*	*
	AT1G75950	4.35	4.25	5.12	4.97	4.34	4.11	4.43						
	AT4G02570	1.91	2.46	2.31	1.90	2.98	2.92	2.61	*			*		*
SA Biosynthesis	AT2G43820	1.09	0.54	0.11	6.30	5.84	6.12	3.36	*	*	*	*	*	*
	AT1G74710	0.05	0.37	5.10	0.78	1.42	0.70	0.33	*	*	*	*	*	*
ET Biosynthesis	AT1G62380	20.15	21.77	28.26	66.32	73.16	49.05	34.25			*	*		*
Photosynthesis	AT1G01090	4.06	4.01	1.98	2.25	2.27	2.81	2.74						
	AT5G54270	20.39	1.92	0.25	8.19	5.40	6.72	0.27	*	*	*	*	*	*
	AT2G21170	10.73	10.35	4.60	8.31	7.42	6.97	9.31		*	*	*	*	
	AT5G66190	16.97	14.20	4.16	4.52	5.16	3.87	5.65		*	*	*	*	*
Primary Metabolism	AT5G40760	0.56	1.57	6.41	2.51	2.44	1.73	1.42	*	*	*	*	*	*
	AT4G26970	3.61	12.35	25.50	15.10	16.77	9.67	11.43	*	*	*	*	*	*

Supplementary Table 7: Hormone levels change overtime in *Arabidopsis thaliana* Col-0. White to red gradient represents values from lowest to highest in each row.

Hormone	Mean ng/g FW							Significance to 0 hrs					
	0	1	3	16	17	19	32	1	3	16	17	19	32
ABA	0.31	0.15	0.10	0.12	0.13	0.12	0.14	*	*	*	*	*	*
IAA	8.59	7.63	6.41	6.00	5.77	6.31	5.65		*	*	*	*	*
JA	1.93	2.95	5.50	5.07	5.65	6.40	5.08	*	*	*	*	*	*
JA-Ile	0.39	0.65	1.02	0.59	0.63	0.70	0.58	*	*		*	*	
OPDA	123.02	950.14	603.64	1095.79	1237.87	1102.75	988.15	*	*	*	*	*	*
SA	64.72	75.65	116.13	157.40	104.31	121.51	140.59		*	*	*	*	*
12-OH-JA	0.92	1.29	2.59	4.06	10.58	9.80	6.82		*	*	*	*	*

Supplementary Table 8: Hormone levels change overtime in Arabidopsis thaliana *myc234*. White to red gradient represents values from lowest to highest in each row.

Hormone	Mean ng/g FW							Significance to 0 hrs					
	0	1	3	16	17	19	32	1	3	16	17	19	32
ABA	0.50	0.20	0.11	0.12	0.11	0.13	0.16	*	*	*	*	*	*
IAA	1.38	1.86	1.46	1.35	1.47	1.65	1.95						
JA	0.96	1.31	1.79	2.23	5.59	8.39	4.00		*		*		*
JA-Ile	0.20	0.24	0.40	0.34	0.94	1.70	0.54		*		*		*
OPDA	26.23	22.34	30.85	108.52	104.49	81.67	51.34				*	*	*
SA	117.77	121.81	165.49	336.16	216.47	280.04	277.50		*	*	*	*	*
12-OH-JA	1.38	1.34	1.12	3.31	7.10	7.84	6.39			*	*	*	*

Supplementary Table 9: qPCR primers list. CYP94B1/3 were adopted from (Zhang et al., 2020).

Gene Name	Gene Accession	Left Primer	Right Primer
4CL1	AT1G51680	ATGCCAAACTCGGTCAGG	GCAAAACCTAACGACATTGCT
AAO1	AT5G20960	ACAACGATCCTGCGTACAGA	CTTGAACAAAGGCTCCTTCAAT
ACO2	AT1G62380	GCTTCTTAAAGATGGTGACTGGAT	TTCCCGTTGGTTATCACCTC
ACONITASE 2	AT4G26970	GGTCAAGACGTCACTGTAACCA	CGTGATCATAGTATGCCAATTCC
ACX1	AT4G16760	GCAATGTCGTTCTGGTGTTC	GCTTCGAAAGCTTCCAGTACA
AOC1	AT3G25760	TGGTATCTCATCTAACGGTCCA	TCGTACACGCTCAGTTCTTGA
ASA2	AT2G29690	CCACGGTAGTAGGTGAATTGC	CAGCTCCATGGCTTTTACCTT
COI1	AT2G39940	GTGTCCTAATTTGGAAGTTCTCG	CTCCATTCCTTGTTCATCTGC
CUL1	AT4G02570	CGATAGAATGCGCAGAATCA	TCAACGACTTTCTTCCTTTCATC
CYP83A1	AT4G13770	TGTTCCAGAGAAAGTGAACAAGTATT	AAAGAAACCAAACATTGAAACAGA

CYP83B1	AT4G31500	ACCGTGTCGCAAGTTTCAG	TCTTGTCCATCATCCGTTGAC
CYP94B1	AT5G63450	ATGCAGCAAACGACGACATT	CCCACACCTTCTCCATCCTT
CYP94B3	AT3G48520	TCAATGTCGACGGTCACTCA	ACGGTTCTCCACTTCGTCTT
CYP94C1	AT2G27690	TTATGCAATGGGTCGGATG	TCCAACCACCTCTCTGGTTT
EDS16	AT1G74710	GCGGGACCTATTGGATTTTT	AGATCAATGCCCCAAGACC
FNR1	AT5G66190	CACCTTTGTTTACATGTGTGGTC	TGTACTCCAACCAATCGATCC
G6PD6	AT5G40760	GAGGCAATGTACATGAAACTAACTG	AGTCTAGTTCACTTTGCACAGTATTCA
IAR3	AT1G51760	GTGCTGCAAAATTGCTCAAA	GCCTCCACAATCTTCTTTGC
JAR1	AT2G46370	ATTGCAACTGTTTCGCACTG	AGCTTTGCCATTGTCATCAA
JOX2	AT5G05600	TTCTTTTCCTCCCACCATAAGA	CAAATGCTTCTTGAAACTTATCCTC
LHCB3	AT5G54270	GAAAAGCTCAAGCCGAGAGA	TTGGGGTAAGAACACTGCTTG
LOX2	AT3G45140	CTTACCCGCGGATCTCATC	ACTCCATGTTCTGCGGTCTT
NIT4	AT5G22300	AACACCGGACTCTGTTGTCTG	TCGTGCTATGTCCCCAAGA
OPR3	AT2G06050	GCGTTGAACGGAGTACCAA	CAGGCACATGTGGGAACC
PAL1	AT2G37040	CGCACTTCAGAAGGAACTTATTAGA	ATCGGATACCGGAAAATCCT
PAT1	AT5G17990	AGCAATTGCGGATTCATTG	CCCAGACGATTGTACTTCACG
PDH-E1 ALPHA	AT1G01090	GAGGACACTCCTTGGCTGAT	GTCTCTAGCCGCGTATTTGG
PEN2	AT2G44490	AGGACATATCCACGCTATTCATC	TGACCATACGTAATAACCTTCCAC
PIN3	AT1G70940	TGCCCAAAATCATTCAACAA	GTTGCAACGCCATGAACA
PIN7	AT1G23080	GTTGCTTTCAGGTGGGATGT	TTGCAATGCCATGAACAAC
PP2A	AT1G13320	GACCGGAGCCAACTAGGAC	AAAACTTGGTAACTTTTCCAGCA
SKP1	AT1G75950	TCGATCAAGCTACTCTCTTTGAAC	TCCTTTGATCATATCCGCAAC
SOT16	AT1G74100	AAAGGTTGGAGATTGGGCTAA	TCTCCTCCACTAAGCCATCAA
TIM	AT2G21170	TGCTTCCAAAACGAGAATCA	GCAAACTCAGGACCCTTCAA
TPR1	AT1G80490	ATGGAAGTGGCAGCGAAAT	GCCACTGCTGAGGAGGTAAA
TPR3	AT5G27030	CAAGATGGAATGTATCCGACAGT	TGCGTACACCGCTGAAGATA
TSA1	AT3G54640	GGTTCAGTCGCTCTTGAAGG	CCCATCCAGCTATCTGTTTCA
TSB1	AT5G54810	ACGAAGAAGCGTTGGAAGC	GGTAAGCTAGTGCGTGTGAGG
UBC21	AT5G25760	CAGTCTGTGTGTAGAGCTATCATAGCAT	AGAAGATTCCCTGAGTCGCAGTT
UGT74F2	AT2G43820	ACCGATGAACGCAAAGTACA	TCTCCTTCTCTGTCTTCACACG

Supplementary Table 10. Polynomial model fits for protein fold change (FCP) calculation in non-steady state PTI. Models based on FCP data of 1,3 and 16 hrs after flg22 addition.

Protein Accession	Protein Name	Equation	R^2
AT1G01090	PDH-E1 ALPHA	y = 0.001x2 - 0.0383x + 1.0165	0.99
AT1G13280	AOC4	y = -0.0027x2 + 0.0224x + 1.0569	0.89
AT1G15750	TPL	y = 0.0074x2 - 0.0888x + 1.0477	0.97
AT1G23080	PIN7	y = 0.0024x2 - 0.0804x + 1.0394	0.98
AT1G24100	UGT74B1	y = -0.0104x2 + 0.2542x + 0.9794	1.00
AT1G26380	FOX1	y = -0.1922x2 + 4.0332x + 1.0255	1.00
AT1G51680	4CL1	y = -0.0138x2 + 0.3334x + 0.9068	0.98
AT1G66430	FRK3	y = -0.0025x2 + 0.0206x + 1.0472	0.91
AT1G70940	PIN3	y = 0.005x2 - 0.1134x + 1.0181	0.99
AT1G74100	SOT16	y = -0.0337x2 + 0.7323x + 0.8676	0.99
AT1G75950	SKP1	y = -0.0045x2 + 0.0528x + 1.0076	1.00
AT2G04400	IGPS	y = -0.0132x2 + 0.322x + 0.9654	1.00
AT2G06050	OPR3	y = -0.0081x2 + 0.1671x + 1.0114	1.00
AT2G20610	SUR1	y = -0.0101x2 + 0.1994x + 0.949	0.96
AT2G21370	XK1	y = -0.0042x2 + 0.0404x + 1.0506	0.94
AT2G27150	AAO3	y = 0.0094x2 - 0.1426x + 1.0377	0.96
AT2G30490	C4H	y = -0.0008x2 + 0.0587x + 1.278	0.53
AT2G37040	PAL1	y = -0.0781x2 + 1.5759x + 0.5464	0.95
AT2G39730	RCA	y = -0.0054x2 + 0.0695x + 0.9777	0.98
AT2G43820	UGT74F2	y = -0.0006x2 + 0.045x + 0.9859	1.00
AT2G44490	PEN2	y = -0.0198x2 + 0.3515x + 0.9596	0.98

AT3G02870	VTC4	y = -0.0034x2 + 0.0275x + 1.0715	0.89
AT3G21240	4CL2	y = -0.0047x2 + 0.1542x + 0.9452	0.99
AT3G24503	ALDH2C4, ALDH1A, REF1	y = -0.0028x2 + 0.0942x + 0.9768	0.99
AT3G25760	AOC1	y = 0.0003x2 + 0.0595x + 0.9478	0.98
AT3G54640	TSA1	y = -0.01x2 + 0.3158x + 0.873	0.98
AT4G02580	NADH-ubiq.oxi.red.24 kDa	y = -0.0015x2 + 0.0022x + 1.0151	0.99
AT4G16760	ACX1	y = -0.0024x2 + 0.0664x + 1.0495	0.93
AT4G20130	PTAC14	y = -0.001x2 - 0.0044x + 0.9712	0.96
AT4G25900	aldose 1-epimerase family protein	y = -0.0026x2 + 0.0857x + 1.0874	0.91
AT4G30530	GGP1	y = -0.0339x2 + 0.6415x + 0.9018	0.98
AT4G31500	CYP83B1	y = -0.0732x2 + 1.4721x + 0.6169	0.96
AT4G35580	NTL9	y = 0.0086x2 - 0.1361x + 1.0488	0.89
AT4G37870	PCK1, PEPCK	y = 0.0025x2 - 0.006x + 0.9941	1.00
AT5G05600	JOX2	y = -0.0018x2 + 0.2713x + 0.9865	1.00
AT5G11670	ATNADP-ME2	y = -0.02x2 + 0.4214x + 0.953	0.99
AT5G11770	NADH-ubiquinone oxidoreductase 20 kDa subunit, mitochondrial	y = -0.0074x2 + 0.1005x + 0.9902	1.00
AT5G17380	pyruvate decarboxylase family protein	y = -0.0049x2 + 0.1145x + 1.0698	0.91
AT5G17990	PAT1	y = 0.0016x2 + 0.1091x + 1.0256	1.00
AT5G18200	UTP	y = 0.0048x2 - 0.0508x + 1.079	0.88
AT5G20960	AAO1	y = 0.0042x2 + 0.0247x + 1.118	0.97
AT5G22300	NIT4	y = 0.0958x2 + 1.508x + 0.2514	1.00
AT5G40760	G6PD6	y = -0.0024x2 + 0.0861x + 1.0029	1.00
AT5G49980	AFB5	y = -0.0013x2 + 0.0036x + 1.0098	0.99

AT5G51830	pfkB-type carbohydrate kinase family protein	y = -0.0056x2 + 0.1643x + 1.004	1.00
AT5G54270	LHCB3	y = -0.0068x2 + 0.0712x + 1.2834	0.53
AT5G54810	TSB1	y = 0.0163x2 + 0.0093x + 1.1023	1.00
AT5G57220	CYP81F2	y = -0.8104x2 + 13.673x + 4.528	0.92
AT5G58260	NDH-N	y = -0.0019x2 + 0.011x + 1.02	0.98
AT5G66190	FNR1	y = -0.0039x2 + 0.0391x + 1.0373	0.96
ATCG00430	PSBG	y = -0.0028x2 + 0.0154x + 0.9625	0.97
ATCG01090	NDHI	y = -0.0025x2 + 0.0167x + 1.0339	0.96

MOHAMMAD ABUKHALAF

Date and place of Birth: 15.04.1989, Damascus
Nationality: Jordanian

WORK EXPERIENCE

- **Research Assistant (PhD), Proteome Analytics**
  Leibniz Institute for Plant Biochemistry, Halle (Saale)
  Jan 2019 – Mar 2021

- **Project & Master Thesis, Proteome Analytics**
  Leibniz Institute for Plant Biochemistry, Halle (Saale)
  Nov 2017 – Dec 2018

- **Medical Representative**
  Bayer AG Middle East (Consumer Care), Jordan & UAE
  Feb 2014 - Feb 2016

- **Medical Representative**
  GSK Pharma, Jordan
  June 2013 - Feb 2014

EDUCATION

- **Martin Luther University Halle-Wittenberg**
  2016-2018
  Masters of Pharmaceutical and Industrial Biotechnology
  Master Thesis "Isolation of Nuclei for LC-MS Measurement of Nuclear Proteome"
  Grade (1.6 ECTS)

- **University of Jordan**
  Doctor of Pharmacy (Pharm.D)
  2007-2013
  Grade (1.8 ECTS)

COURSES

- Conflict management in academia, Golin wissenschaftsmanagement (October 2021)
- Introduction to Python, InGrA (June 2021)
- Project management in academia, Golin wissenschaftsmanagement (January 2020)
- Critical Reasoning and Logic, InGrA (September 2019)
- Slidewriting and Storylining, InGrA (July 2019)

- Introduction to Statistic and R, InGrA (April 2019)
- Problem Solving and Decision Making, Informa (2015)
- Advanced Negotiation Skills, Informa (2014)
- Communication and Selling Skills, Actando (2014)

LIST OF PUBLICATIONS

- Ayash, M., Abukhalaf, M., Thieme, D., Proksch, C., Heilmann, M., Schattat, M.H. and Hoehenwarter, W. 2021. LC–MS Based Draft Map of the Arabidopsis thaliana Nuclear Proteome and Protein Import in Pattern Triggered Immunity. Front. Plant Sci. 12:744103. doi: 10.3389/fpls.2021.744103

- Abukhalaf, M., Bassal, M., Majovsky, P., Thieme, D., Herr, T., Ayash, M., Tabassum, N., Al Shweiki, M. R., Proksch, C., Hmedat, A., Ziegler, J., Lee, J., Neumann, S. & Hoehenwarter, W. 2020. Reshaping of the Arabidopsis thaliana Proteome Landscape and Co-regulation of Proteins in Development and Immunity. Mol Plant, 13, 1709-1732. doi: 10.1016/j.molp.2020.09.024

Halle (Saale), _____

Mohammad Abukhalaf

Declaration of Academic Honesty

Hereby I declare that I have prepared this work independently and without outside help. I did not use other than the listed sources / resources, and that all material which has been quoted either literally or by content from the used sources is particularly marked.

With this dissertation I am applying for the first time to obtain a doctoral degree.

Halle (Saale), _____

Mohammad Abukhalaf